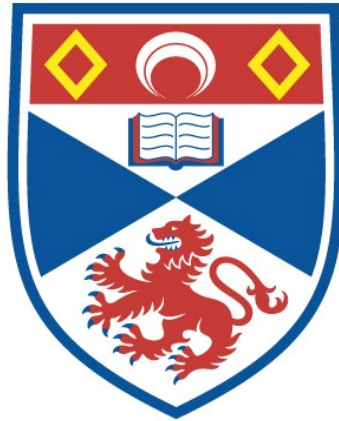


THE EVAPORATION KINETICS OF LIQUID HELIUM II

George Hutton Hunter

A Thesis Submitted for the Degree of PhD
at the
University of St Andrews



1968

Full metadata for this item is available in
St Andrews Research Repository
at:
<http://research-repository.st-andrews.ac.uk/>

Please use this identifier to cite or link to this item:
<http://hdl.handle.net/10023/13941>

This item is protected by original copyright

THE EVAPORATION KINETICS OF LIQUID HELIUM II

A thesis presented by
George Hutton Hunter, B.Sc.,
to the
University of St. Andrews
in application for the degree of
Doctor of Philosophy.



ProQuest Number: 10171006

All rights reserved

INFORMATION TO ALL USERS

The quality of this reproduction is dependent upon the quality of the copy submitted.

In the unlikely event that the author did not send a complete manuscript and there are missing pages, these will be noted. Also, if material had to be removed, a note will indicate the deletion.



ProQuest 10171006

Published by ProQuest LLC (2017). Copyright of the Dissertation is held by the Author.

All rights reserved.

This work is protected against unauthorized copying under Title 17, United States Code
Microform Edition © ProQuest LLC.

ProQuest LLC.
789 East Eisenhower Parkway
P.O. Box 1346
Ann Arbor, MI 48106 – 1346

Tm 5484


DECLARATION

I hereby declare that this thesis has been composed by me, that the work of which it is a record has been done by me, and that it has not been previously submitted for a higher degree to this or any other university.


George H. Hunter.

CERTIFICATE.

I certify that George H. Hunter has spent nine terms as a research student under my supervision, that the first six were spent at the University of St. Andrews, and that in all other respects the conditions of the regulations have been fulfilled.


D.V. Osborne.

PERSONAL PREFACE

I first matriculated in St Salvators College, University of St Andrews, in October 1959. In 1963, I graduated B.Sc with first class honours in Natural Philosophy, and during these four years I held a Harkness Residential Scholarship. In October 1963 I started research in the School of Natural Philosophy, St Andrews University, under the supervision of Dr. D.V. Osborne. At the same time I was admitted as a research student under Ordinance General No.12, and in October 1964 I was admitted as a candidate for the degree of PhD. under Ordinance No. 88. In July 1965 I moved to the University of East Anglia and continued my research there until September 1966.

SUMMARY

This work is concerned with the evaporation and condensation processes occurring when liquid helium II is in equilibrium with its saturated vapour. We define the condensation coefficient α as the fraction of atoms incident on the liquid vapour interface which cross it to form part of the liquid. Experiments to measure α are described, and the results are discussed in terms of microscopic condensation processes.

The measurements are made by reflecting second sound pulses from the liquid vapour surface at normal incidence and measuring the reflection coefficient. An account is given of the phenomenological theories of Osborne (1962a) and Chernikova (1964), which describe the reflection of second sound from the surface and the associated effect, its transformation into first sound in the gas. Neither of these agree with the experimental results, and Osborne's theory is modified by taking account of the conditions in the gas a small fraction of a mean free path above the surface (rather than many mean free paths above the surface, as in Osborne's original theory). Thus modified,

the theory is shown to be in agreement with the measurements of the reflection coefficient.

Also described are measurements made on second sound pulses generated at the interface by first sound pulses, themselves generated at the interface by second sound, propagated up the tube, and reflected from its closed end back to the surface. From the time intervals between these pulses the velocity of first sound in the vapour is deduced, and found to be in agreement with previous work. Measurements of pulse amplitude corroborate the reflection coefficient measurements, and taking the two sets of measurements together we have concluded that α is probably 1 and not less than 0.8 between 1.0°K and 2.14°K.

The microscopic processes by which condensation can take place are considered. Experiments due to Beenaker^k (unpublished, see Osborne, 1962a) and Osborne (1962b) are described, which indicate that the vapour exchanges momentum with the normal fluid only. We have therefore supposed that processes in which a gas atom condenses to form excitations must conserve energy and momentum.

Processes involving both bulk excitations and surface excitations are considered, but effects due to the finite lifetime of the excitations and the linewidth of the excitation spectrum are neglected. No attempt has been made to calculate the matrix elements for condensation processes, but plausible estimates have been made of their

relative magnitudes. In particular, only processes involving one gas atom and one or two excitations have been considered. Using the requirements of conservation of energy and momentum, it is shown that as the temperature decreases, a decreasing fraction of the incident atoms have enough energy to form two excitations, and condensation must take place by the collision of an atom with an existing excitation, and the subsequent decay of the pair into a second excitation. A rough estimate of the collision probability for such a process leads to the conclusion that at 1°K , α should be about 0.2. This disagreement with experiment has not been resolved.

Finally, some remarks are made about the implications for other work on liquid helium II, and some suggestions for future work.

TABLE OF CONTENTS

	Page
Declaration	ii
Certificate	iii
Personal Preface	iv
Summary	v
Table of Contents	viii
List of Figures	xi
List of Tables	xii
Chapter 1 - Introduction	
1.1 - Liquid Helium	1
1.2 - The Condensation Coefficient	5
1.3 - Evaporation from Classical Liquids	10
Chapter 2 - Phenomenological Theories of Evaporation	
2.1 - Introduction	12
2.2 - Osborne's Theory	12
2.3 - Chernikova's Theory	16
2.4 - Comparison of the Two Theories	19
2.5 - Modification of Osborne's Theory	23
Chapter 3 - Apparatus	
3.1 - General Methods	32
3.2 - The Heaters and Thermometers	33
3.3 - Propagation Tubes	35
3.4 - The Cryostat and General Cryogenic Arrangements	37

	Page
3.5 - Temperature Measurement and Control	39
3.6 - Electronics (Pulse Method)	40
3.7 - Electronics (Resonance Method)	43
3.8 - The Pulse Generator	44
Chapter 4 - The Experiments	
4.1 - General Remarks on Experimental Procedure	47
4.2 - Resonance Experiments	49
4.3 - The Observed Pulse Shapes	51
4.4 - The Thermometer Response Times	55
Chapter 5 - The Reflection Coefficient Measurements	
5.1 - Analysis of the Photographs	58
5.2 - Experimental Procedure	60
5.3 - Analysis of the Results	62
5.4 - Open Tube Results	64
5.5 - Closed Tube Results	68
5.6 - The Free Surface Reflection Coefficient	73
Chapter 6 - The Coupling between First Sound in the Vapour and Second Sound in the Liquid	
6.1 - Introduction	78
6.2 - The Closed Tube Case	78
6.3 - The Velocity of First Sound in the Vapour	79
6.4 - The Amplitude of the Vapour Pulses	81

	Page
6.5 - The Open Tube Case	85
Chapter 7 - Evaporation on a Microscopic Scale	
7.1 - Introduction	88
7.2 - Surface Excitations	91
7.3 - Some Numerical Calculations Relevant to Condensation Processes	93
7.4 - Tilley's Theory of Evaporation	96
7.5 - Condensation Processes Involving Bulk Excitations	98
7.6 - Processes Involving Surface Excitations	102
7.7 - The Condensation Coefficient at Low Temperatures	105
Chapter 8 - Discussion	
8.1 - Conclusions	109
8.2 - Johnston and King's Experiment	110
8.3 - The Condensation Coefficient in Helium Films	113
8.4 - Suggestions for Future Work	116
Appendix A - The Surface Area of a Liquid Meniscus	119
Appendix B - The Kinetic Theory Calculations on Evaporation	
B.1 - The Distribution Functions Close to the Surface	126
B.2 - Momentum and Mass Flux	127
B.3 - Momentum, Mass and Energy Conditions Close to the Surface	128

	Page
B.4 - Momentum and Energy Conditions Far from the Surface	130
Appendix C - The Computer Programme	132
References	143
Acknowledgements	147

LIST OF FIGURES

	following page
1.1 - The Vapour Drag Experiments	6
1.2 - The Distillation Experiment	8
2.1 - (a) The Equivalent Circuit for Evaporation	23
(b) The Velocity Distribution Close to the Surface	23
(c) The Velocity Distribution Far from the Surface	23
3.1 - The Propagation Tube and the Wall Thermometer	35
3.2 - Block Diagram of the Pulse Experiment Electronics	40
3.3 - The Thermometer Supply Circuit	42
3.4 - Block Diagram of the Resonance Experiment Electronics	43
3.5 - The Pulse Generator	44
4.1 - Argand Plots of S and 1/S	49
4.2 - The Observed Pulses	51
4.3 - The Observed Pulses	56
5.1 - The Propagation Tubes (schematic)	58

	following page
5.2 - A Typical Plot of Log H vs n	59
5.3 - The Closed Tube Reflection Coefficient	69
5.4 - The Free Surface Reflection Coefficient	74
6.1 - The Pattern Produced by the Vapour Pulses	79
6.2 - The Velocity of First Sound in Helium Vapour	80
6.3 - The Vapour-Liquid Coupling - the Coefficient r	84
7.1 - The Energy Spectrum of Liquid Helium II	89
7.2 - Momentum Vector Diagrams for Surface Excitations	103
C.1 - The Computer Programme	134

LIST OF TABLES

Table 5.1	65
Table 5.2	72
Table 7.1	95
Table 7.2	95

CHAPTER ONE

INTRODUCTION.

'..... art thou but

A dagger of the mind,

A false creation

Proceeding from the heat-oppresed brain?'

William Shakespeare.

CHAPTER 1

INTRODUCTION

1.1 Liquid helium

The He^4 atom is well known to be an extremely stable entity. The nucleus contains two protons and two neutrons, and the two orbital electrons completely fill the first shell. The atom has no electric or magnetic dipole moment, and its electric polarizability is small. As a result, the atom has a high ionization potential, it does not form chemical compounds in the normal way, and the van der Waals forces between atoms are very weak.

Because of this last fact helium is the most difficult of the permanent gases to liquefy. The critical temperature is 5.2°K and the boiling point is 4.2°K , and at these temperatures all the other permanent gases are solid. The liquid has a number of unusual properties, not the least of which is that it almost certainly remains liquid at the absolute zero. The third law of thermodynamics requires that the melting pressure tends to a constant value at the absolute zero, and at the lowest temperatures at which measurements have been made (-0.3°K) the melting pressure has in fact reached a constant value of about 25 atmospheres. Consequently, no triple point has been observed. This behaviour is at least qualitatively explained by the fact that the helium atom has a large zero point energy (as a consequence of its small mass) and it

indicates the importance of quantum effects in determining the liquid's properties.

The liquid undergoes a second order phase change at about 2.2°K , above which it is known as Helium I, and below as Helium II. A large number of the liquid's properties show anomalous behaviour near the transition temperature, which is known as the λ point. Below the λ point, the liquid is 'superfluid' - that is it behaves in certain circumstances as though it had zero viscosity. In addition the thermal conductivity is very high, and there are certain other unusual thermal effects.

These effects are explained by supposing (Tisza, 1940, Landau, 1941) that the liquid is a mixture of two components, a normal component, which carries all the entropy, and a superfluid component. Each of these components is characterised by a separate density, ρ_n for the normal fluid and ρ_s for the superfluid, such that $\rho_n + \rho_s = \rho$, the total liquid density. In addition, many of the thermodynamic properties of the liquid can be explained by assuming that the normal fluid consists of a gas of excitations dissolved, as it were, in the superfluid background (Landau, 1941, 1947). The excitations are to be thought of as collective modes of motion of many atoms, and are of two kinds. The long wavelength excitations are merely longitudinal

phonons, and the short wavelength excitations, called rotons, are envisaged as kinds of microscopic vortex rings. The energy spectrum of these excitations finally proposed by Landau (1947) has been measured by neutron scattering experiments (e.g. Henshaw and Woods, 1961), and the results are shown in figure 7.1. Strictly speaking this approach is only valid if the excitations can be regarded as non-interacting, a situation which occurs in practice below about 1.5°K . However, the interactions can be allowed for to some extent by taking account of the temperature dependence of the parameters of the excitation spectrum. In this way Bendt, Cowan and Yarnell (1959) have derived values of the normal fluid density, the specific heat and the entropy from the experimentally determined energy spectrum which agree to within a few per cent with direct measurements for temperatures up to 1.8°K .

The property with which we shall be most concerned in this work is the ability of the liquid to sustain two kinds of wave motion, called first and second sound. First sound is the ordinary sound which can be propagated in other liquids i.e. it is a pressure wave accompanied by oscillations in the total density of the liquid. Second sound is a mode in which the two fluids oscillate in antiphase, so that there is no first order density oscillation (there is a second order one due to the non-zero thermal expansion coefficient), but a first order entropy oscillation, since the normal fluid carries all the entropy. Second sound therefore appears as a temperature wave, and can be generated by

the joule heating of an A.C. current in a resistor in thermal contact with the liquid.

Since second sound was first detected by Peshkov (1944), it has been extensively investigated. Its velocity u_2 is given by (Landau, 1941)

$$u_2^2 = (\rho_s / \rho_n) (TS^2 / C)$$

where T is the temperature, C the specific heat and S the entropy of the liquid. u_2 varies little with temperature between about 1°K and 1.9°K, having a value of about 20 metres/sec (to be compared with a first sound velocity of about 240 metres/sec). Above 1.9°K u_2 falls rapidly to zero at the λ point. Associated with the temperature oscillation is a heat flow W , and it can be shown (Osborne, 1948) that W is related to the temperature amplitude θ , by

$$\theta = W / \rho C u_2 = \beta W$$

where C is the specific heat of the liquid and u_2 the velocity of second sound. β is called the characteristic impedance of the liquid for second sound, by analogy with electrical transmission line theory.

The attenuation α_B is given by (Khalatnikov, 1952a)

$$\alpha_B = (W^2 / 2\rho u_2^2) \left[(\rho_s / \rho_n) \left\{ \frac{4}{3} \gamma_n + \eta_2 - \rho (\eta_1 + \eta_4) + \rho^2 \eta_3 \right\} + \chi / C \right]$$

where w is the angular frequency, η_n and χ the coefficients of first viscosity and thermal conductivity, and $\zeta_1, \zeta_2, \zeta_3$ and ζ_4 are four coefficients of second viscosity. However, above 1°K dissipative effects at the walls of the propagation tube (which increase as the square root of the frequency) are more important.

1.2 The condensation coefficient

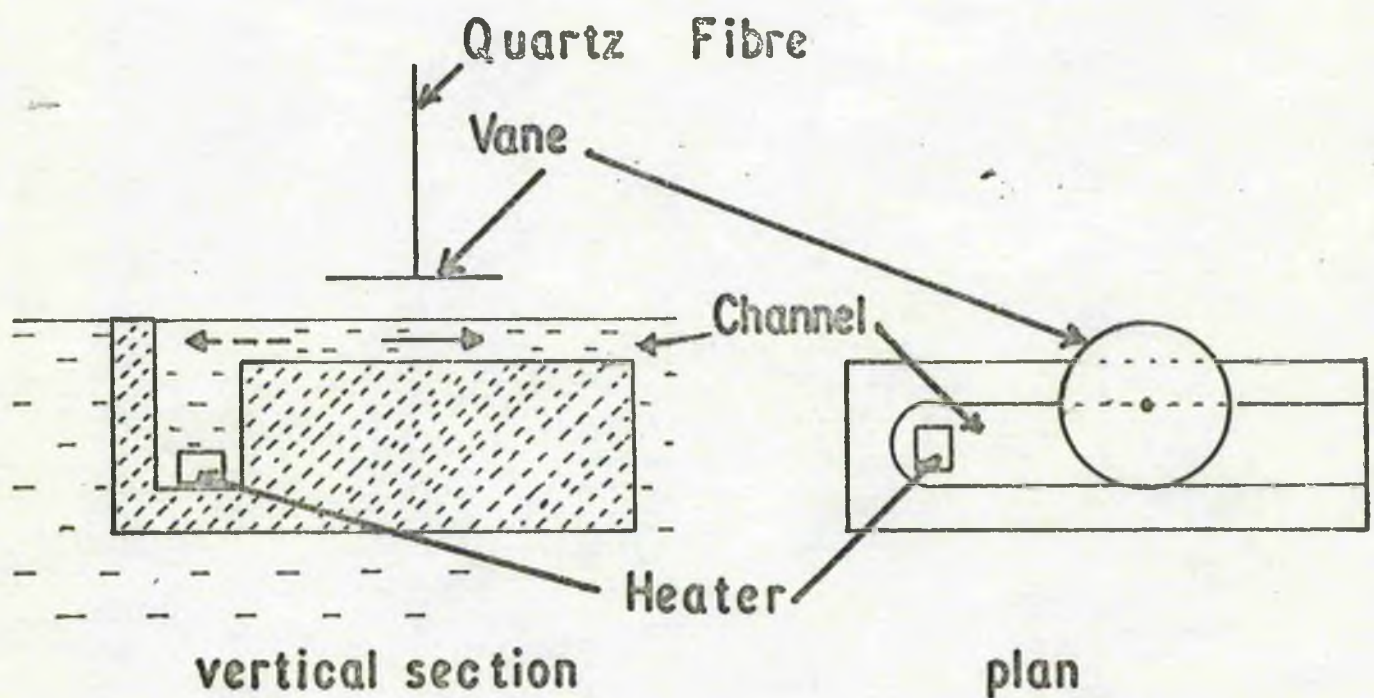
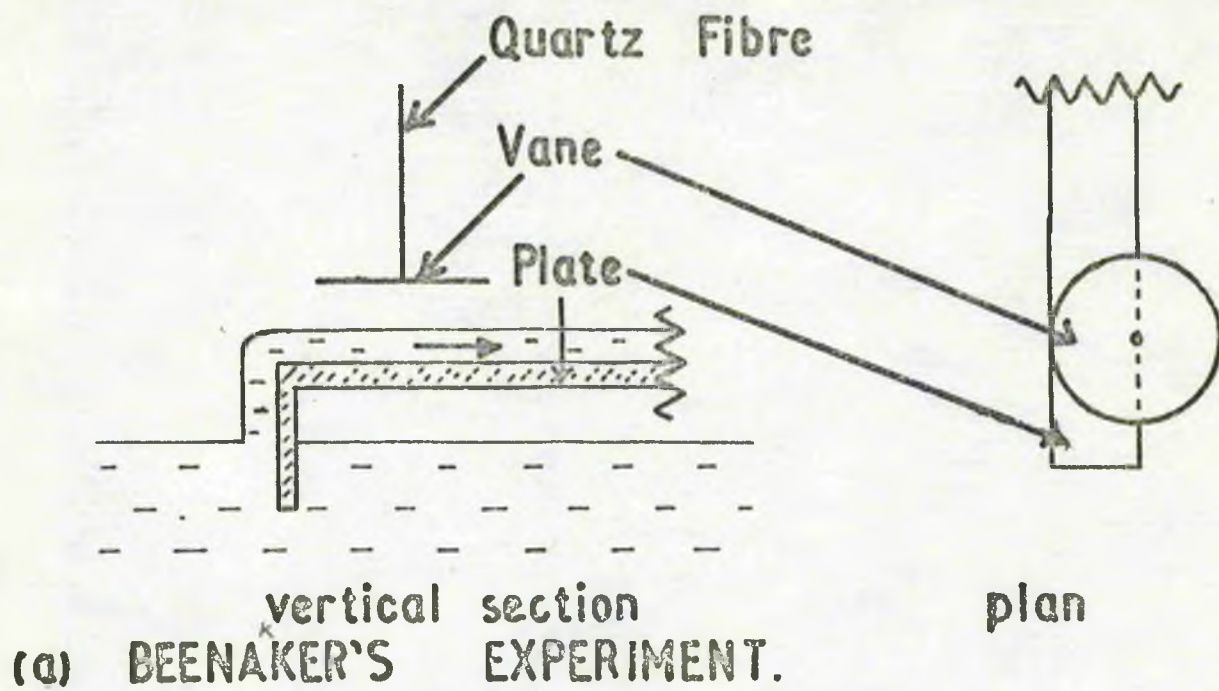
When a liquid is in equilibrium with its vapour, there is a continuous exchange of molecules between the two phases. The rate at which molecules from the vapour strike the liquid surface is known from kinetic theory, and this is clearly the maximum rate at which the vapour molecules can condense, and we define the condensation coefficient α to be the fraction of vapour molecules incident on the liquid surface which condense into the liquid. Similarly we can define the evaporation coefficient α' as the fraction of liquid molecules striking the surface which evaporate.

The case of liquid Helium II in equilibrium with its vapour presents an unusual problem, because the liquid is now thought of as a gas of excitations dissolved in a superfluid background, and it is this system which is in equilibrium with the vapour, which is adequately described as an ideal classical gas. Some light is thrown on the problem by an

experiment due to Beenaker^k (unpublished, see Osborne 1962a). He caused the superfluid film to flow across a flat plate, (figure 1.1a) and attempted to detect the motion of the vapour just above it by a small vane and a quartz fibre suspension system. The vapour was found to be stationary, or at least to have a velocity several orders of magnitude smaller than the superfluid velocity.

A similar type of experiment has been done by Osborne (1962b). A steady heat current was used to produce a counterflow of superfluid and normal fluid in a channel, and a vane suspended by a quartz fibre measured the vapour velocity (figure 1.1b). Above 1.3°K (his lowest temperature) the vapour velocity was in the same direction as the normal fluid velocity, and up to 1.7°K, they were proportional and at least approximately equal. Above 1.7°K, the experiment was more difficult to perform, and the results were not so clear cut, but the vapour was still moving with the normal fluid, and apparently faster than it.

These experiments suggest that there is no momentum exchange between the vapour and the superfluid, and that the evaporation process concerns only the vapour and the normal fluid. Fig. 7.1 shows both the energy spectrum of the excitations which make up the normal fluid and the energy of a free gas atom as a function of momentum. Each atom when it condenses acquires an energy L/R (L is the latent heat of vaporisation and R the gas constant) and a corresponding amount of momentum, and since $L/R \approx 8^\circ\text{K}$, we see that condensing atoms have



(b) OSBORNE'S EXPERIMENT

—→ superfluid velocity.

-- → normal fluid velocity.

FIG. 1.1 THE VAPOUR DRAG EXPERIMENTS.

enough energy to form rotons, but not enough momentum. Also, they have too much momentum to form phonons. There are a number of processes involving the gas atom and two excitations which conserve energy and momentum, e.g. the transformation of a gas atom into a phonon and a roton. These processes will be discussed in more detail in Chapter 7, but we note here that it may not always be possible for every gas atom to condense. If, for example, the above process were the only one possible, then only gas atoms with energies lying above the excitation spectrum could condense, and these become an increasingly large fraction of the total number of gas atoms as the temperature increases.

The problem is accentuated by the fact that if $\alpha = 1$ then evaporation takes place very rapidly. The number of gas atoms striking the surface per cm^2 per sec is $n\bar{v}/4$, where n is their number density and \bar{v} their mean speed. From this it follows that the mass condensing per cm^2 per sec is $p(M/2\pi RT)^{\frac{1}{2}}$, where p is the pressure, M the molecular weight, R the gas constant and T the temperature. In equilibrium, this is also the mass evaporating. If $\alpha = 1$, then the mass evaporating per cm^2 per sec is 0.014 gm at 1.0°K , 0.34 gm at 1.5°K , and 2.5 gm at 2.1°K . That these rates are large may be gauged by the fact that a helium film 3×10^{-6} cm thick will be completely

evaporated and recondensed in a time of the order of microseconds.

In the light of these considerations, it is of interest to determine α experimentally. Atkins, Rosenbaum and Seki (1959) have measured α in the temperature range 1.1 to 1.25°K by a direct distillation method (figure 1.2). An inverted U-tube with one limb closed was placed with both ends beneath the liquid surface, in such a way that liquid was trapped in the closed limb up to a level above the outside bath level. The liquid in the closed limb was evaporated by a heater, and the temperature difference ΔT between it and the bath measured by two thermometers. The vapour above the liquid in the closed limb was then at a pressure slightly below the vapour pressure, and α could be determined from the rate of fall of the liquid in the closed limb. Corrections were applied for surface tension effects, film flow of the liquid and viscous flow of gas. The values of α obtained ranged from 0.8 to 1.01, but depended on the U-tube diameter. Atkins et al suggested that the flow of gas in the U-tube was more complex than they had allowed for, and might have been accompanied by convection currents, for example.

In an attempt to overcome these difficulties, a second sound technique has been used in the present work. When a second sound wave strikes the liquid-vapour interface the temperature oscillation in the liquid causes evaporation to take place at the surface and the puff of vapour produced appears as a first sound wave in the vapour. The

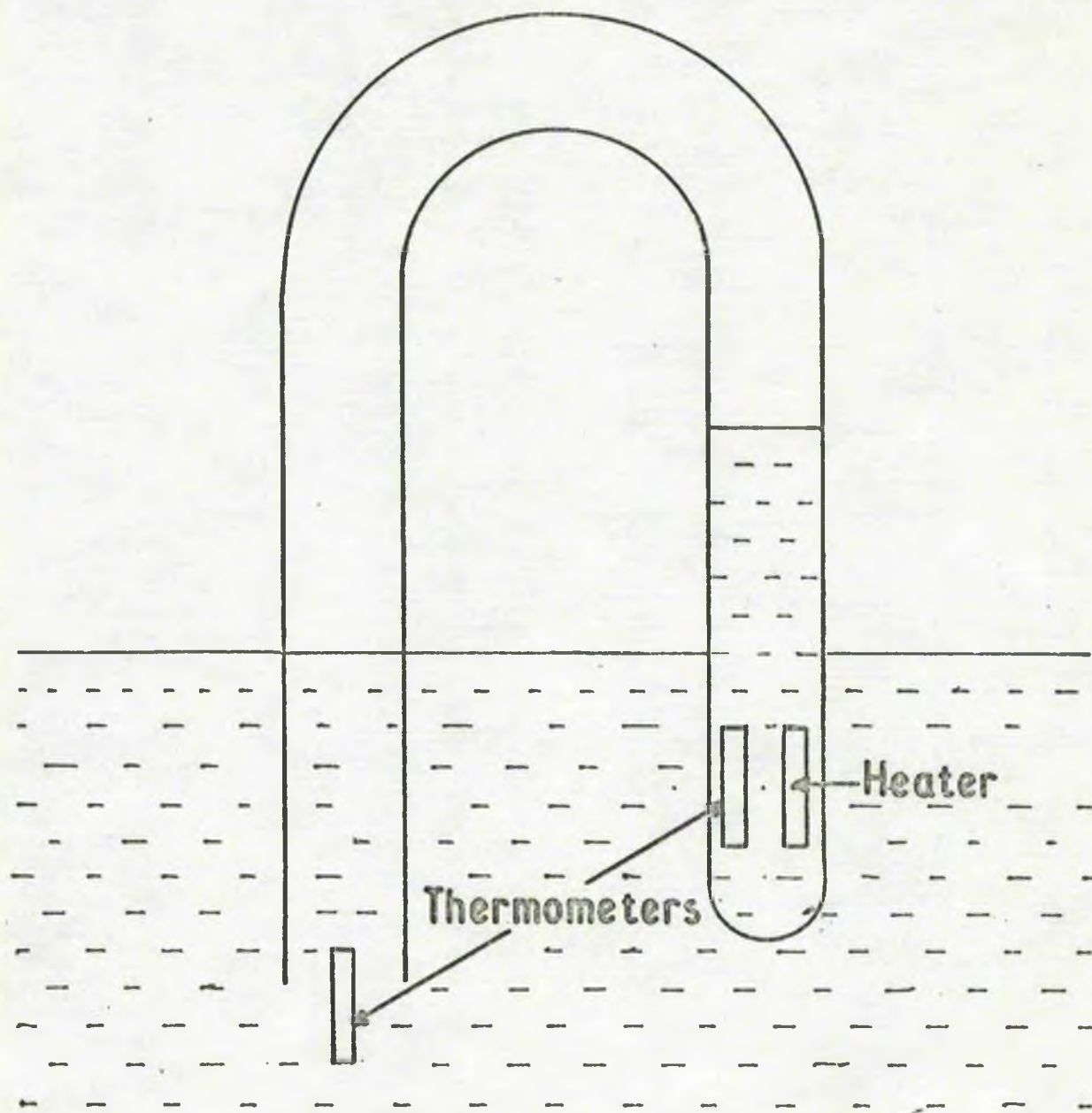


Figure 1.2 The Distillation Experiment.

amplitudes of the first sound wave in the vapour and the reflected second sound wave in the liquid are clearly determined by the boundary conditions at the interface. In particular, they can be related to the condensation coefficient. If α is very small, we would expect very good reflection from the interface.

An experiment of this kind has already been done, by Lane and his co-workers (Lane, Fairbank, Schultz and Fairbank, 1946, Lane, Fairbank and Fairbank, 1947). Using a resonance method they detected the first sound waves in the vapour with a conventional microphone, and from the separation of the resonance peaks deduced the velocity of second sound. They have also done the converse experiment, generating second sound in the liquid from first sound in the vapour (Fairbank, Fairbank and Lane, 1947). Pellam (1949) and Osborne (1962a) have observed first sound pulses in the vapour generated by second sound pulses in the liquid. None of these experiments were intended to measure α , but the fact that the amplitude of the first sound in the vapour was comparable to the second sound amplitude suggests intuitively that α cannot be very small. A detailed analysis (Osborne 1962a) confirms this impression and places a lower limit on α of about 0.1. However, the boundary conditions at the surface on which Osborne's analysis is based are a matter of some dispute, and before discussing them in detail, we shall

briefly review what is known about evaporation from classical liquids.

1.3 Evaporation from classical liquids.

The condensation coefficient has been measured for a large number of classical liquids, by a variety of methods. In one of the earliest experiments, Knudsen (1915) measured the condensation coefficient of mercury by a direct distillation method, and found it to be one. He also found that if the surface was not kept scrupulously clean, α could become as low as 0.001. Later work has confirmed these conclusions, and it is now generally accepted (e.g. Hirth and Pound, 1963) that for non-polar liquids α is one.

For polar liquids the situation is not so clear. Values of α ranging from 0.001 to 1 have been reported for water (see Hirth and Pound), using a wide variety of experimental techniques. For example Alty and Mackay (1935) measured the weight lost by a drop as it formed on a glass tip in a vessel maintained at a pressure below the saturated vapour pressure, and deduced a value for α of 0.036. More recently Jamieson (1964) has used a radioactive tracer technique and found $\alpha > 0.35$. The disparity in the experimental results is sufficient evidence that the experiments are difficult to perform. In addition to the surface contamination noted by Knudsen, there is the additional problem that

as the liquid evaporates the surface cools, and if this is not properly corrected for it leads to a low value for α .

Various theories have been proposed to account for values of α less than 1 in polar liquids (see Hirth and Pound). These mostly rest on the fact that the liquid surface is slightly polarised and only molecules approaching the surface with the appropriate orientation can enter the liquid. (Experiments to test them must therefore seek not to disturb the surface dipole, which does not make the experiments any easier). However, the latest work (a conference entitled Liquid Vapour Interfacial Phenomena, Rochester, N.Y., 1966, private communication by D.T. Jamieson) suggests that the true value of α for water is probably one, and that low results have been obtained as a result of inadequate experimental precautions.

CHAPTER TWO

PHENOMENOLOGICAL THEORIES OF EVAPORATION

'Two truths are told,
As happy prologues to the swelling act
Of the imperial theme.'

William Shakespeare.

CHAPTER 2

Phenomenological Theories of Evaporation

2.1 Introduction

Theories of the conversion of second sound to first sound at a liquid vapour interface have been published by Osborne (1962a), and by Dingle (1948), Pellam (1948) and Chernikova (1964). The last three give essentially the same result, and of these only that of Chernikova, which is the most general treatment, will be discussed in detail. Another theory due to Onsager has not been published (see Lane et al., 1947, and Pellam, 1948).

2.2 Osborne's Theory

Osborne assumes that the amplitudes of first and second sound are small, that the vapour behaves like an ideal gas, that the liquid has zero coefficient of expansion and compressibility and that the vapour density is negligible in comparison with the liquid density. He then considers a second sound wave approaching the surface normally from below, having a heat flow W per unit area towards the surface. If the reflected wave has a heat flow $W-w$ per unit area away from the surface, and the total temperature amplitude at the surface is θ , then

$$\theta = \beta (2W - w)$$

where $\beta = 1/\rho C u_s$ is the characteristic impedance of liquid HeII for second sound, ρ is the liquid density, C its specific

heat and u_2 the velocity of second sound. We rewrite this equation as

$$\theta = \beta w X_L \quad 2.1$$

where $X_L = (2w-w)/w = (1 + R_L)/(1 - R_L)$, and R_L is the reflection coefficient for second sound incident on the liquid vapour interface.

The second sound produces in the vapour an adiabatic sound wave of temperature amplitude ϕ , pressure amplitude p_0 and velocity amplitude v , related by

$$p_0 = \sigma uv \quad 2.2$$

$$\text{and } \phi = \frac{M_1}{R} \frac{\gamma-1}{\gamma} v \quad 2.3$$

where σ is the vapour density, u the velocity of sound in the vapour, M the molecular weight, R the gas constant and γ the ratio of the specific heats of the vapour.

Osborne gives an equation for conservation of mass

$$\sigma v = w/L$$

where L is the latent heat. In order to make comparison with experiment it is necessary to take account of the surface area A of the liquid meniscus in a propagation tube of finite radius r .

$$\pi r^2 \sigma v = A w/L$$

$$\text{or } v = A_0 w/L \quad 2.4$$

A_0 is calculated in appendix A.

Finally, Osborne relates the temperature difference at the surface to the net rate of evaporation. If the vapour is at a temperature T and the pressure p , then the mass condensing into the liquid is, from kinetic theory

$$G = \alpha p \left(\frac{M}{2\pi RT} \right)^{\frac{1}{2}} = \alpha \alpha_0 (T)p$$

where α is the condensation coefficient. If the vapour is in equilibrium with the liquid this is also the mass evaporating. Osborne assumes that the mass evaporating is always $G = \alpha \alpha_0 (T)p$ even if equilibrium does not exist. In this case, the mass evaporating at a temperature $T + \theta$ is

$$\begin{aligned} G(T+\theta) &= \alpha \alpha_0 p + \frac{d(\alpha \alpha_0 p)}{dT} \theta \\ &= \alpha \alpha_0 p + \alpha_0 p \frac{d\alpha}{dT} \theta + \alpha p \frac{d\alpha_0}{dT} \theta + \alpha \alpha_0 \frac{dp}{dT} \theta \end{aligned} \quad 2.5$$

Osborne implicitly assumes that $d\alpha/dT$ is negligible.

Then, using the Clausius-Clapeyron equation for dp/dT he gets

$$\begin{aligned} G(T+\theta) &= \alpha \alpha_0 p - \frac{1}{2} \alpha p \alpha_0 \theta/T + \alpha \alpha_0 (ML/RT)p\theta/T \\ &= \alpha \alpha_0 p (1 + \xi \theta/T) \end{aligned}$$

where $\xi = (ML/RT) - \frac{1}{2}$

Now the mass condensing is

$$\begin{aligned} G(T + \phi) &= \alpha \alpha_0 p - \frac{1}{2} \alpha \alpha_0 p \phi/T + \alpha \alpha_0 \frac{dp}{dT} \cdot \phi \\ &= \alpha \alpha_0 p (1 - \phi/2T + p_0/p) \end{aligned} \quad 2.6$$

since p_0 is not necessarily the vapour pressure corresponding to a temperature $T + \phi$.

Thus finally

$$\begin{aligned} w/L &= G(T+\theta) - G(T+\phi) \\ &= \alpha_0 p (\xi \theta/T - p_0/p + \phi/2T) \end{aligned} \quad 2.7$$

Substituting in this equation from equations 2.1 to 2.4 (and using the ideal gas equation $PM = \sigma RT$) gives X_L

$$X_L = (T/pL\beta \xi) (1/\alpha_0 + A_0 u (\gamma + 1)/2\gamma) \quad 2.8$$

and hence

$$R_L = (X_L - 1)/(X_L + 1)$$

This is the result we are principally interested in, but it is convenient to derive here two results required for Chapter 6.

Firstly, we note from 2.1 and 2.2

$$p_0/\theta = (\sigma uv)/(\beta w X_L) = (A_0 u)/(L\beta X_L)$$

and since $\theta = 2w\beta X_L/(1 + X_L)$

$$p_0/\beta w = 2(A_0 u/L\beta)/(1 + X_L) \quad 2.9$$

which gives the pressure amplitude in the vapour in terms of the temperature amplitude of the incident second sound wave. Secondly we extend Osborne's treatment to the reverse case, i.e. a sound wave in the gas of velocity amplitude V incident on the liquid vapour interface and being reflected with amplitude $V-v$.

$$\text{We have } p_0 = \sigma u(2V-v) = \sigma uv X_V \quad 2.10$$

$$\theta = w\beta \quad 2.11$$

$$\phi = \frac{p_0}{p} \frac{\gamma-1}{\gamma} T$$

$$\sigma v = A_0 w/L$$

$$\text{and } w/L = \alpha \alpha_0 p (p_0/p - \phi/2T - \xi \theta/T)$$

since the net mass flow is now in the opposite direction.

Solving for X_V gives

$$X_V = 2\gamma(1/\alpha \alpha_0 + pL\beta \xi /T)/A_0 u(\gamma+1) \quad 2.12$$

$$\text{and } R_V = (X_V - 1)/(X_V + 1) \quad 2.13$$

where R_V is now the reflection coefficient for first sound in the gas incident on the liquid vapour interface.

Also, 2.10 and 2.11 give

$$\theta/p_0 = w\beta / \sigma uv X_V = L\beta / u A_0 X_V$$

$$\text{and since } p_0 = 2V\sigma u X_V / (1 + X_V)$$

$$\theta/V\sigma u = (2L\beta / A_0 u) / (1 + X_V)$$

$$\text{If we now write 2.8 as } X_L = (b_1 + c_1) a_1$$

$$\text{and 2.12 as } X_V = (b_1 + 1/a_1)c_1 = (a_1 b_1 + 1)/a_1 c_1$$

$$\text{we see that } (X_V + 1) = (X_L + 1)/a_1 c_1$$

$$\text{Thus } \theta/V\sigma u = 2(T(\gamma+1)/2\gamma\beta \xi) / (1 + X_L) \quad 2.14$$

which gives the temperature amplitude in the liquid in terms of the incident pressure amplitude in the gas.

2.3 Chernikova's Theory

Chernikova considers the reflection of any type of sound wave (second sound, first sound in the liquid or first sound in the vapour) from the liquid vapour interface, and the transformation into either

of the other kinds. The treatment is for any angle of incidence, but we shall discuss here only the case of normal incidence. She remarks that her solutions are valid only for frequencies so low that the first and second sound wave lengths are very large compared with the mean free paths of the vapour atoms and the liquid excitations, respectively. At any given temperature this condition is satisfied for all frequencies for which it has so far been possible to propagate second sound. She also states that, on the basis of some calculations which she does not describe, in this frequency region the liquid is in equilibrium with its vapour.

She makes the same assumptions as Osborne about small amplitudes and likewise supposes $\rho \gg \sigma$. She does not neglect the transformation of second sound into first at the boundary, but shows that this is negligible, and in the discussion that follows it will be neglected. Also, ideal gas behaviour of the vapour is assumed here for purposes of comparison, though not in her original paper. Finally, she neglects the liquid entropy in comparison with that of the vapour, while here the entropy difference is written (exactly) as L/T .

With these assumptions and approximations, Chernikova's equations can be written as follows

$$L\rho_c/u = w$$

which is just conservation of energy. It is the same as equation 2.4 which we have written

$$p_0/u = A_0 w/L \quad 2.15$$

Her second equation arises from her boundary condition that the temperature is continuous across the surface

$$\theta = \phi + T_0 \quad 2.16$$

where T_0 is the temperature amplitude of the thermal conductivity wave in the vapour. However, no contribution to the energy flow due to thermal conduction is included in 2.15. Finally, equating chemical potentials on both sides of the surface gives

$$p_0/\sigma = L\theta/T$$

which can be written as

$$p_0 = (ML/RT) p\theta/T = (dp/dT)\theta \quad 2.17$$

That is, Chernikova has taken p_0 to be the vapour pressure corresponding to a temperature $T + \theta$.

These three equations 2.15 to 2.17, together with 2.1, which is merely a matter of definition, give

$$X_L = A_0 u T / p L \sigma \eta \quad 2.18$$

where $\eta = ML/RT$. As before

$$R_L = (X_L - 1) / (X_L + 1)$$

Using 2.17 and 2.1 gives

$$p_0/w\beta = 2p\eta \frac{X_L}{T(1+X_L)} = 2(A_0u/L\beta)/(1+X_L) \quad 2.19$$

For a first sound wave in the vapour incident on the liquid, Chernikova gives

$$\sigma v = A_0w/L$$

$$\theta = \phi + T_0$$

$$p_0/p = \eta \theta/T$$

(We note in passing a printer's error in Chernikova's paper (present in the Russian and the translation), in that her set of equations 2.2 contains σ_L (the liquid entropy in her notation) in the last term of the last equation, which should be σ_v , the entropy of the gas. Similarly, in her expression 2.3 for $T_2^{(0)}/P_1^{(0)}$ (our $\theta/V\sigma u$) there is a term $1/\rho_L \sigma_L$ which should be $1/\rho_v \sigma_v$)

Solving the above three equations for X_V gives

$$X_V = (pL\beta \eta)/(A_0uT) = 1/X_L \quad 2.20$$

$$\text{Thus } R_V = (X_V - 1)/(X_V + 1) = -R_L \quad 2.21$$

$$\text{Also } \theta/V\sigma u = 2TX_V/\eta p(1+X_V) = (T/\eta p)/(1+X_L) \quad 2.22$$

2.4 Comparison of the two Theories

If we write $T/pL\beta \xi = a_1$, $A_0u(\gamma+1)/2\gamma = c_1$, $T/pL\beta \eta = a_2$

and $A_0u = c_2$, then equations 2.8 and 2.18 become

$$X_L \text{ (Osborne)} = a_1(1/a_2c_2 + c_1)$$

$$X_L \text{ (Chernikova)} = a_2c_2$$

Chernikova's theory applies only when the liquid and the vapour are in equilibrium, i.e. when their temperatures are the same (equation 2.16), and when the pressure in the gas is the vapour pressure for that temperature (equation 2.17). Recognising that for a given p_0 , ϕ is determined by equations 2.2 and 2.3, she is obliged to introduce the thermal conductivity wave to get equality of temperatures. (Even if this procedure is correct in principle, it is not clear that the temperature amplitudes of the two waves can be added to give the total temperature excursion in the gas, as 2.16 implies).

Equations 2.16 and 2.17 together imply no net mass flow across the surface. This in turn implies that no energy is lost across the surface, i.e. the energy loss from the second sound wave is entirely taken up by the first sound and thermal conductivity waves in the vapour, though Chernikova neglects the latter contribution.

Osborne's theory, on the other hand, does not assume equilibrium. p_0 is not the vapour pressure corresponding to a temperature $T+\theta$ and there is a net mass flow $G(T+\theta) - G(T+\varphi)$ across the boundary. This mass flow requires energy, and introduces a dissipative term $1/\alpha_0$ in the final result. The situation is analogous to the transmission line system of figure 2.1(a) for which the reflection coefficient is

$$(Z_2 + R - Z_1) / (Z_2 + R + Z_1)$$

Z_1 is to be identified with β , the impedance of the liquid. R is then $a_1\beta/\alpha_0$, the 'evaporation resistance' of the surface. $Z_2 = a_2c_2\beta$ is then the effective impedance of the vapour for second sound as seen from the liquid. Then the energy lost on reflection by an incident wave of amplitude $I Z_1$ is $I^2 Z_1 - (I-i)^2 Z_1$, that carried away by the transmitted wave is $i^2 Z_2$, and the difference is $i^2 R$, the energy lost in getting from one line to the other. Chernikova's theory, however, puts $R = 0$ (no $1/\alpha_0$ term), and so no energy is lost crossing the surface. For the analogy to be exact, R must be regarded as nonlinear, since α_0 is a function of T . If $d\alpha_0/dT$ is neglected, then a_1 and c_1 go over to a_2 and c_2 .

Dingle (1948) obtains exactly the same result as Chernikova, for the same reasons. His boundary conditions are (1) p_0 is the vapour pressure corresponding to a temperature $T+\theta$, and (2) there is no energy loss crossing the surface. Pellam (1948) is interested in deriving resonance conditions for the Lane experiments (Lane et al 1946, 1947, Fairbank et al, 1947) and not in deriving heights and widths of resonances. He makes the same assumptions as Chernikova and Dingle, stating that they are sufficient for the former purpose, though probably not for the latter. However, in obtaining, for example, the total pressure at the surface due to a first sound wave incident on it from the vapour, he writes for the total pressure (his equation 35)

$$p(\text{total}) = \sigma uV - \sigma u(V-v)$$

where V is the velocity amplitude of the incident wave and $V-v$ the velocity amplitude of the reflected wave.

In obtaining the net velocity amplitude he makes the converse error (his equation 37).

$$V(\text{total}) = V+(V-v)$$

Consequently his final equation gives the reciprocal of the reflection coefficient and not the reflection coefficient as he implies. He determines θ from a relation

$$\frac{\Delta p_n}{p_n} = r\theta/T$$

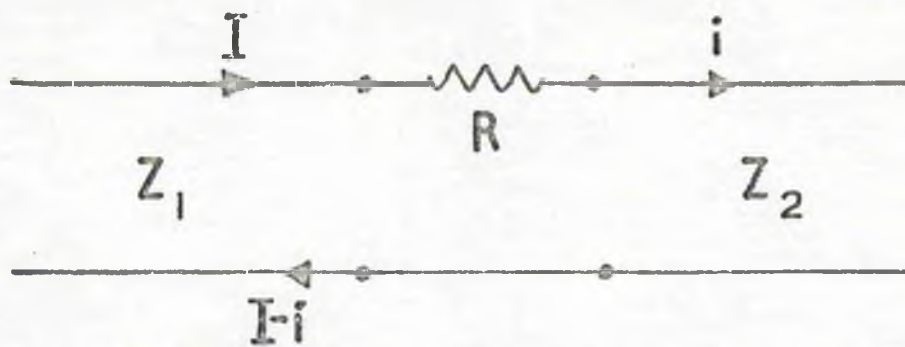
where ρ_n is the density of the normal fluid and r is an empirically determined constant. His corrected result is of the same form as Chernikova's (equation 2.18) but differs from it by a factor C/rS (-1.1) where S is the entropy of the liquid.

It should be noted that $1/\alpha\alpha_0 = 2c_1$ and so Osborne's value of X_L is three times as large as Chernikova's, and his value of R_L about 20% higher. Graphs of R_L as a function of temperature for both theories are shown in Chapter 5 (Figure 5.4), together with the experimental measurements.

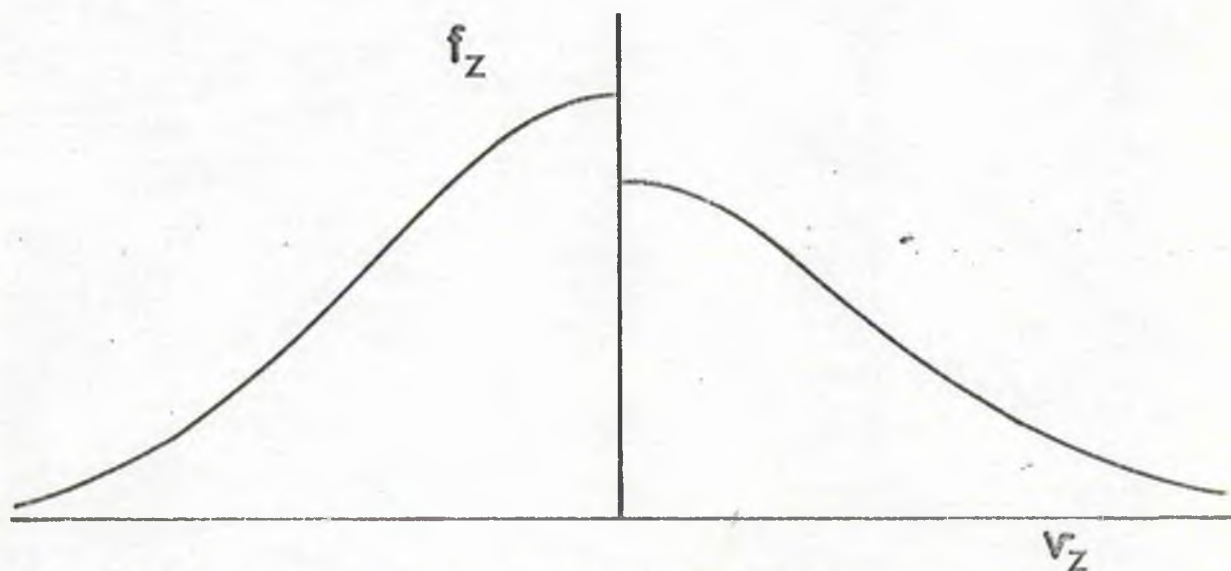
2-5 Modification of Osborne's Theory

As will be seen in Chapter 5, the experimental results agree with neither of these theories, and it is necessary to re-examine them and decide how they should be modified.

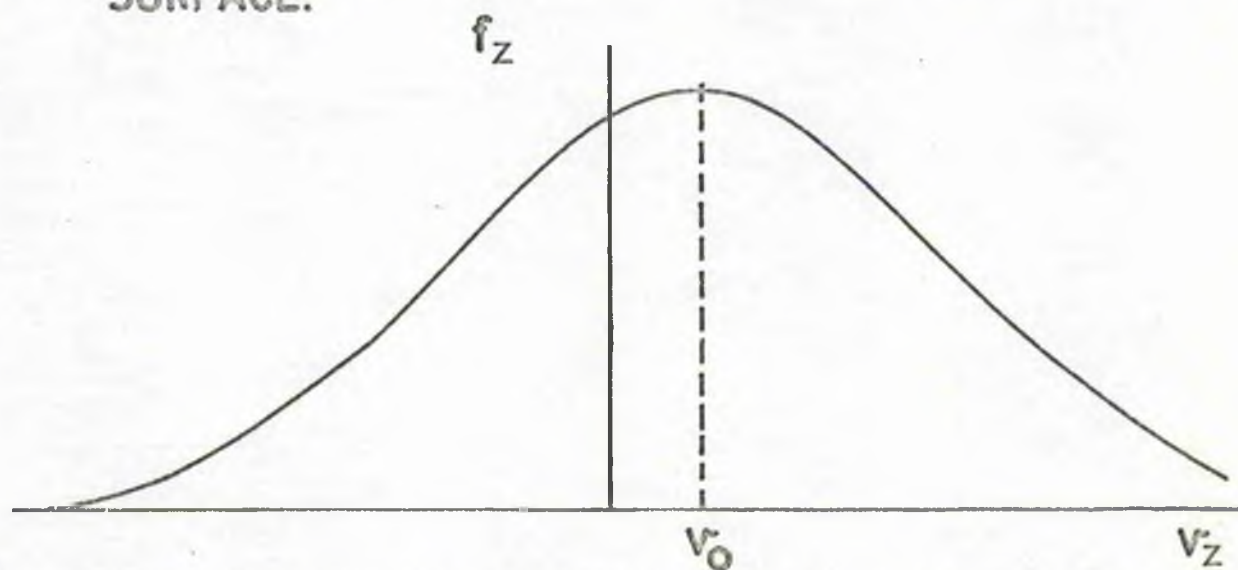
Chernikova's basic assumption, that the liquid and vapour are in thermodynamic equilibrium with each other, seems to the present author to be untenable. Her argument seems to be that thermodynamic equilibrium will exist unless there are relaxation effects (Khalatnikov, private communication), and the only relaxation times she has considered are the mean times between collisions of gas atoms or of



(a) THE EQUIVALENT CIRCUIT FOR EVAPORATION.



(b) THE VELOCITY DISTRIBUTION CLOSE TO THE SURFACE.



(c) THE VELOCITY DISTRIBUTION FAR FROM THE SURFACE.

FIG. 2.1

excitations. It is possible that there is a relaxation time associated with the evaporation process, but it is hard to see what it might be. However, the direct distillation experiment of Atkins et al (1959) is essentially a zero frequency experiment, in which no relaxation effects can be important, and it is clear that even in this case the vapour and the liquid are not in thermodynamic equilibrium.

Osborne's theory assumes that the rate of condensation is determined by the temperature ($T + \phi$) and pressure ($p+p_0$) of the gas. But $T + \phi$ and $p+p_0$ relate to the conditions in the gas many mean free paths away from the surface, and Osborne has subsequently suggested (private communication) that it is more reasonable to suppose that the condensation rate is determined by the conditions in the gas very close to the surface, i.e. a small fraction of a mean free path above the surface. In this region, he suggests that the distribution function f_z for the z components of velocity of the gas atoms has the form shown in figure 2.1(b), since all the atoms moving up (positive v_z) have come from the liquid, and all those moving down have come from the gas. (To simplify the treatment we take $\alpha = 1$.) Further, these two

distributions are characterised by different temperatures. But at distances many mean free paths from the surface, the function f_z has the form shown in figure 2.1(c) - it is merely the normal Maxwell-Boltzmann distribution shifted by a velocity v_0 . On the basis of these considerations, we now proceed to a detailed calculation of the net evaporation rate.

Consider first the region close to the liquid surface. We assume that both halves of the distribution are Maxwellian, i.e. that the distribution function for the atoms moving up has the form

$$f_{z+} = \beta_1 \exp(-mv_z^2/2kT_1)$$

and for those moving down

$$f_{z-} = \beta_2 \exp(-mv_z^2/2kT_2)$$

Then if there are $\frac{1}{2}n_1$ atoms/cc moving up and $\frac{1}{2}n_2$ atoms/cc moving down, it is shown in Appendix B (equation B.4) that the mean energy of an atom is

$$(\frac{3k}{2})(n_1T_1 + n_2T_2)/(n_1 + n_2)$$

and that the flux of z momentum across the x - y plane per cm^2 per second is (equation B.5)

$$\frac{1}{2}n_1kT_1 + \frac{1}{2}n_2kT_2$$

We now consider a region of the gas a distance x from the liquid surface, such that $x \gg \ell$, the mean free path. If the theory is to be applicable to sine waves, it is necessary that x be chosen at a point where the phase of the wave is the same as at the surface (or differs from it by an integral multiple of 2π). In practice it is always possible to choose x such that $\lambda \gg x \gg \ell$, where λ is the first sound wavelength. (In the worst case, at 1°K , $\lambda = 5$ cm and $\ell = 4 \times 10^{-4}$ cm). Then we find that the mean energy of an atom is (equation B.9)

$$\frac{3}{2}kT_s + \frac{1}{2}m v_0^2$$

and the momentum flux is (equation B.10)

$$n_s k T_s + n_s m v_0^2$$

v_0 is the particle velocity in the sound wave; it is proportional to ϕ , the temperature amplitude of the sound wave (equation 2.3). But T_s , the temperature of the gas, is merely $T + \phi$, and so terms in v_0^2 are second order and will be neglected.

We now assume that the mean energy of the atoms is the same in both regions, and that the momentum fluxes are also equal.

Then

$$(n_1 T_1 + n_2 T_2) / (n_1 + n_2) = T_s \quad 2.23$$

and $\frac{1}{2}(n_1 k T_1 + n_2 k T_2) = n_s k T_s \quad 2.24$

As already noted $T_2 = T + \phi$ in our previous notation, and clearly also $n_2 k T_2 = p + p_0$. By our assumption about evaporation under non equilibrium conditions T_1 is to be identified as $T + \theta$, and $n_1 k T_1$ as $p + p_1$, the vapour pressure corresponding to this temperature.

(Although the number density of the molecules moving up in the region close to the surface is $\frac{1}{2}n_1$, in equilibrium those moving down also have a density $\frac{1}{2}n_1$, and it is thus the total density n_1 which determines $p + p_1$).

We write $n_1 = n + dn_1$, $n_2 = n + dn_2$ and $T_2 = T + \Delta T$ and since θ , ϕ , p_0 and p_1 are small quantities it is clear that dn_1 , dn_2 and ΔT are also small quantities. Equation 2.23 can then be written

$$(n + dn_1)(T + \theta) + (n + dn_2)(T + \Delta T) = (2n + dn_1 + dn_2)(T + \phi)$$

whence, neglecting second order terms

$$\theta + \Delta T = 2\phi \quad 2.25$$

It is shown in appendix B (equation B.6) that the net mass transfer across the x-y plane close to the surface is

$$n_1 k T_1 \left(\frac{M}{2\pi R T_1} \right)^{1/2} - n_2 k T_2 \left(\frac{M}{2\pi R T_2} \right)^{1/2}$$

This is clearly just the mass evaporating, w/L . Rewriting we get

$$w/L = \alpha_0 \left[n_1 k T_1 (1 - \theta/2T) - n_2 k T_2 (1 - \Delta T/2T) \right]$$

Substituting from 2.24 for $n_2 k T_2$ gives

$$w/L = 2\alpha_0 \left[n_1 k T_1 (1 - \theta/4T - \Delta T/4T) - n_2 k T_2 (1 - \Delta T/2T) \right]$$

Substituting from 2.25 for ΔT and writing the $n k T$'s in terms of pressures

$$w/L = 2\alpha_0 p \left[(1 + \eta \theta/T)(1 - \phi/2T) - (1 + p_0/p)(1 - \phi/T - \theta/2T) \right]$$

where the Clausius-Clapeyron equation has been used for p_1 , and $\eta = ML/RT$. Finally we get

$$w/L = 2\alpha_0 p \left(\xi \theta/T - p_0/p + \phi/2T \right) \quad 2.26$$

This is to be compared with equation 2.7. Since Osborne's other equations remain unaltered, X_L and R_L are obtained by ^{replacing} putting a by 2 in equation 2.8.

Osborne's original theory rests on the assumption that if the liquid is maintained at a temperature T , evaporation takes place from the surface as if the liquid were in equilibrium with its vapour, whether it is or not. As modified here, it requires three additional assumptions.

The first is the supposition that both halves of the distribution close to the surface are Maxwellian. Loeb (1961) shows that for a classical liquid in equilibrium with its vapour, the evaporating molecules have a Maxwellian distribution, if it is assumed that the distribution of molecular velocities in the liquid is also Maxwellian. Because the latent heat of liquid helium is 8°K per atom and only atoms with at least this energy can escape, their velocity distribution will be Maxwellian even if Bose-Einstein statistics are more appropriate for the liquid as a whole. While this argument is not conclusive, a Maxwellian distribution is the only one that it seems reasonable to assume for the evaporating atoms.

We have also assumed that (a) the mean energy of an atom is the same close to the surface as it is far from the surface, and (b) that the flux of z momentum across an x - y plane is the same in both regions.

These two together (equations 2.23 and 2.24) imply that there is no first order density change between the two regions. In equilibrium, we have regarded the surface as well defined on a microscopic scale; the temperature and pressure of the gas are independent of the distance from the surface as a matter of definition. When the liquid and vapour are not in equilibrium with each other, our assumptions are equivalent to saying that the temperature and pressure amplitudes of the sound wave are independent of the distance from the surface. (Also, if the momentum flux was not the same in both regions, momentum would be accumulating somewhere, and this seems rather unlikely. It is not so obvious that the energy distribution must be uniform, and the best justification for equating temperatures in the two regions is that the theory is in agreement with experiment).

One other point about microscopic theories of evaporation should be mentioned, and that is that the first sound wave is being propagated in a saturated vapour. We note, however, that the velocity has been measured at the saturated vapour pressure in helium gas by van Itterbeek and de Laet (1958), Grimsrud and Werntz (1967) and Meyer, Meyer, Halliday and Kellers (1963), and also in the present work (see Chapter 6). Only van Itterbeek and de Laet and Grimsrud and Werntz were able to detect any deviation from $u = (\gamma RT/M)^{\frac{1}{2}}$.

These results extended from 2°K to 4.2°K, and at the lowest temperature the deviation was only about 1%. Above 1.8°K their extrapolated values of u have been used in calculating theoretical reflection coefficients; below this temperature the extrapolated values agree with the perfect gas curve. In this temperature region we have also used van Itterbeek and de Laet's experimental values of γ .

CHAPTER THREE

APPARATUS

'The higher we fly on the wings of Science, the worse
our feet seem to get entangled in the wires'

The New Yorker, February, 1931.

CHAPTER 3

Apparatus

3.1 General Methods

Two methods of measuring α were tried, a pulse method and a resonance method.

In the pulse method, second sound was generated by applying electrical pulses to a heater resistance, placed across the bottom end of a vertical tube, arranged so that the liquid level is below the top. The second sound pulses were propagated up the tube, reflected from the free surface, and detected by a resistance thermometer situated somewhere below the surface. The thermometer was supplied with a constant current to convert resistance fluctuations to voltage fluctuations, which were then amplified, filtered, and displayed on an oscilloscope. The oscilloscope trace showed the initial pulse and echoes caused by successive reflections, first from the open end, then from the closed end. The traces were photographed, and measurements of pulse heights from the photographs enabled the reflection coefficient at the open end to be calculated.

In the resonance experiments, the thermometer was placed at the bottom of the tube. The heater was fed from an oscillator, and standing waves were set up when the length of the liquid column in the tube was an integral number of half wavelengths. As the helium boils off, a resonance is swept through, and the Q (which is related to X_L) was measured.

3.2 The Heaters and Thermometers

The heater has to be placed at the bottom of the tube to produce a second sound flow along the axis, and the question then is where to put the thermometer. For a resonance experiment, it must clearly be at a temperature antinode, and the most convenient antinode is the bottom of the tube. Two such arrangements were tried.

In the first, the heater consisted of a flat plate of glass whose top surface was electrically conducting, placed across the end of the tube. This conducting glass had a resistance of ≈ 50 ohms/square, which was virtually independent of temperature between 1°K and 300°K . It was obtained from J.A. Jobbling Ltd., Sunderland. Electrical contacts were made by soldering wires to thin copper strips just large enough to cover the ends of the plate, and 'gluing' these strips on with 'silver dag' (a commercially available suspension of silver in methylisobutylketone). The heater used in all the experiments was $15\text{ mm} \times 13\text{ mm}$ and had a resistance of 100 ohms at helium temperatures. The thermometer in this arrangement consisted of an enamelled copper wire (36 S.W.G.) which was coated with aquadag. It was placed across a diameter of the propagation tube, and located by two recesses cut in the bottom of tube. This thermometer was used for all the resonance experiments.

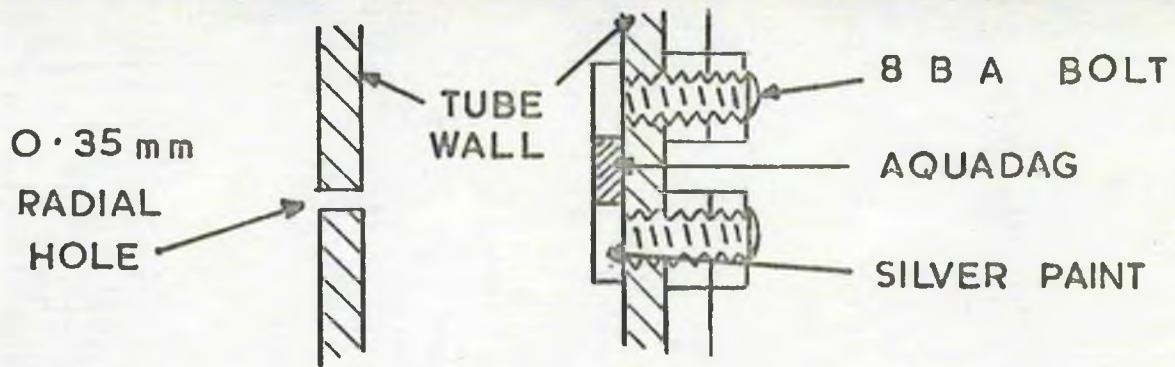
The second method tried was to paint both the heater and thermometer on a glass plate, which was then placed across the end of the tube. The thermometer was a thin strip of aquadag painted across the centre, the heater a strip of aquadag or silver dag on either side. This arrangement was troublesome for four reasons. Firstly, it was necessary, in the pulse experiments, to be able to generate pulses of amplitude about 1 watt/cm^2 for measurements near the λ point. The aquadag heater had such a high resistance, and the silver dag one such a low resistance, that it was not easy to meet this requirement. Secondly, the electrical pick up in the thermometer was so large that the thermometer amplifier was saturated for an inconveniently long time. This could be remedied by earthing the heater in a suitable way (see 3.8) but only at the expense of increased hum. Thirdly, the temperature variation of the heater resistance was so large and unpredictable that it was difficult to do meaningful tests of the system at room temperature. Finally, it was discovered that the thermometer was responding to the heat pulse generated by the heater and transmitted through the glass backing. This last produced a large and slow distortion of the base line which made the pulse photographs so obtained unusable.

A third heater thermometer arrangement was used, in which the thermometer was placed on the tube wall sufficiently far from the heater that thermal conduction effects did not occur. The heater was again a conducting glass plate across the end of the tube. The construction of the thermometer is shown in figure 3.1 (a). A small patch of aquadag - 2 mm wide (i.e. along the tube) and - 4 mm long was painted on the inside wall of the tube. Two 8 B.A. holes were drilled and tapped in the wall, one above and one below the aquadag. Brass bolts with their ends filed flat were screwed into the holes until the ends were just flush with the inside surface. They were then locked in place with nuts, and contact made between the aquadag and the bolt ends with silver dag.

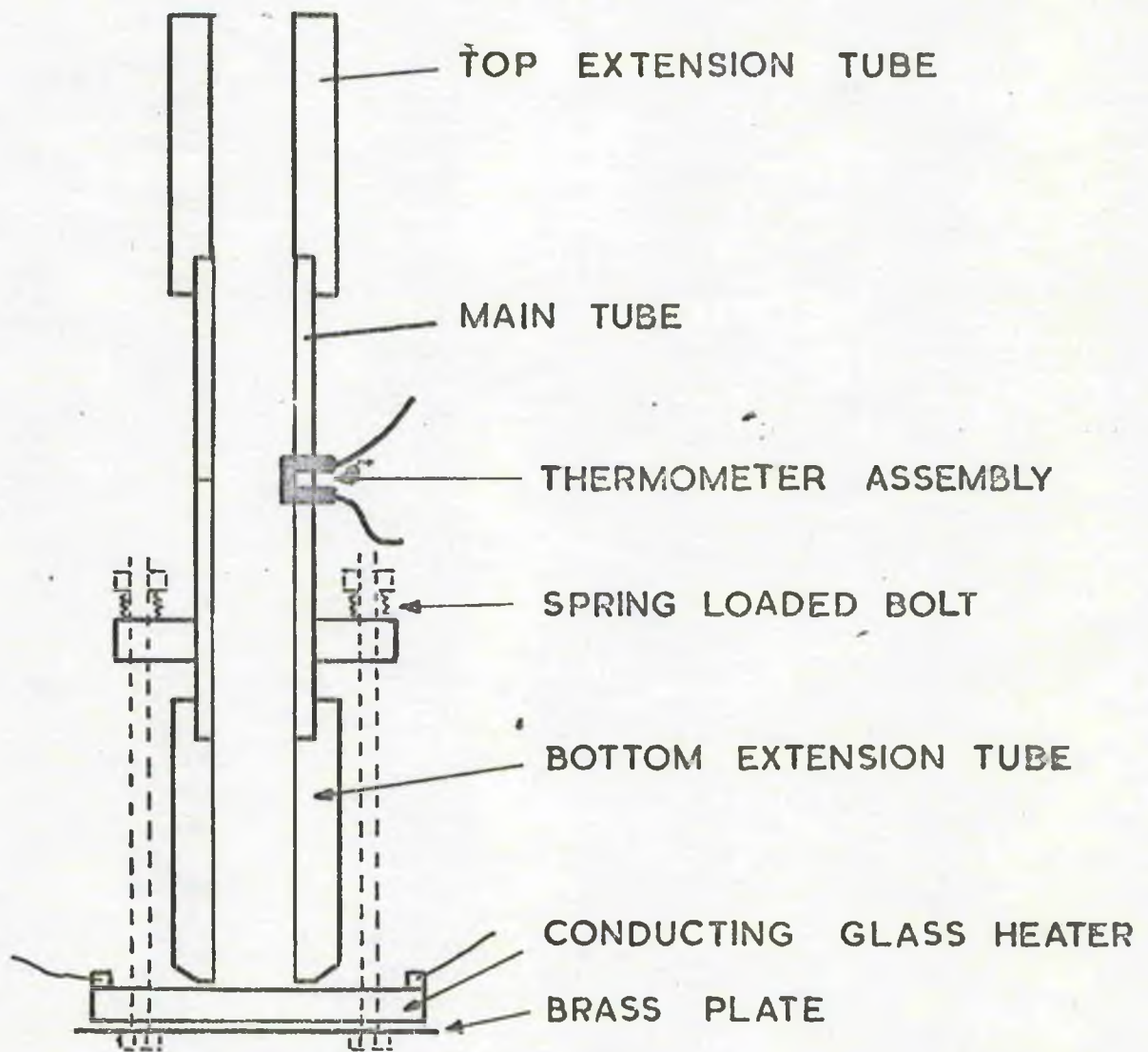
This thermometer had a rather poor response time, ≈ 1.5 ms presumably caused by the good thermal contact with the backing. This arrangement was used for all the results discussed in Chapters 5 and 6.

3.3 Propagation tubes

The propagation tubes used were made from perspex of 1 cm internal diameter and from 7 to 14 cm long. Figure 3.1(b) shows the type of tube used in the final pulse experiments. The tube



(a) THE WALL THERMOMETER



(b) THE PROPOGATION TUBE

Figure 3.1 The Propagation Tube and the Wall Thermometer.

with the thermometer on the wall was made in parts to avoid placing the thermometer too close to one end. Extension tubes of various lengths were made which could be pushed on to either end. Those for the bottom were tapered at the lower end to leave $\frac{1}{2}$ mm wide annulus in contact with the heater. This was to reduce any spurious effects caused by local heating at the part of the heater surface in contact with the tube wall. A small hole (0.34 mm) was drilled in the tube wall opposite the thermometer to allow good thermal contact with the bath. A brass plate beneath the heater was bolted to a flange near the bottom of the main tube by 10 B.A. bolts tightened against compression springs, which kept the tube flat on the heater when the perspex contracted at low temperatures.

The tubes used in resonance experiments were slightly different. Extension tubes were not used, and the bottom end of the tube was not tapered off from the full wall thickness of 2 mm. The thermometer, located by two recesses in the end, was insulated from the heater by a thin perspex ring placed between them.

The brass plate was part of a cage (not shown) used to suspend the tube from the top of the cryostat. In dummy experiments the top of the tube was closed by another conducting glass plate, held by a spring placed between it and the top of the cage. Also mounted on the cage were a plumb line and a pointer, roughly adjusted to be in

line when the propagation tube was vertical. Fine adjustments were made with the 10 B.A. bolts holding the tube to the brass plate. The tube was positioned (approximately) on the axis of the cryostat, and a mirror mounted behind the plumb line and pointer at 45° to the line of sight permitted the tube to be vertically aligned during a run using levelling screws on the cryostat top plate.

3.4 The cryostat and general cryogenic arrangements.

The brass cage containing the propagation tube was bolted on the end of a $1/8$ inch diameter thin walled stainless steel tube, which could slide vertically through a hat gland seal on the top plate. Current and potential leads to the thermometer were taken down inside this tube to a multiple plug, the socket being mounted on the brass cage. The stainless steel tube then provided some screening of the thermometer leads, and the whole cage assembly was arranged to be easily demountable. A small hole was drilled in the stainless steel tube about half way up, to prevent thermal oscillation in it, and a stop was mounted just above the hole to prevent the hole being pulled past the seal when the cryostat was under vacuum. The cryostat also contained a resistance thermometer

for measuring the bath temperature, and a 2 kohm heater for controlling the temperature at low temperatures. The dewars were made of glass, the helium ones of Monax, which required repumping about every 20 runs.

Temperatures down to 1.25°K were reached using a high capacity rotary pump. From 1.25°K to 1°K an Edwards 9B4 vapour booster pump was used.

Because it was used only in the latter stages when time was short, it was installed without much consideration for pumping speeds, and was connected to the cryostat by a rather long and narrow pipe. This consisted, essentially, of three lengths of tube, the first (nearest the cryostat) 7.1 cm long and 1.8 cm diameter, the second 9.2 cm long and 4 cm diameter, the third 17.8 cm long and 4.25 cm diameter. Assuming laminar flow in the pipe, the mass flow/sec., G , is given by (e.g. Present, 1958).

$$G = \frac{\pi a^4 M}{16 \eta RT \ell} (p_0^2 - p_1^2)$$

where a is the radius, ℓ the length, and p_0 and p_1 are the pressures at the input and output ends of one of the sections of pipe. G can be calculated from the helium boil off rate, which was ~ 1 cm/hr in a dewar of 6 cm internal diameter. This gives $G \sim 1.4 \times 10^{-2}$ gm./sec. η for Helium gas at 1°K is $\approx 2\mu$, and p_0 for the first section is

taken as the vapour pressure at 1°K, i.e. 0.12 torr. Using these values, one finds that the pressure drop across three sections of pipe is quite negligible ($\approx 5 \times 10^{-4}$ torr).

The conclusion is that the ultimate pressure is limited by the throughput. Using a three level polished copper radiation shield reduced the ultimate pressure from 0.2 torr to 0.11 torr, which according to the makers performance figures (for air) gives a reduction in throughput of $\sim 8\%$. Rotating the nitrogen dewar so that stray light did not fall on the helium, or on the absorbent perspex tube, had no appreciable effect. The cryostat would have had to be redesigned to have a lower heat leak before lower temperatures would have been obtained.

3.5 Temperature measurement and control

Above 1.3°K, temperatures were determined from the vapour pressure, measured on an oil manometer one side of which was continuously pumped, the other side being connected to the cryostat. Conversions from vapour pressure to temperature were made using the T_{58} scale of van Dijk and Durieux (1958a).

Below 1.3°K, temperatures were determined from the resistance of a $1/8W$ 12 ohm nominal Allen Bradley resistor. The resistor

was calibrated between 1.3°K and 2.1°K, and the temperature at lower temperatures determined from a linear extrapolation of a log-log plot of vapour pressure against resistance (Cunsolo, Santini and Vincenti-Missoni, 1965). A potentiometer was used to measure both the potential across the thermometer and the current through it (by measuring the potential across a standard resistance in series). The measuring current used was 4 μ a, corresponding to a maximum heat dissipation of 16×10^{-9} watts.

Above 1.25°K the temperature was controlled by valves on the pumping line, while monitoring the temperature with the resistance thermometer. At the lowest temperatures a fine control on the nearly shut baffle valve of the booster pump gave adequate temperature stability (better than 1 mdeg.), while at temperatures between 1.1 and 1.25°K the bath heater was used to control the throughput. It was fed from a 12v D.C. power supply, giving up to 70 mw heat input, but 30 mw was the largest heat input used.

3.6 Electronics (Pulse Method)

The block diagram is shown in figure 3.2. Two amplifier systems were used. The first consisted of a Brookdeal L.F. amplifier

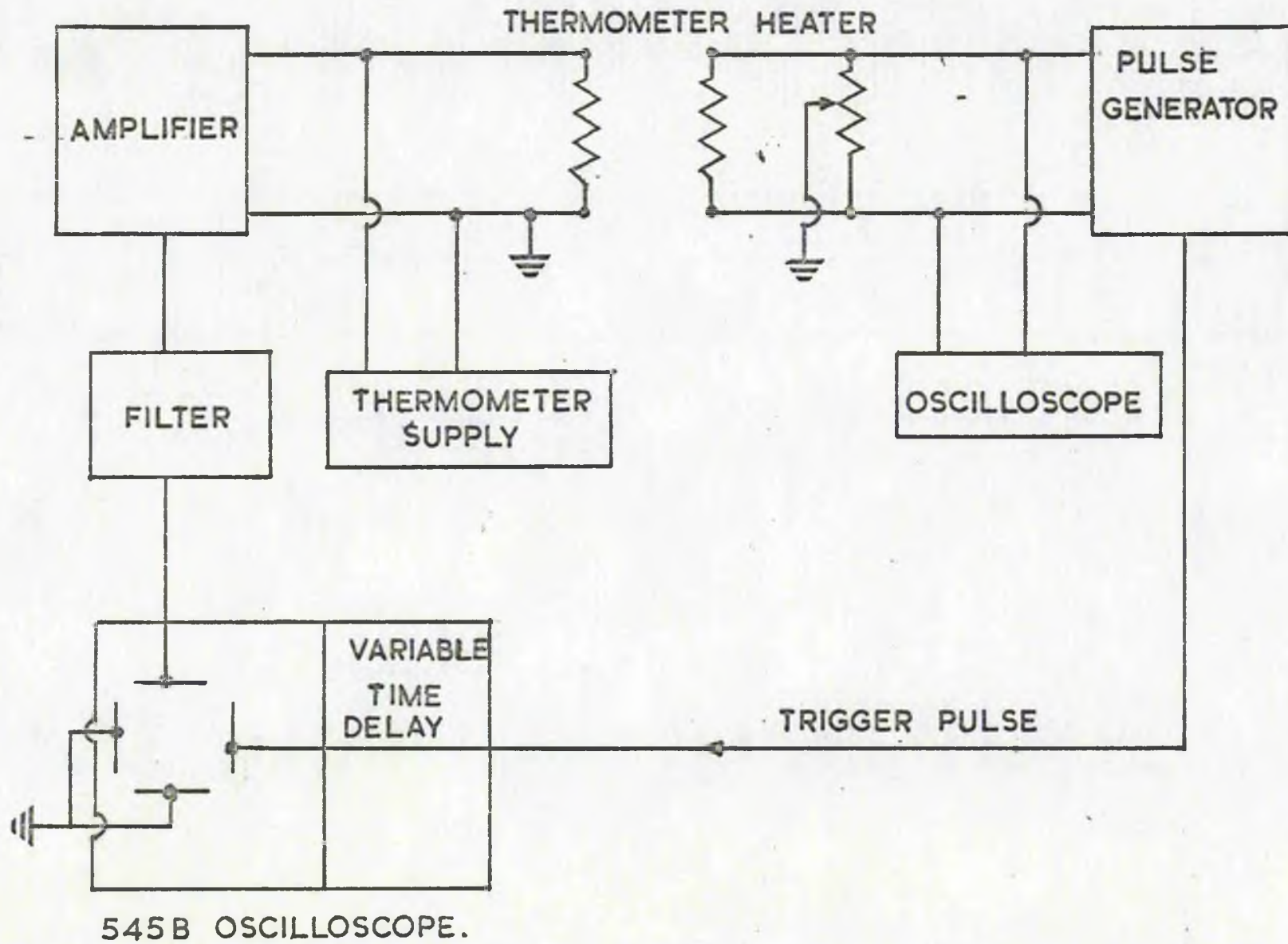


Figure 3.2 Block Diagram of the Pulse Experiment Electronics.

followed by a Dawe variable filter and a CA type plug-in unit on a Tektronix 545B oscilloscope. The Brookdeal had a gain of 94 db, a bandwidth from 5c/s to 100 kc/s, and an input noise level of \approx μ v. The Dawe filter was used in the low pass mode, set at 20kc/s. The thermometer was fed with a constant current of about 1 ma, supplied by a 120v. H.T. battery and a 100 kohm resistance, placed in an earthed metal box to reduce 50 cycle pick up problems. Higher currents than 1ma increased the noise level, and lower currents decreased the signal.

This system was not very satisfactory because, at the lowest sweep speeds (10ms/cm) the Brookdeal low frequency response caused the base line of the scope trace to become distorted. It was therefore replaced by a Fenlow type A102 D.C. amplifier with a gain of 26 db, and a type E differential amplifier plug in unit, used in the single ended mode. The type E plug in had a maximum sensitivity of 50 μ v/cm compared with the 50 mv/cm of the C A type. It has a bandwidth from 0.02 c/s to 80kc/s, and its own high and low pass filters, set at 0.02 c/s and 10kc/s respectively.

With this system it was necessary to modify the thermometer current supply circuit to prevent saturation of the D.C. amplifier.

The circuit used is shown in Figure 3.3. Essentially it was two constant current sources of opposite polarity feeding two parallel resistors R_1 and R_2 in such a way that the net current through R_1 (the D.C. amplifier) input was zero, while that through R_2 (the thermometer) was not. For this to be so, we require that $I_1/I_2 = (1+r/R_1)$. Since R_1 was temperature dependent, it was necessary to adjust r every time the temperature was changed.

Incorporated in the oscilloscope was a variable time delay which enabled the start of the sweep to be delayed by a known time after the arrival of the triggering pulse from the pulse unit. With the delay set to zero, the start of the sweep could be made to coincide with a graticule mark on the screen, and the delay times necessary to bring successive pulses into coincidence with the same mark could be used to measure the time intervals between pulses. This is the basis of the level measurements in Chapter 5 and the velocity measurements in Chapter 6.

50c/s pick up was very troublesome, and a considerable amount of time was devoted to earthing problems. It was necessary to adopt a systematic single point earthing system, and then introduce strategically situated earth loops (across the Fenlow D.C. amplifier for

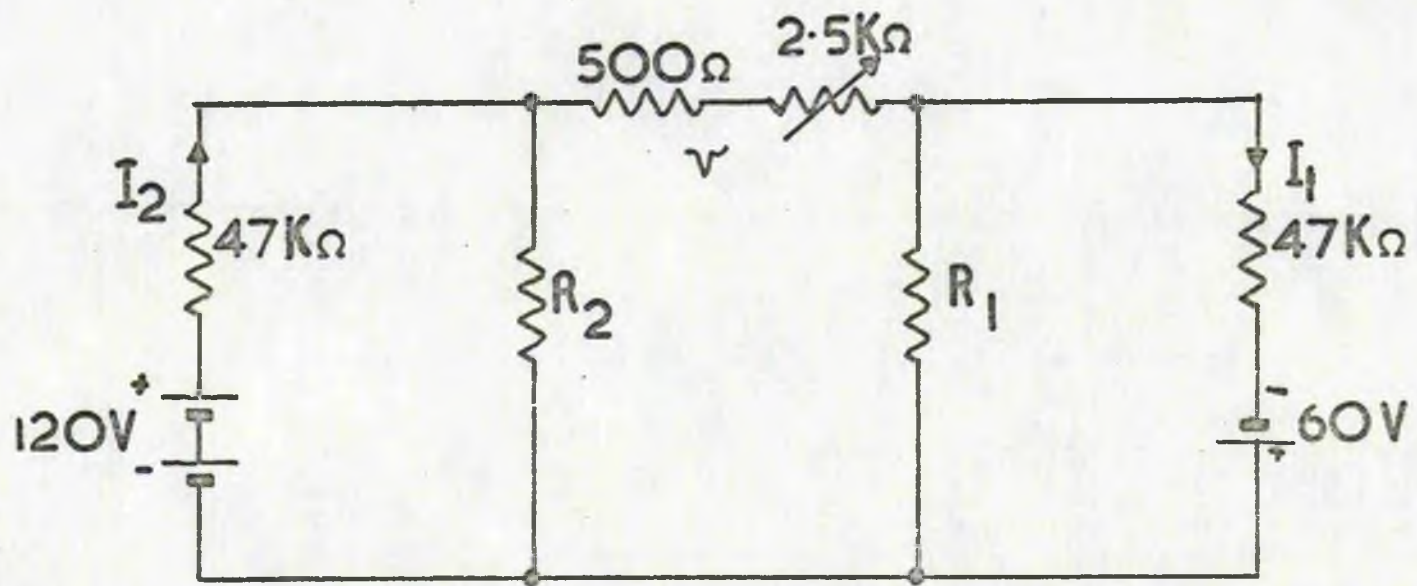


Figure 3.3 The Thermometer Supply Circuit.

example). It was also necessary to break the earth line to the oscilloscope, and earth it separately to the common earth point (usually the cryostat top plate). It was possible in the high temperature runs to isolate the system from the mains earth, which meant electrical isolation from the pumping line. This was achieved by inserting a teflon washer between two of the flanges on the line, and bolting them together with brass bolts insulated by teflon bushes and washers. For the low temperature runs, it was sufficient to exploit the fact that the Fenlow amplifier was directionally sensitive to pick up. It was mounted on a clamp stand and could be rotated about any of three mutually perpendicular axes to give minimum hum.

3.7 Electronics (Resonance Method)

The signals were generated by the oscillator and detected by the d.c. fed thermometer, amplified, filtered and applied to the Y plates of an oscilloscope. (see Figure 3.4). The X plates were driven from the oscillator and so the signal appears as a 2:1 Lissajou figure, since the second sound frequency is twice the

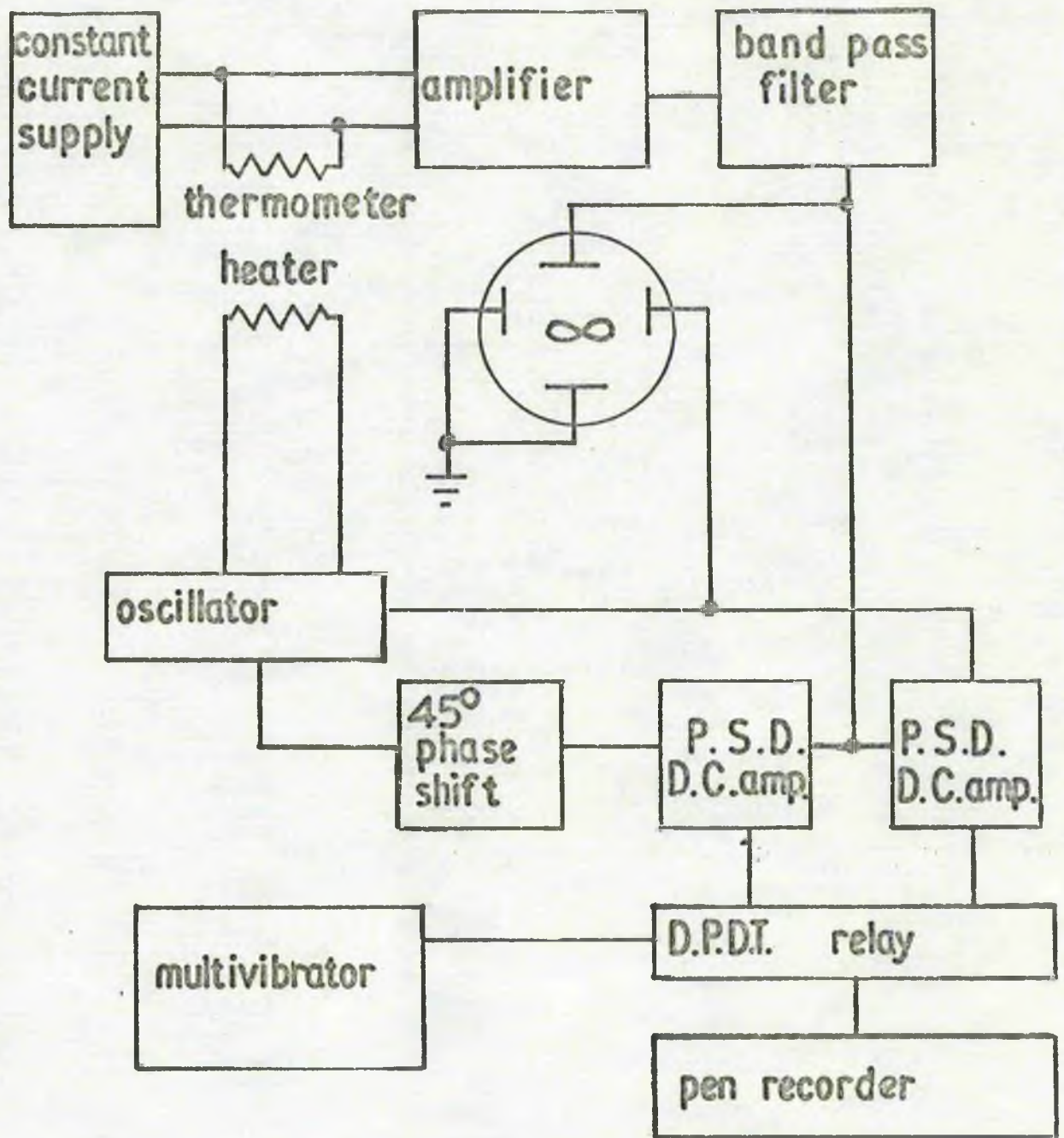


Figure 3.4 Block Diagram of the Resonance Experiment Electronics.

oscillator frequency. The oscilloscope was used for detecting resonances. In order to measure them, the signal was fed to two phase sensitive detectors, one supplied with a reference direct from the oscillator, the other with a reference 45° out of phase with it. The two outputs, 90° out of phase, were applied to a pen recorder via a multivibrator driven relay acting as a chopping device. As the helium level dropped, it was observed through a cathetometer, and the marking pen on the pen recorder used to register the time at which the level passed each division.

3.8 The Pulse Generator

This consisted of a free running multivibrator, V1 (Figure 3.5), controlling the repetition frequency, which drove a monostable multivibrator, V2, controlling the pulse length, and an output stage.

One period of V1 was fixed, at 45 ms, and the other had 4 values selected by a switch (≈ 5 ms, 55 ms, 155 ms and 455 ms with $C_1 = 0.1 \mu\text{f}$). The monostable circuit V2 was triggered by positive going pulses, and the intervals between these were then approximately 50, 100, 200 and 500 ms. In the later stages of the experiment when photographs were being taken, C_1 was increased to $0.2 \mu\text{f}$, to give a

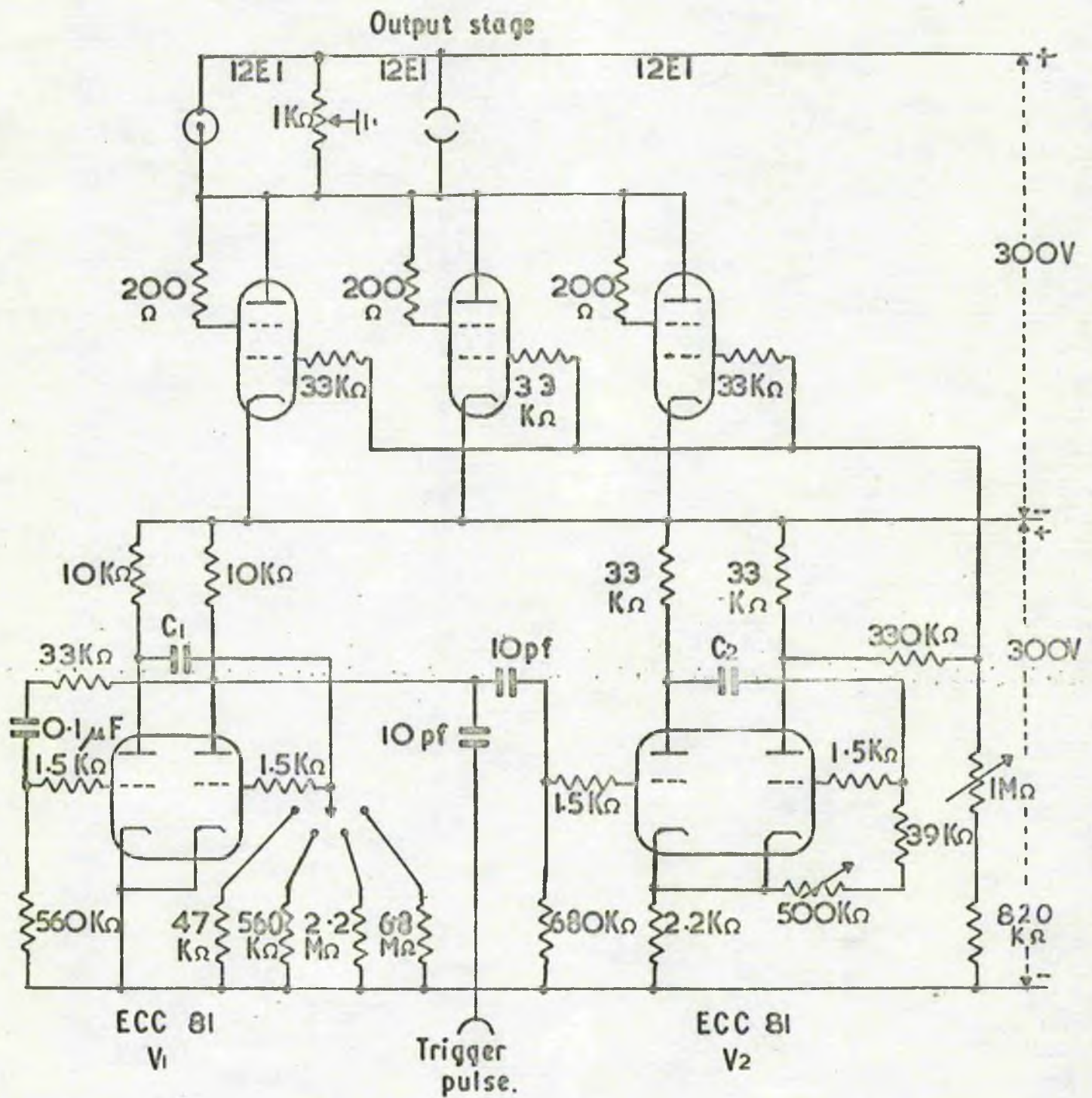


FIG. 3.5 THE PULSE GENERATOR.

minimum repetition rate of about 1 pulse/second.

The pulse length was determined by the time constant RC_2 . In the early experiments R was 39 Kohm plus 2 Mohm variable and C_2 was 12 kpf, giving a pulse length variable from 0.6 ms to 20 ms, though the longest pulses used were 2.5 ms. Later R was altered to 47 Kohm plus 500 Kohm variable, and C_2 to 3.3 kpf, to give a pulse length variable from 150 μ s to 1.5 ms.

Near the λ point pulses of ~ 1 watt/cm² were required to generate useful second sound signals. The heater had a resistance of 100 ohms and an area of 1.95 sq.cms., which meant developing a 14 volt, 140 ma pulse. At this high current, the H.T. voltage tended to fall off during the pulse, causing the output stage anode voltage to rise, and the pulse to lose its flat top. If the output stage was run off the same power supply as the rest of the circuit the voltage at the second anode of the monostable multivibrator also rose, causing a fall in voltage at the second anode, a fall in voltage at the output grids and a further rise at the output anodes. This effect is avoided by using two power supplies, and, by making the positive rail of one the negative rail of the other, a convenient large negative voltage is obtained to provide bias for the output

grids. This is such that the output valves are cut off, except when a pulse arrives. The pulse height is then controlled by varying the bias conditions. In these circumstances it is convenient to d.c. couple the output of the monostable multivibrator to the output grids.

Because of its low resistance, and the long pulses used, the heater was also d.c. coupled to the output. A 500 ohm pot with an earthed centre tap placed in parallel enabled the earth point of the heater to be varied to give minimum heater-thermometer coupling. In practice it was found that this was in any case small, and, if the heater earth was not the same as the chassis earth, there was a rather large amount of 50c/s pick up on the signal.

Apart from the heater, the pulse circuit provides two other outputs. One, in parallel with the heater, is used to measure the input pulse heights on a second oscilloscope. The other, from the output of the free running multivibrator, is used to trigger the main oscilloscope.

CHAPTER FOUR

THE EXPERIENTS

'But, Mousie, thou art no thy lane
In proving foresight may be vain :
The best laid schemes o' mice an' men
Gang aft a-gley,
An' lee'e us nought but grief an' pain,
For promised joy.'

Robert Burns.

CHAPTER 4

THE EXPERIMENTS

4.1 General remarks on experimental procedure.

The basic experiment is to measure either the Q of a resonator closed at one end by the free liquid surface, or to measure the reflection coefficient from it. In practice such measurements by themselves are too low, because of imperfect reflection from the heater end and losses in the tube due to attenuation. In addition to the free surface experiments therefore, it is necessary to perform dummy experiments with the tube closed at both ends and totally immersed in liquid to correct for these losses.

The free surface experiment will also give too low a result if the free surface is not perpendicular to the axis of the tube i.e. if the tube is not vertical. Using the plumb line described in Chapter 4 the tube could be aligned to within 0.5° of the vertical and this was done for all the resonance experiments and the early pulse experiments. However, the sound frequencies used in resonance experiments were between 140 and 1150 c/s and the pulse lengths used were between $400 \mu\text{s}$ and 2.5 ms. This corresponds to a wavelength range from 1.75 to 14 cm for the resonance experiments, and for the pulse experiments,

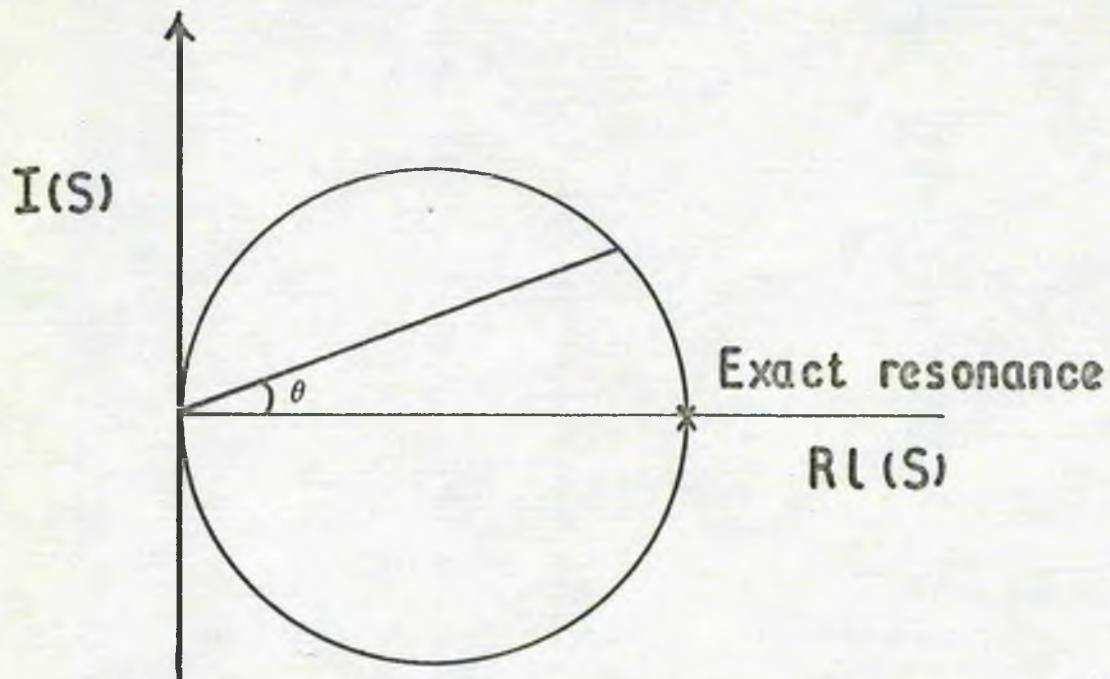
the wavelength range of the principal Fourier components of the pulses was from 1.6 to 5 cm. A misalignment of 0.5° is equivalent to a 0.1 mm difference in the second sound path between opposite sides of a 1 cm diameter tube, and so this degree of misalignment is quite unimportant for the range of frequencies used. In view of this it was decided in the later pulse experiments (including those discussed in Chapters 5 and 6) to dispense with the plumb line, and adjust the tube by eye. This could be done to within 5° , giving a length difference of 1 mm, which is still much less than the shortest wavelength used. As a check, the risetime of the first pulse reflected from the free surface was measured, first with the tube aligned with the plumb line, then at an angle $\approx 10^\circ$ from the vertical, and no significant difference was observed.

A check was also made that the amplitudes of the observed pulses were reasonable. For instance, at 1.43°K , with a 10v, 1.3 ms input pulse and an amplifier gain of 30db the observed signal was 2.4 volts. The heater area was 1.95 sq. cm. and its resistance 100 ohms, and at this temperature β , the characteristic impedance of second sound, is 3.98×10^{-3} deg cm² watt⁻¹, and so the expected temperature amplitude is 2.04 mdeg. The thermometer sensitivity was

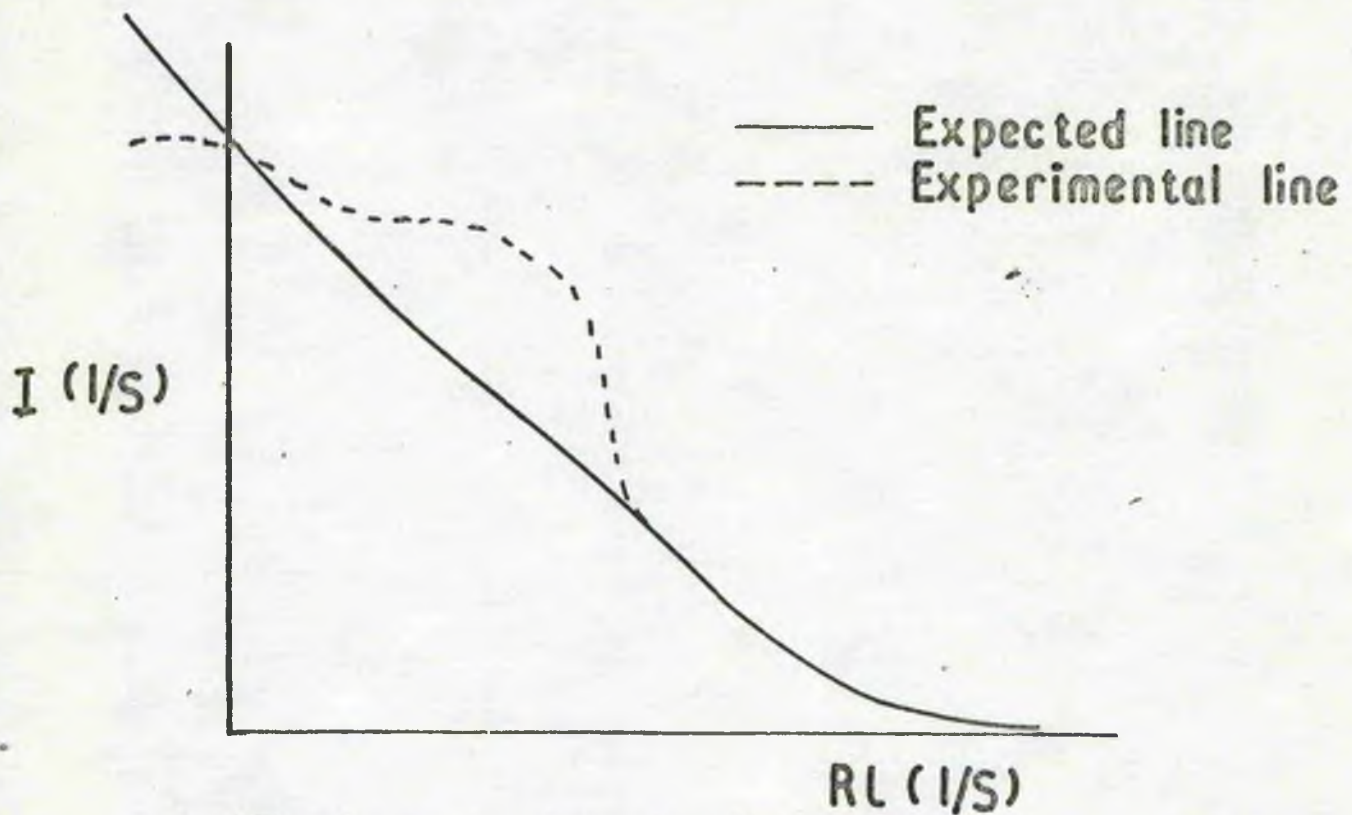
200 ohms/deg, and the thermometer current was 1 ma, so the expected signal at the thermometer is $410\mu\text{v}$, or 4.1 volts on the oscilloscope. This is reasonable agreement, since there are a variety of reasons for expecting a smaller signal than 4.1v. For example, not all the power is used to generate second sound - some is lost in the heater leads. The amplifier specification allows an error of $\pm 1\text{db}$ in the gain. And the thermometer does not respond fully to a 1.3 ms pulse (see 4.4).

4.2 Resonance experiments.

We can regard the two outputs P,Q, of a resonance experiment as the real and imaginary parts of the signal, S. It can be shown that the Argand plot of $S = P + iQ$ is, sufficiently near resonance, a circle passing through the origin (figure 4.1(a)). If we can determine the point on the circle corresponding to exact resonance, then the phase angle of any other point is the angle subtended by that point and the exact resonance point at the origin. If we also know the helium level readings corresponding to these two points, we can determine the phase angle in terms of λ , and from these two relations determine Q.



(a) Argand plot of S



(b) Argand plot of $1/S$.

Figure 4.1 Argand Plots of S and $1/S$.

In practice there are two modifications to this procedure. (a) the phase angle for all points to which there corresponds a level reading is plotted against level reading, and the slope is measured. This gives Q without requiring the level reading at exact resonance. (b) It is much better to determine the phase angle from the Argand plot of $1/S$, which is a straight line, close to resonance.

The results obtained in free surface runs gave Argand plots of $1/S$ which were far from the expected straight lines (figure 4.1(b)). The theory predicts a straight line parallel to the $Re(1/S)$ axis, and the observed rotation represents a phase shift occurring between the heater and the phase sensitive detector inputs, possibly due to the thermal capacity of the heater and/or thermometer.

The results obtained in closed tube runs gave Argand plots of $1/S$ which were straight lines near resonance. From them values of the phase angle θ were obtained corresponding to known level readings, L , and Q was obtained from the slope of a plot of L versus $\tan \theta$. This graph was not the expected straight line, but was such that Q was a monotonic function of θ . It was suspected that this was because the oscillator frequency stability was not good enough.

At this stage it was decided to abandon the resonance experiments and use the pulse method. The advantage is that the analysis is much simpler, and it is consequently much easier to detect the causes of unexpected results such as those described above. The disadvantage is that the quantity measured in a pulse experiment is R_L , rather than X_L in a resonance experiment, and R_L is much less sensitive than X_L to changes in α , or, for that matter, to the theory used to determine it.

4.3 The observed pulse shapes

The first pulse experiments used the wire thermometer placed across the bottom end of the tube. A typical photograph from an open tube experiment is shown in figure 4.2(a). The pulse shape changed as the pulse progressed, and, at the same time, the base line was noticeably distorted. A similar effect was observed in closed tube experiments, e.g. figure 4.2 (b).

It was at first thought that the change of pulse shape was caused by the wire thermometer across the end of the tube. It was therefore replaced by the second heater thermometer arrangement described in Chapter 3, with both heater and thermometer on a glass

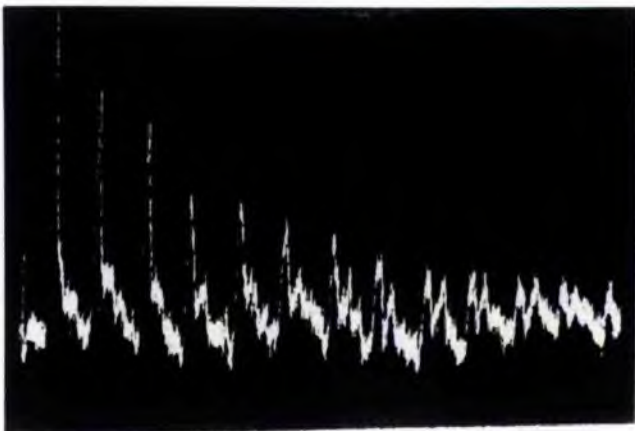
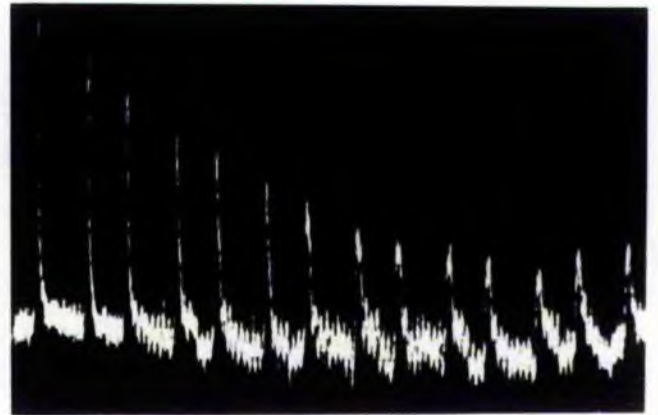
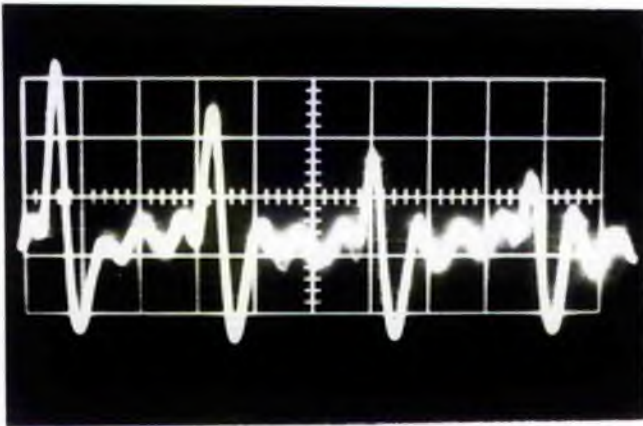
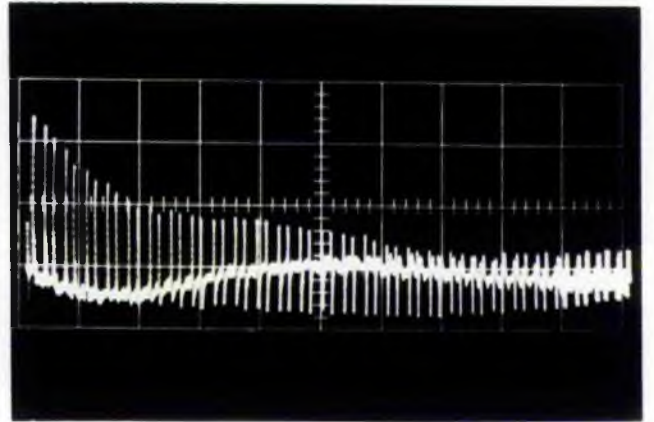
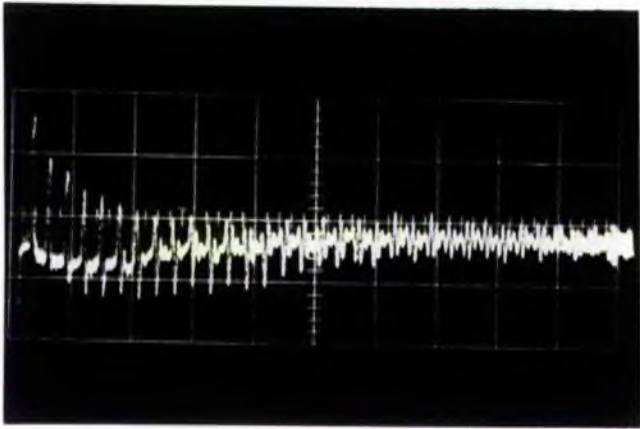


plate across the end of the tube. The pulses still changed their shape as they progressed, but, in addition, the base line became enormously distorted. The latter effect disappeared when the thermometer current was switched off, and was ascribed to thermal conduction from the heater to the thermometer through the glass backing.

The third thermometer arrangement, where the thermometer is placed on the tube wall about 3 cm from the bottom end, was then tried with essentially the same results as the wire thermometer. A detailed investigation showed that as the pulse progressed it developed the shape shown in figure 4.2 (c). Successive reflections made the top part smaller and the bottom larger, until the top part disappeared completely and the pulse appeared to have turned upside down. We can define the pulse number N at which the top and bottom parts have equal amplitude, and use N as a measure of how badly distorted the pulses are. The dependence of N on thermometer current, input pulse height, temperature, pulse length and height of liquid in the tube was investigated. N was found to be independent of thermometer current. N increased with pulse length, until for 1.9 ms pulses no change of pulse shape was detectable. N was also found to

increase with the height of the liquid in the tube, and no change of shape was observed with the tube full. N varied with input pulse size and temperature in such a way as to suggest that N/θ was constant, where θ is the second sound amplitude, proportional to $(\text{second sound impedance}) \times (\text{input pulse height})^2$. Finally, N seemed to be greater in dummy experiments than in closed tube experiments.

At this stage it was decided to work with long pulses (i.e. about 2 ms). All the work so far described had been done with a 7 cm propagation tube with the thermometer situated 3 cm from the bottom end. With this arrangement the time between the end of one pulse and the beginning of the next was only 1 ms for reflections from the bottom of the tube and 2 ms for those from the top and so extension tubes were made to fit on both ends. With this arrangement it was found that even short pulses (i.e. 600 μ s) were propagated without change of shape in closed tube experiments (e.g. figure 4.2(d)). The explanation seems to be connected with the fact that although the wire thermometer had been removed from the original tube, the recesses used to locate it had not. It is therefore supposed that part of the second sound wave approaching the heater saw the two recesses, connected to the helium bath outside the tube, as an open end and was reflected

with a phase change of π , i.e. upside down. The rest, of course, was reflected normally. When an extension was used, however, the recesses were isolated from the bath, and the effect disappeared. The effect reappeared in a later run when the top end of the tube jammed and came off as the tube was lowered, but disappeared as the tube was raised and the top reseated itself.

Cleaning up the tube geometry in this way did not affect the open tube experiments, where a progressive change of pulse shape was still observed. This was thought to be due to the first sound pulses in the vapour (which were generated when the second sound pulses were reflected from the surface) being reflected from the open end of the tube (with a pulse change of π), travelling back down, and generating second sound pulses in the liquid when they struck the surface. A cotton wool plug placed in the top of the propagation tube completely removed the progressive change of shape observed without it (see figure 4.2(e)). A careful examination of the photographs showed that pulses generated in this way were still present, though much smaller and the right way up now. Such pulses can be seen after the 4th and subsequent pulses in figure 4.2(e). A fuller discussion of the

coupling between first sound in the vapour and second sound in the liquid is given in Chapter 6.

The base line distortion mentioned in the last paragraph (figure 4.2(a)) increased with increasing pulse height and pulse length. It was very sensitive to the low frequency characteristics of the amplifier system and to give a straight base line the D.C. amplifier system was used.

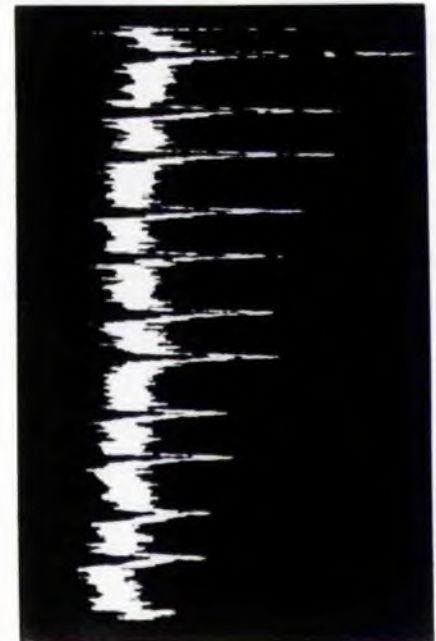
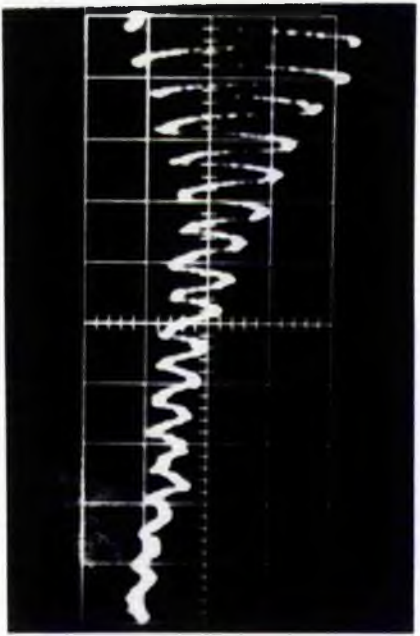
4.4 The Thermometer Response Times

Figure 4.2 (f) shows the first received pulse for a 2 ms input pulse, using the tube wall thermometer. The input pulse had a risetime of about 150 μ s, and the transit time of the leading edge across the thermometer was about 100 μ s. The long observed risetime may be due to poor thermal response of either the heater or the thermometer. Both the heater and thermometer were in good thermal contact with their backings, which were rather more substantial than have normally been used in previous second sound work. The tube wall was 2 mm thick and the conducting glass plate was 4 mm thick.

The risetime of pulses observed with the carbon wire thermometer was about 800 μ sec, and it seems possible that most of this was due

to the thermal capacity of the heater. Whether this is true or not, the thermal capacity of the tube wall thermometer was clearly responsible for the much larger risetime observed with it.

The propagation tubes used were too short to resolve pulses which were sufficiently long for the thermometer to respond fully to them. Figure 4.3(a) shows the effect produced, where pulses become piled on top of the tails of the preceding ones. It would have been possible, of course, to use a much longer tube, but this was not done for two reasons. Firstly, as we shall see in Chapter 5, it is advantageous if the tube used in dummy runs is twice as long as that used for free surface runs. This would have meant a dummy tube 20 to 30 cm long, and required considerable modification to the apparatus at a late stage in the project. Secondly, long pulses aggravated the base line distortion, and a longer tube, implying longer transit times and more low frequency bandwidth to detect a given number of pulses, might have made matters even worse. Short pulses (400 μ s) were therefore used for all the results discussed in Chapters 5 and 6. (The signal so obtained was, of course, only about half the height of a fully developed pulse). It is necessary to check that the observed pulse



amplitudes are linearly dependant on the input heat flow, i.e. on (input pulse height)². This was done at two temperatures, 1.3°K and 1.0°K. Further, the observed pulse was cut off on its leading edge at a point where it was still rising fairly fast, but had the exponential tail of the fully developed pulse. Consequently the pulses seemed to have faster risetimes than fall times, an effect clearly seen in figure 4.2(e).

Finally, it should be mentioned that the hum level varied widely from run to run for no very obvious reason. Figure 4.3(b), for example, was taken under essentially similar conditions to 4.3(c) but is clearly much less reliable, merely because of increased hum.

CHAPTER FIVE

THE REFLECTION COEFFICIENT MEASUREMENTS

'There are three kinds of lies; lies, damned lies, and statistics'

Mark Twain

CHAPTER 5

THE REFLECTION COEFFICIENT MEASUREMENTS

5.1 Analysis Of the Photographs

Figure 4.2(e) shows a typical photograph from an open tube experiment using a 400 μ s pulse. To analyse such a photograph it is necessary to consider the behaviour of a pulse when the reflection coefficients at either end are different. Let H_1 be the height of the first pulse, i.e. the pulse as it passes the thermometer going up for the first time. Then the height of the second pulse, H_2 is given by

$$H_2 = H_1 R \exp(-2\alpha l_2) = aH_1$$

where α is the attenuation coefficient, R is the reflection coefficient from the free surface, and l_2 is the distance between the thermometer and the free surface (see figure 5.1). Then

$$H_3 = H_2 R_0 \exp(-2\alpha l_1) = aa_1 H_1$$

where R_0 is the reflection coefficient from the closed end.

$$H_4 = a^2 a_1 H_1$$

$$H_5 = a^2 a_1^2 H_1$$

and $H_n = H_1 (aa_1)^{(n-1)/2}$ when n is odd

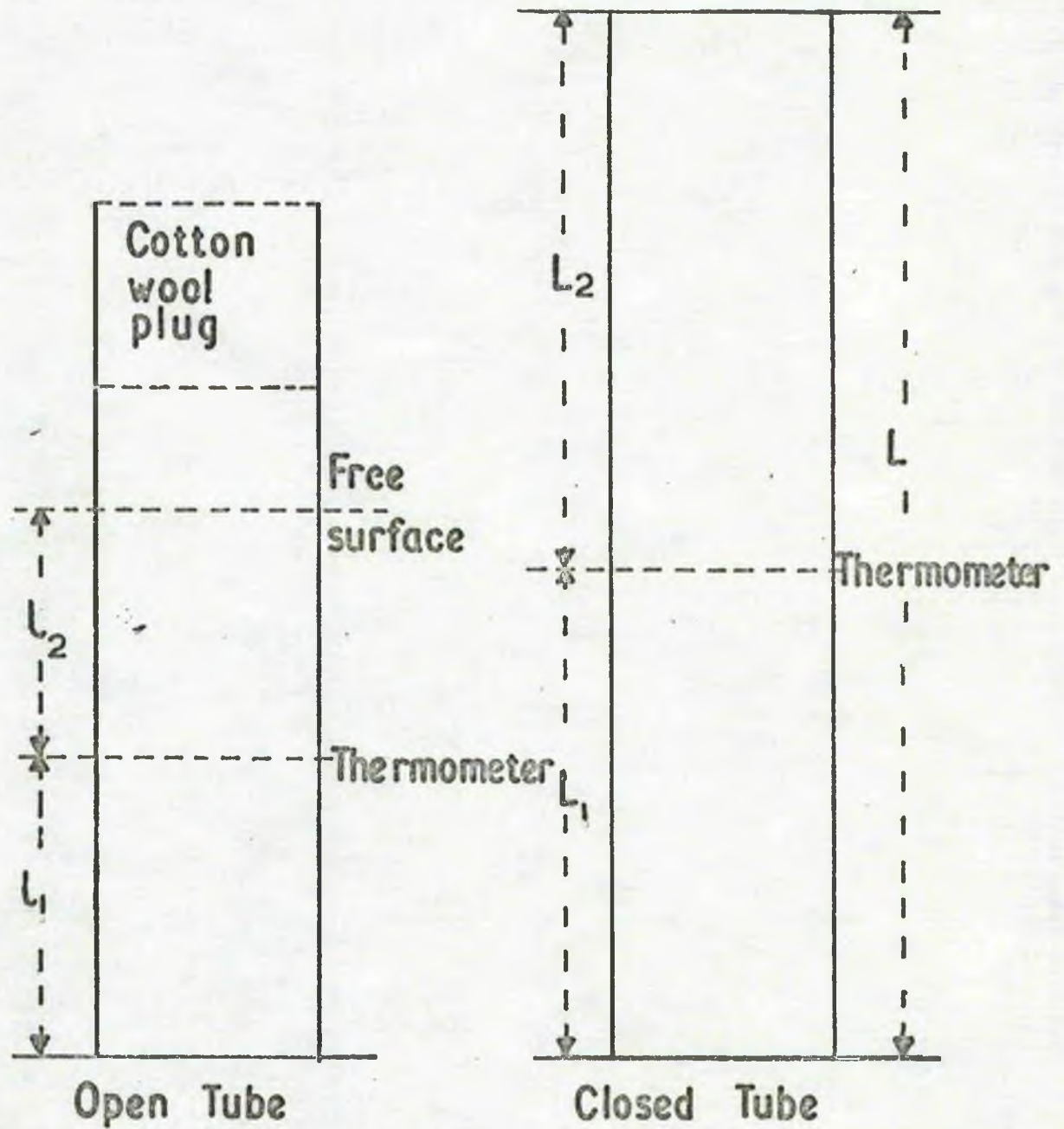


Fig. 5.1 THE PROPOGATION TUBES. (schematic)

$$= H_1 a_1^{n/2} a_2^{n/2-1} \text{ when } n \text{ is even}$$

$$\text{Thus } \log H_n = \frac{1}{2}n \log a a_1 - \frac{1}{2} \log a a_1 + \log H_1 \text{ for } n \text{ odd}$$

$$= \frac{1}{2}n \log a a_1 - \log a_1 + \log H_1 \text{ for } n \text{ even}$$

So a plot of H_n against n should fall on two parallel straight lines of slope $\frac{1}{2} \log a a_1$. Figure 5.2 shows a typical graph. The intercept of the line through the odd points ('the odd line') is $\frac{1}{2} \log (H_1^2/a a_1)$ and the intercept of the line through the even points ('the even line') is $\log(H_1/a_1)$. Then if we express the slope of the lines as a measured reflection coefficient R_F , we have

$$R_F = (RR_0)^{\frac{1}{2}} \exp -\alpha(l_1+l_2)$$

The same analysis for a closed tube experiment gives for the measured reflection coefficient R_C

$$R_C = R_0 \exp -\alpha(L_1+L_2) = R_0 \exp -\alpha L \quad 5.1.$$

whence

$$R = (R_F^2/R_0) \exp -2\alpha(\frac{1}{2}L - l_1 - l_2) \quad 5.2$$

If L and l_1 are suitably chosen, l_2 can be adjusted so that

$$l_2 = \frac{1}{2}L - l_1 = l_0$$

Alternatively R_F can be measured as a function of l_2 , and $R_F(l_0)$ found by plotting a graph of $\log R_F$ versus l_2 . In either case

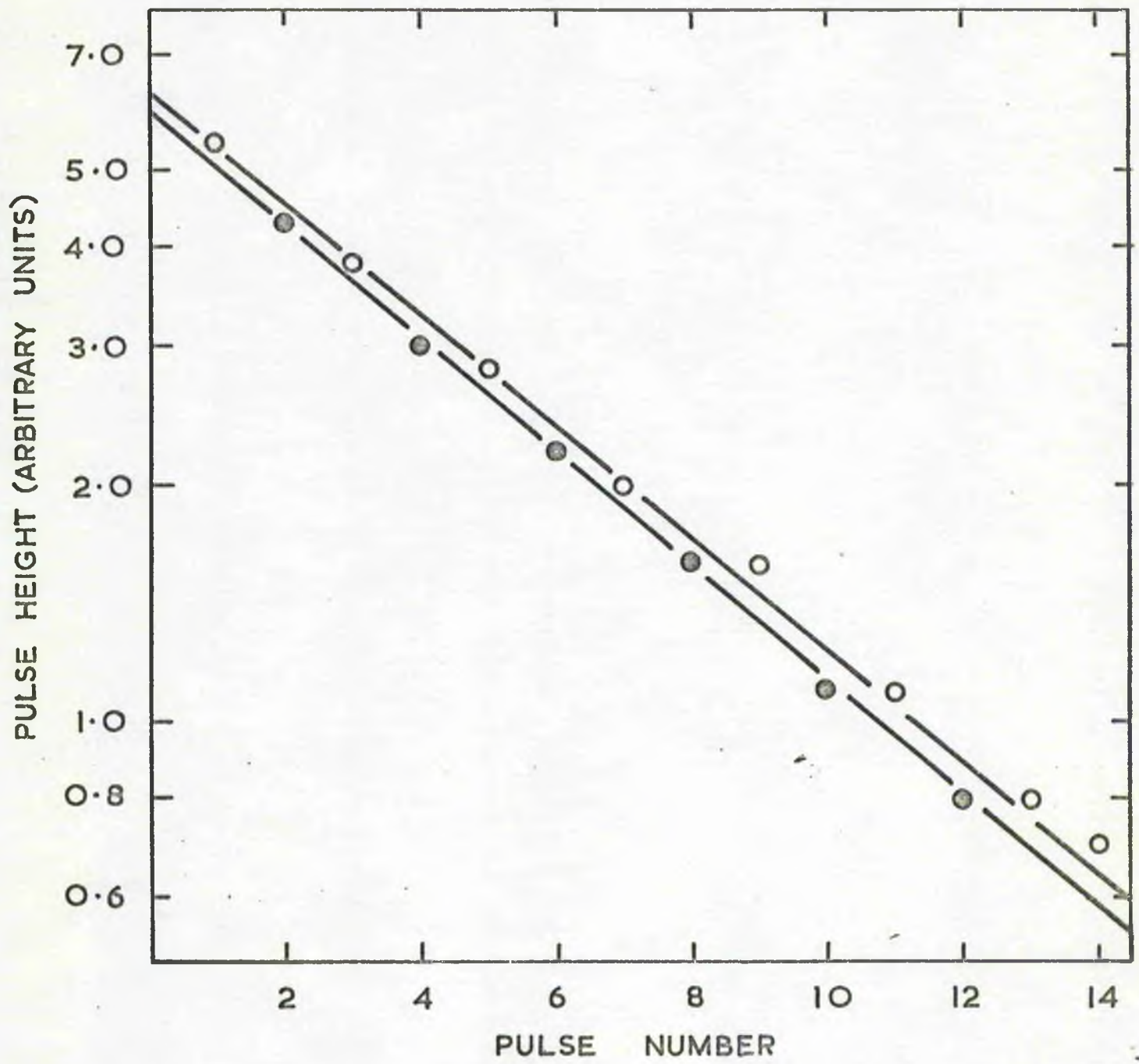


Figure 5.2 A Typical Plot of Log H vs n.

equation 5.2 can then be used to find R .

We note also that the ratio of the intercepts of the odd and even lines gives $(R_o/R)^{\frac{1}{2}} \exp - \alpha(\ell_1 - \ell_2)$ for an open tube experiment and $\exp - \alpha(L_1 - L_2)$ for a closed tube experiment.

We can therefore measure a top reflection coefficient R_T and a bottom reflection coefficient R_B , given by

$$\begin{aligned} R_T &= R \exp(-2\alpha\ell_2) \\ R_B &= R_o \exp(-2\alpha\ell_1) \end{aligned} \quad 5.3$$

for an open tube experiment, and

$$\begin{aligned} R_T &= R_o \exp(-2\alpha L_2) \\ R_B &= R_o \exp(-2\alpha L_1) \end{aligned} \quad 5.4$$

for a closed tube experiment.

5.2 Experimental procedure

In practice ℓ_o was rather small, and pulses tended to pile up. R_p was therefore measured at each temperature for three values of ℓ_2 , from about 1 cm to 3 cm greater than ℓ_o . The exact values of ℓ_2 were obtained by measuring the time intervals between pulses, using the calibrated time delay, and assuming the velocity of second sound. As a check, the total length L of the closed tube

was determined in this way, and found to be 13.62 ± 0.15 cm, compared with a length of 13.736 cm measured at room temperature with a travelling microscope.

At each temperature and level, a group of from 3 to 6 photographs were taken for each of three input powers. In a separate run, another group of photographs was taken for the same temperature and input powers, with the tube closed and totally immersed. The heights of successive pulses were then measured from the photographs under a magnifying glass, using a rule graduated in 0.02 inch divisions. The error in determining the pulse height (about half a division) is one of definition rather than of scale reading, so a higher magnification and a finer scale would not have improved the accuracy.

Altogether about 600 photographs were taken, though about 100 were rejected as unusable. Some frames were double exposed, a very few were too under exposed, and some at the end of films were fogged or partially fogged. But the most frequent cause of rejection was low frequency noise, which caused the trace to run too high or too low across the screen.

The two amplifiers used were tested to check that the output varied linearly with input over the input range used. The oscilloscope

optics were checked by measuring the height of a vertical line at various positions across the screen. Finally, the camera was tested for distortion by measuring the oscilloscope graticule from the photographs.

5.3 Analysis of results-

The pulse height measurements were fitted to a straight line of the form $\log H_n = a - bn$ using a computer programme. Each point was assigned a weight proportional to the inverse square of the error associated with it. Since the error in H is constant the error in $\log H$ is $\propto 1/H$, and the weights are $\propto H^2$. In practice the programme did rather more than this. It fitted one line through all the points from a given photograph. It also fitted two separate lines through the odd and even points. It calculated the standard errors of the slopes and intercepts so obtained and the corresponding reflection coefficients and standard errors. It also calculated the ratio of the intercepts of the odd and even lines, and the corresponding reflection coefficients R_T and R_B given by equations 5.3 and 5.4.

In addition, for each group of photographs, it calculated the weighted mean and two standard errors of (a) the slopes obtained by fitting one straight line through all the data, (b) the slopes

of the even lines and the slopes of the odd lines, and (c) the slopes corresponding to the R_T 's, and (d) the slopes corresponding to the R_B 's. It then calculated the reflection coefficient corresponding to these mean slopes.

The two standard errors are

$$\beta_e = \left[\frac{\sum (b_i - \bar{b})^2 / \alpha_i^2}{(n-1) \sum 1/\alpha_i^2} \right]^{1/2}$$

$$\text{and } \beta_1 = (1 / \sum 1/\alpha_i^2)^{1/2}$$

where the b_i are the slopes, \bar{b} their mean, α_i their standard errors and n the number of them. If the b_i 's are normally distributed about \bar{b} then $Z = \beta_e / \beta_1 = 1$, with standard error

$$\Delta Z = 1 / [2(n-1)]^{1/2}$$

(see, e.g. Topping, 1962). We note that

$$Z = \beta_e / \beta_1 = \left[\frac{\sum (b_i - \bar{b})^2 / \alpha_i^2}{(n-1)} \right]^{1/2} \quad 5.5$$

and that if we have a large number of values of Z we would expect them to be normally distributed about 1 with a standard deviation of ΔZ . Throughout this chapter the standard error of a weighted mean is taken to be the larger of β_e and β_1 .

No straight line was fitted to less than four points. This means that there must have been eight points per line before the computer fitted odd and even lines, and it either fitted both or it fitted neither. A fuller description of the programme is given in Appendix C.

5.4 Open tube results

Table 5.1 shows all the results discussed in this chapter. The first column gives the temperature, the second gives the size of the input pulse, and the others give the reflection coefficients measured under these conditions. The third, fourth and fifth columns give the open tube reflection coefficients R_p measured at three values of l_s , approximately equal to $l_0 + 3$ cm, $l_0 + 2$ cm and $l_0 + 1$ cm, respectively. (The exact values of l_s are not displayed, since they seem to be of little significance). Each entry represents a weighted mean of results from between 2 and 6 photographs. Where values of R_p have been obtained at the same temperature in different runs, they have been displayed separately.

Column 6 is the weighted mean of all the individual measurements of R_p at that temperature and input pulse size (which is not

necessarily the same as the mean of the entries in columns 3 to 5). Column 7, R_c , is the closed tube reflection coefficient measured in a separate run at the same temperature and input pulse size. Where results have been obtained in separate runs at temperatures differing by more than 10m deg, the results have again been displayed separately; in these cases the entries under R_c at the temperature at which the R_f 's were measured have been obtained by graphical interpolation of figure 5.3. Column 8 is calculated from the corresponding entries in columns 6 and 7 ($R = R_f^2/R_c$). Finally column 9 gives the weighted mean of all the entries in column 8 for that temperature.

Although up to 15 echoes could be observed in open tube experiments, measurements of pulse height became increasingly unreliable for the later pulses as the error in measurement became an increasing fraction of the pulse height. This is the more important because the error in $\log H$ is \propto to $1/H$. Consequently the inclusion of all of the later pulses provides little extra information and a good deal more uncertainty. And as we have seen, the cotton wool did not completely suppress the first sound pulses from the vapour, and this would produce a systematic error in height measurements

TABLE 5.1

TEMP. °K	INPUT VOLTS	R _f			AVERAGE R _f	R _C	R	AVERAGE R
		$l_2 \approx l_0 + 3\text{cm}$	$l_2 \approx l_0 + 2\text{cm}$	$l_2 \approx l_0 + 1\text{cm}$				
0.99	3	82.58 ± 0.57	79.81 ± 0.81	81.26 ± 0.65	80.77 ± 0.44	86.87 ± 0.50	75.11 ± 1.02	77.10 ± 1.21
	4	80.64 ± 0.42	81.28 ± 0.36	81.43 ± 0.33	82.00 ± 0.76*	86.61 ± 0.45	77.64 ± 0.99	
	5	80.13 ± 0.49	80.30 ± 0.22	80.61 ± 0.11	81.05 ± 0.50*	84.28 ± 1.09	77.96 ± 1.23	
1.11	4	81.85 ± 1.75	85.59 ± 1.30	85.63 ± 0.76	83.54 ± 0.85	91.23 ± 0.53	76.50 ± 1.77	77.77 ± 0.32
	5	82.75 ± 0.33	84.65 ± 0.40	84.27 ± 0.47	83.46 ± 0.28	89.18 ± 0.55	78.11 ± 0.79	
	6	83.34 ± 0.44	82.84 ± 0.49	81.95 ± 0.41	82.77 ± 0.27	88.19 ± 0.59	77.69 ± 0.80	
1.14	5					90.43 ± 0.42		
	6					89.13 ± 0.78		
	8					87.97 ± 0.87		
1.20	5	86.73 ± 1.00		87.20 ± 0.12	87.13 ± 0.31	91.7 ± 0.5**	82.75 ± 0.80	78.93 ± 1.44
	6	84.42 ± 0.76	82.99 ± 0.77	85.23 ± 0.28	85.12 ± 0.21	91.55 ± 0.5**	79.14 ± 0.65	
	8	82.90 ± 0.34	82.17 ± 0.22	83.75 ± 0.19	83.28 ± 0.19	90.8 ± 0.5**	76.37 ± 0.63	
1.30	6	86.26 ± 0.85	90.28 ± 0.71	82.95 ± 1.00	83.99 ± 0.72	92.87 ± 0.43	76.00 ± 1.50	83.71 ± 1.29
	8	88.50 ± 0.44	88.26 ± 0.88	88.73 ± 0.27	88.36 ± 0.08	93.62 ± 0.46	88.39 ± 0.49	
	10	89.42 ± 0.68	89.71 ± 0.17	88.54 ± 0.66	89.57 ± 0.18	93.73 ± 0.32	85.57 ± 0.48	

1.38	7	85.29 ± 0.44	85.56 ± 0.80	85.23 ± 0.35	85.32 ± 0.26	91.78 ± 0.39	79.29 ± 0.65	77.90 ± 0.54
	8	85.70 ± 0.68	84.79 ± 0.39	84.85 ± 0.44	84.90 ± 0.25	92.30 ± 0.41	78.09 ± 0.65	
	10	83.52 ± 0.52	84.00 ± 0.22	84.47 ± 0.18	84.18 ± 0.16	91.60 ± 0.20	77.36 ± 0.38	
1.45	8		86.44 ± 0.35		85.25 ± 0.24	94.30 ± 0.5**	77.07 ± 0.69	77.07 ± 0.69
	10		85.13 ± 0.32					
1.50	7	91.39 ± 0.64		92.49 ± 1.32	91.87 ± 0.62	94.61 ± 0.49	89.19 ± 1.33	87.50 ± 0.94
	8	89.78 ± 0.93		89.63 ± 1.24	89.72 ± 0.71	94.88 ± 0.51	84.84 ± 1.51	
	10	90.78 ± 0.64		91.08 ± 0.36	91.04 ± 0.25	94.59 ± 0.58	87.62 ± 0.77	
1.61	8	88.29 ± 0.89	84.44 ± 0.71	86.69 ± 0.87	86.34 ± 0.57	96.05 ± 0.59	77.61 ± 1.28	77.38 ± 0.86
	9	83.48 ± 1.11	88.59 ± 0.74	87.87 ± 0.67	86.81 ± 0.71	95.14 ± 0.33	79.21 ± 1.46	
	10	83.08 ± 0.55	86.10 ± 0.64	86.91 ± 0.81	85.05 ± 0.52	95.06 ± 0.35	76.17 ± 1.10	
1.74	9		87.30 ± 0.53	87.78 ± 0.54	87.51 ± 0.35	94.61 ± 0.92	80.93 ± 1.16	80.15 ± 1.17
	10		85.49 ± 0.59	86.41 ± 0.23	86.37 ± 0.18	94.81 ± 0.54	78.70 ± 0.65	
	12		87.42 ± 0.53	88.84 ± 0.48	88.30 ± 0.40	94.63 ± 0.35	82.41 ± 0.87	
1.74	9	87.28 ± 2.61			87.28 ± 2.61	94.61 ± 0.92	80.52 ± 5.3	85.79 ± 0.73
	10	90.00 ± 0.68			90.00 ± 0.68	94.81 ± 0.54	85.43 ± 1.46	
	12	90.38 ± 0.61			90.38 ± 0.61	94.63 ± 0.35	86.34 ± 1.27	
1.80	9	85.86 ± 0.60	88.36 ± 0.52	87.85 ± 1.03	87.25 ± 0.44	96.13 ± 0.58	79.18 ± 1.05	81.1 ± 0.96
	10	88.68 ± 0.55	88.95 ± 1.31	90.57 ± 1.20	89.16 ± 0.65	95.49 ± 0.60	83.28 ± 1.43	
	12	88.25 ± 0.19	87.08 ± 0.44	88.06 ± 0.97	88.02 ± 0.21	95.10 ± 0.67	81.47 ± 0.79	

TABLE 5.1 (continued)

TEMP. °K	INPUT VOLTS	R_F			AVERAGE R_F	R_C	R	AVERAGE R
		$\ell_2 \approx \ell_0 + 3\text{cm}$	$\ell_2 \approx \ell_0 + 2\text{cm}$	$\ell_2 \approx \ell_0 + 1\text{cm}$				
1.93	10	94.23 ± 2.55	88.76 ± 0.46	91.23 ± 0.72	89.72 ± 0.52	96.00 ± 0.85	83.85 ± 1.35	86.52 ± 1.94
	12	88.88 ± 0.77	89.59 ± 1.17	91.75 ± 1.35	89.23 ± 0.55	94.01 ± 0.57	84.70 ± 1.24	
	15	89.80 ± 1.33	88.55 ± 2.06	92.70 ± 0.14	92.30 ± 0.49	94.79 ± 0.56	89.89 ± 1.13	
2.02	10	89.32 ± 1.39	86.75 ± 2.72	85.06 ± 1.30	86.20 ± 1.00	92.77 ± 1.25	80.09 ± 2.36	83.24 ± 1.64
	12	87.17 ± 0.92	87.65 ± 0.87	92.43 ± 0.71	87.90 ± 0.56	91.98 ± 1.07	84.01 ± 1.55	
	15			90.98 ± 2.45	90.98 ± 2.45	92.45 ± 0.62	89.56 ± 5.56	
2.12	10	89.88 ± 2.42	89.52 ± 0.66	86.24 ± 1.18	89.07 ± 0.63	92.14 ± 1.77	86.08 ± 2.17	78.48 ± 3.84
	12	84.11 ± 0.92	86.66 ± 1.05	84.38 ± 0.58	85.66 ± 0.52	91.67 ± 0.28	80.05 ± 1.08	
	15	77.27 ± 1.03	83.07 ± 0.67	84.88 ± 1.42	78.20 ± 0.73	88.49 ± 0.96	69.10 ± 1.75	

* Extrapolated to ℓ_0

** Interpolated from Fig. 5.3

which might be significant, and which would be larger for the later pulses. So for the open tube experiments only the first 8 pulse measurements on each photograph have been used in working out the results.

The values of R_T and R_B (equations 5.3) calculated by fitting two straight lines differed significantly from each other, and this implies that the two lines had different intercepts and that the points did in fact fall on two separate lines. This interpretation is confirmed by comparing the standard errors of the values of R_p obtained by fitting two lines to the data with the errors obtained by fitting only one. For any given photograph the former error was about the same or slightly smaller than the latter, while an increase by a factor of $\sqrt{2}$ would have been expected (because the number of points per line had been halved) if the points had only been distributed about one line. The open tube results (Table 5.1) have therefore been calculated by fitting two straight lines to the first eight points.

An analysis has been made of the values of Z (equation 5.5) and the way in which they were distributed. This analysis is of limited value, because of the large sampling errors involved in fitting

a line to only four points, and averaging the slopes of only three to six such lines. For example, the effect of reducing the number of points fitted to a line, either by reducing the total number of points, or by fitting two lines instead of one, is almost always to increase the mean of the Z distribution. The only exception was when one line is fitted and the total number of points is reduced from 16 ($Z=1.0 \pm 0.1$) to 8 ($\bar{Z} = 0.7 \pm 0.1$). The latter result, implying that the standard errors were too large for the given scatter of slopes about the mean slope, is expected for a one line fit. The higher value of Z when 16 points were fitted is presumably due to higher scatter resulting from the large errors in the extra points.

In these circumstances, it is not clear what weight should be attached to the fact that \bar{Z} was significantly greater than 1 for the two line distribution, being 1.7 ± 0.2 when 16 points were fitted and 2.5 ± 0.2 when 8 points were fitted. The distributions were approximately normal, but the standard deviations were rather large, $(1.5 \pm 0.1) \Delta Z$ in both cases. It ought to be remarked that the final values of R (figure 5.4) are relatively insensitive to the

number of points used and the number of lines fitted. The variation between extreme cases moves the points by about 1%, and mostly but not always in the same direction. This is scarcely significant in view of the standard errors in the values of R_p , and we therefore suppose that the high values of \bar{Z} are mostly caused by sampling fluctuations, and that any systematic errors present do not make the true error much larger than the standard errors of table 5.1 and figure 5.4.

Table 5.1 shows there is no dependence of R_p on l_2 , except at 1°K where it has been corrected for. The mean slope for all photographs taken at a given temperature and input power has been calculated ab initio from the individual slopes in each of three groups, and this value (Average R_p in the table) has been taken to be $R_p(l_0)$. But there does seem to be a slight dependence of R_p on input power, which disappears when R_p^2/R_c is calculated.

5.5 Closed tube results

The reflection coefficients in closed tube experiments are much larger than in open tube runs, and consequently a larger number of pulses can be measured to the same degree of accuracy. And, of course, there are no systematic errors due to coupling with the vapour. Also, the values of R_T and R_B obtained by fitting two lines to the data

agree with R_c , indicating that the points fall on one line and not two. So the results have been calculated by fitting one straight line to the first 16 pulse height measurements from each photograph (see table 5.1 and figure 5.3). The Z distribution is close to the expected one - \bar{Z} is 1.2 ± 0.2 with a standard deviation of $(1.20 \pm 0.15)\Delta Z$, and the distribution is approximately normal. Once again it is not clear whether this means that the closed tube results are relatively free from systematic error compared with the open tube ones, or whether they are merely less liable to sampling errors.

If we suppose that $R_0 = 100\%$, we can use equation 5.1 to get a maximum estimate of the attenuation, α . Between 1.5°K and 1.9°K we get $\alpha = 0.0037 \text{ cm}^{-1}$, and at 1.0°K $\alpha = 0.017 \text{ cm}^{-1}$. Since $L_1 - L_0 = 1.7 \text{ cm}$, we would then expect R_T and R_B to differ from R_0 by ≈ 1.7 at 1°K . Both these figures are much smaller than the standard errors in R_T and R_B , and the difference is consequently not detected. Similarly, in an open tube experiment, the variation in R_F with L_2 is close to the limit of measurement. The expected difference between the largest and smallest values of $R_F(z_2)$ at 1.5°K is -0.66 , and at 1.0°K is -1.7 . At 1.5°K this value is comparable with the standard error, and accounts for the lack of any observed dependance of R_F

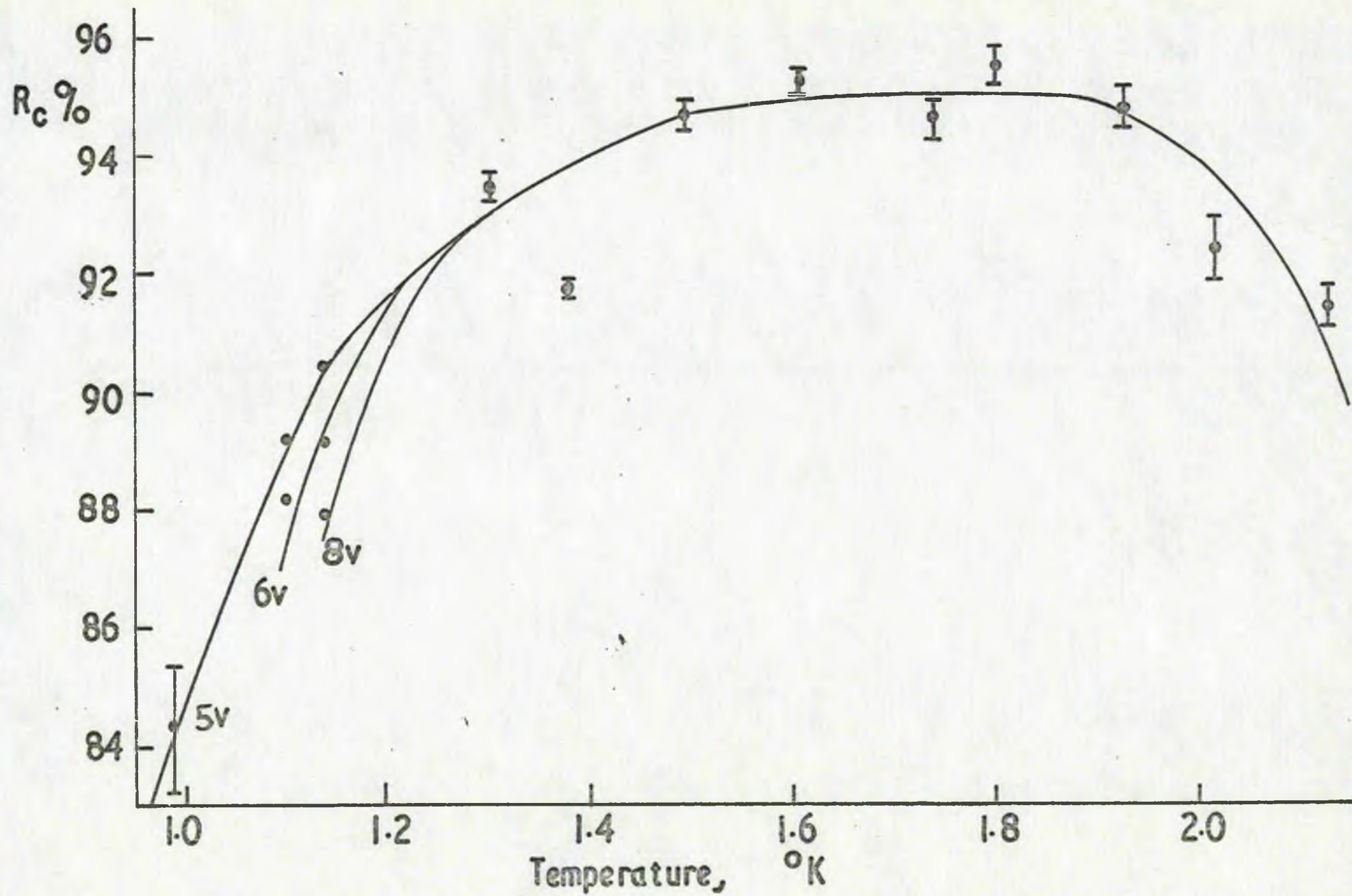


Figure 5.3 The Closed Tube Reflection Coefficient.

on ϵ_a . At 1.0°K , the observed variation is smaller than expected, though the errors in R_T do not rule out the possibility that the true variation is much larger. And, of course, the expected variation is a maximum one.

At the lowest temperatures, below 1.3°K , the attenuation becomes amplitude dependant, increasing with increasing input power, W . (Above 1.3°K the points shown in figure 5.3 are the averages of all the results obtained at that temperature. Below 1.3°K , some points have been omitted for the sake of clarity. All the data are given in table 5.1). This effect has been observed before by Atkins and Hart (1954), and Zinoveva (1956), and the present results are in qualitative agreement with theirs. Atkins and Hart found $da/dW = 1.3 \times 10^{-2} \text{cm}^{-1}/(\text{watts/cm}^2)$ at 1.18°K and 20 kc/s, Zinoveva found a value 10×10^{-2} at 1.27°K and 1 kc/s and the present results at 1.14°K give $da/dW = 1 \times 10^{-2}$. The results of Atkins and Hart suggest that $da/d\theta (= (1/\beta) da/dW)$ is not strongly temperature dependant and so da/dW is large only when β is large, i.e. at low temperatures. The range of input powers used in the present work is largest at low temperatures and these two points explain why the effect has only been observed below 1.3°K .

The attenuation coefficients deduced above are much larger than those measured in the bulk liquid (e.g. Atkins and Hart, 1954) but in this temperature and frequency region surface losses are much more important (Zinoveva, 1956). According to Khalatnikov (1952b), the surface attenuation α_s is given by

$$\alpha_s = \left(\rho_s / \rho \right) r u_w (\rho_n w \eta / 2)^{\frac{1}{2}} + (\beta / r) \left[(1/4K) + (2/\rho_0 C_0 \chi w)^{\frac{1}{2}} \right]^{-1} \quad 5.6$$

where ρ , ρ_s , ρ_n are the total, superfluid and normal densities of the liquid, r is the tube radius, w the angular frequency, η the liquid viscosity, β the characteristic impedance of second sound, and ρ_0 , C_0 and χ the density, specific heat and thermal conductivity of the walls of the propagation tube. The first term represents attenuation due to the viscous drag of the liquid at the tube walls. The second term represents losses due to the thermal conductivity of the tube walls, and depends on K , the Kapitza thermal boundary resistance between the tube walls and the helium. In our case, however, the second term is negligible compared with the viscous losses. (In the same paper Khalatnikov gives a theoretical expression for the reflection coefficient from the closed end

$$R_0 = 1 - 2r u_T$$

where α_T is the second term in equation 5.6, which gives a value of R_0 less than 0.01%.)

The measured attenuation is still rather larger than the surface attenuation calculated from equation 5.6, and it seems likely that the amplitude dependant attenuation is also important. The present work gives values of da/dW from 1.0°K to 1.14°K, and Atkins and Hart give values of $da/d\theta$ at 1.18°K, 1.3°K and 1.50°K. Using these to calculate the power dependant attenuation and combining this with the surface attenuation gives a total attenuation within 20% of the measured value below 1.5°K. (Table 5.2 shows the contributions to the total attenuation α_T from the bulk attenuation α_B , the surface attenuation α_s (viscous losses) and the power dependant attenuation α_w , together with the measured attenuation α_m .) Since the measured attenuation is greater than that calculated this is fairly reasonable agreement in view of the uncertainty in the power dependant attenuation, especially large at low temperatures. Above 1.5°K, however, the calculated attenuation (using Atkins and Hart's value of $da/d\theta$ at 1.5°K) steadily diverges from the experimental value, being ten times smaller at 2.12°K. The amplitude dependant attenuation is probably

TABLE 5.2

$T, ^\circ\text{K}$	α_B	α_S	α_W	α_T	α_e
1.0	2.4	10.7	1.6	14.7	12.4
1.2	0.2	4.3	1.7	6.2	6.4
1.4	0.0	2.1	1.9	4.0	4.6
1.6	0.0	1.2	0.9	2.1	3.8
1.8	0.0	0.7	0.6	1.3	3.6
2.0	0.0	0.4	0.6	1.0	5.0
2.1	0.0	0.4	0.6	1.0	6.9
2.15	0.1	0.2	3.3	3.6	7.3

Units of attenuation are $\text{cm}^{-1} \times 10^{-9}$.

A frequency of 1.25kc/s has been assumed in calculating α_B and α_S .

a consequence of second order terms in the hydrodynamical equations, but no detailed theory seems to have been worked out, nor do there seem to be any measurements of $da/d\theta$ other than those already mentioned. The amplitude dependant attenuation is therefore unknown above 1.5°K, though were it large enough to completely explain the experimental attenuation a dependance of R_p on input power should probably have been observed in this temperature range. In fact, the results at 2.12°K show a dependance on amplitude which is possibly not significant because of the rather large errors. But if this is regarded as a real effect, the amplitude attenuation so calculated gives a value for the theoretical attenuation about half the experimental one, a discrepancy which is almost completely explained by the error in determining $da/d\theta$.

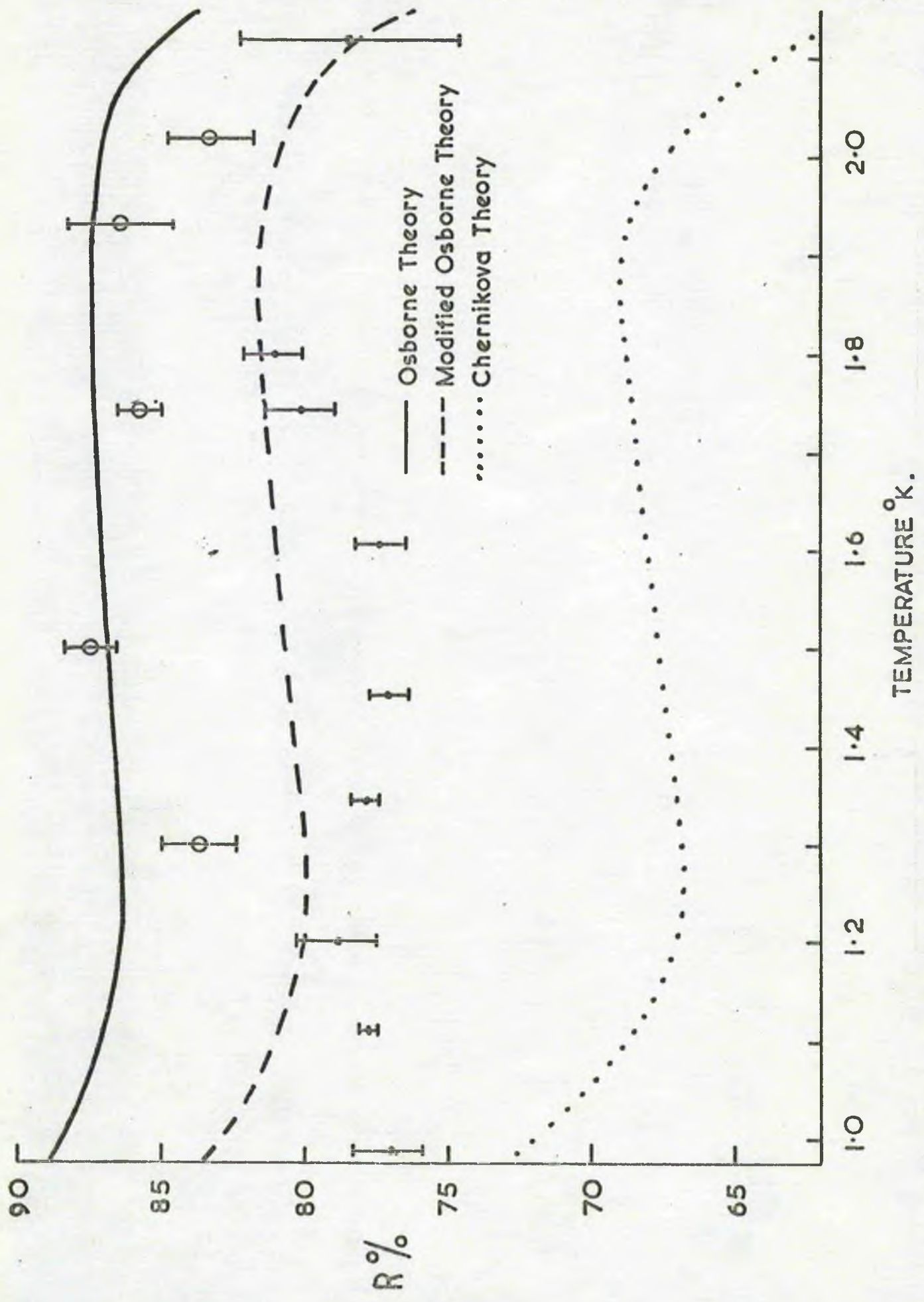
Finally we note that there exist two further possible surface loss mechanisms, namely the thermal conductivity and second viscosity of the liquid, which have not been treated theoretically, and for which no allowance has been made in the foregoing discussion.

5.6 The free surface reflection coefficient

Figure 5.4 shows the free surface reflection coefficient as a function of temperature, and Table 5.1 shows the data from which

the graph has been constructed. Also shown are the theoretical predictions of Osborne (both theories) and Chernikova.

These results were obtained in three open tube runs and two closed tube runs. During the first of the open tube runs the 50 cycle pick up level was much higher than in the other two, and the low pass filter was set at 3 kc/s, compared with 10 kc/s in the later runs. The results obtained in ^{this} these runs ^{is} are marked with a circle in figure 5.4, and it can be seen that they are systematically ^{these obtained in the other two open tube runs.} higher than ~~the other~~ results. A comparison of the photographs (e.g. figures 4.3(b) and 4.3(c)) suggests that the results from the later runs should be much more reliable. The reason for the discrepancy is probably connected with the fact the measured reflection coefficients are rather sensitive to the base line used in making pulse height measurements. In photographs like 4.3(c) the base line has been taken as the top of the noise level, and measurements of pulse heights have been made between there and the top of the pulse. An attempt has been made to follow the same procedure for the earlier photographs (figure 4.3(b)), but it is clearly much less satisfactory in these cases, where the base line is badly defined because of the lack of high frequency noise and distortion by mains



pick up. Typically, the measurements of the height of the first pulse were about 0.5 ins., the error in determining the base line was about 0.01 ins. for good photographs, and the base line thickness was about 0.06 ins. A systematic error of 0.01 ins. in determining the base line gives an error of 0.7 in R_f and 1.4 in R . So an error of 0.03 ins. in the base line would account for the observed difference between the two sets of results.

A poorly defined base line might also be expected to give a larger scatter in the results but this effect was partially eliminated while doing experiments by taking more photographs in each set in the first run.

An analysis of the Z distribution when the early results are included (they were not included in the results discussed in 5.4) confirms the impression that they should be largely discounted. Neither \bar{Z} nor S , the standard deviation, is much altered, but the distribution is much too broad to be normal.

The remaining results are seen to agree best with Osborne's modified theory. (For values of a less than 1 Osborne's theory predicts higher values of R). They are perhaps systematically low because the scatter of results has obscured the dependence of R_f

on l_2 . Since the range of l_2 over which R_p was measured is about the same as the difference between l_0 and the mid point of the range of l_2 , the averaged values of R_p are low by an amount of the order of (or less than) the standard error in R_p . Since R depends on R_p^2 , this is usually the dominant source of error in R , and the results of figure 5.4 may be systematically low by an amount comparable with the error bars. This makes the agreement even better, and is about the same as would be obtained if the results were corrected using the values of the attenuation coefficient estimated in the last section. In any case, no reasonable correction for attenuation will bring the results into agreement with Osborne's original theory. It is also clear that Chernikova's theory is incorrect, at least for 400 μ s pulses.

Agreement with Osborne's modified theory implies that α is close to 1. Since we have supposed $\alpha=1$ in the derivation, we cannot say what limits on α are implied by an error in R . However, it is reasonable to assume that R will be rather insensitive to variations in α , as in Osborne's original theory, where $\alpha=0.85$ gives only a 1% increase in R .

At first sight this seems to give good agreement with the results of Atkins et al (1959). But to interpret their results they have used an equation which is essentially equation 2.7, equivalent to Osborne's original theory, rather than the modified form (2.26). This reduces their values of α by a factor of 2. However, they have neglected da_c/dT , which increases α by 5 to 10%. But more important is the fact that their values of α are increasing with tube radius. The reason for this is not known (it is perhaps that there is a pressure drop along the U tube due to viscous flow of the gas), and until it is, there is no way of estimating what condensation coefficient would be measured in a very wide tube.

CHAPTER SIX

THE COUPLING BETWEEN FIRST SOUND IN THE VAPOUR
AND SECOND SOUND IN THE LIQUID.

'Great fleas have little fleas upon their backs to bite 'em,
And little fleas have lesser fleas, and so ad infinitum'

Augustus de Morgan.

CHAPTER 6

The coupling between first sound in the vapour and second sound in the liquid.

6.1 Introduction.

When a second sound pulse arrives at the surface it generates a first sound pulse in the vapour. This pulse travels up the tube, is reflected from the end, travels back down the tube, and when it reaches the surface generates a second sound pulse in the liquid.

For a tube of radius r and a sine wave of wave vector k the reflection coefficient at the open end is -1 when $2kr \ll 1$, and 0 when $2kr \gg 1$ (Kinsler and Frey, 1962). The important Fourier components of a $400 \mu\text{s}$ pulse are in the region of 1.25 kc/s , giving $2kr = 1.3$ at 1.0°K and 0.93 at 2.1°K . In this case only the low frequency components are reflected (with a phase change of π). But the poor frequency response of the thermometer does not detect the higher frequencies in any case.

6.2 The closed tube case

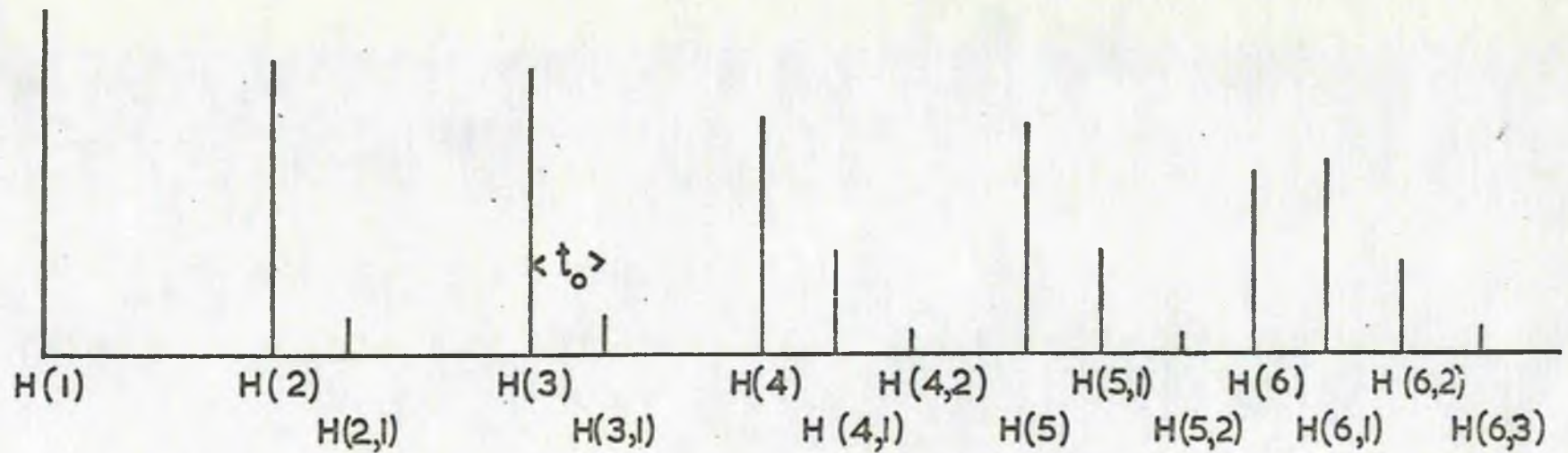
We consider first an experiment where the liquid level is between the thermometer and the top of the tube, which is closed with a flat plate. The pulse in the vapour is reflected without a phase

change and the pulse it generates in the liquid is then the same way up as the original pulse in the liquid. The pattern of pulses that is observed is shown in figure 4.3(d), and schematically in figure 6.1(a). $H(1)$ is the pulse generated by the heater (the main pulse) travelling up the tube, $H(2)$ is the main pulse returning and $H(2,1)$ is the pulse generated by the vapour pulse produced by $H(1)$ (or 'vapour pulse' for short). $H(3)$ is the main pulse travelling up, and $H(3,1)$ is the vapour pulse following it. $H(4)$ is the main pulse travelling down, and $H(4,1)$ is a vapour pulse with two components, one due to reflection at the surface of $H(3,1)$ and one due to a separate vapour pulse generated by $H(3)$. $H(3,1)$ also generates a vapour pulse, $H(4,2)$.

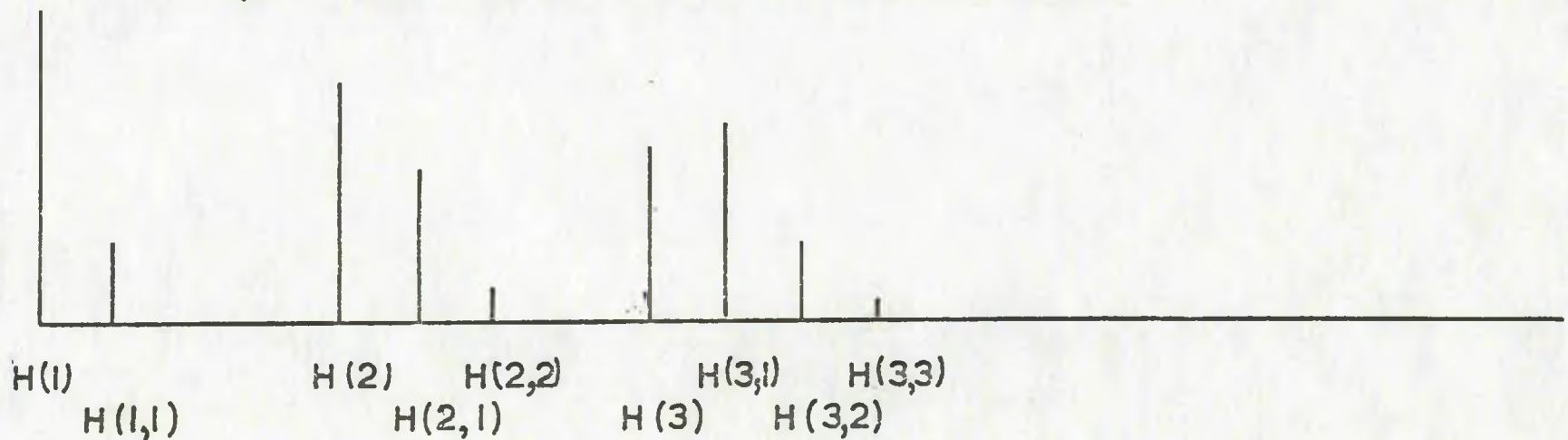
Each successive reflection generates another vapour pulse and at each reflection some of the energy lost by each pulse is transferred to the next member of the chain. Consequently each pulse increases in amplitude at every reflection until it becomes as large as the preceding pulse.

6.3 The velocity of first sound in the vapour

We can verify this interpretation by measuring the velocity of sound in the vapour, u . Denoting by l the length of the liquid



(a) thermometer below the surface.



(b) thermometer on the surface.

Figure 6.1 The Pattern Produced by the Vapour Pulses.

column between the thermometer and the surface, we have, in the notation of the last chapter (figure 5.1)

$$L_1 + \ell + (L_2 - \ell) = L$$

and $(L_2 - \ell) = ut_0$

whence $u = (L - L_1 - \ell)/t_0$ 6.1

where t_0 is the time interval defined in figure 6.1. The results obtained in this way are shown in figure 6.2, along with those of van Itterbeek and de Laet (1958), Grimsrud and Werntz (1967) and Meyer et al (1963) for comparison. The latter results extend up to 1.9°K, and above 1.2°K are in agreement with the velocity calculated from the ideal gas equation, viz $u = (\gamma RT/M)^{1/2}$. The present results have a precision of 2 or 3 per cent, but there are a number of sources of systematic error remaining. These include non-linearity of the time base (small), temperature drift while measurements are being taken, which is only important near the λ point, and finite amplitude effects. The second sound velocity is a function of amplitude (Dessler and Fairbank 1956) and this causes $L_1 + \ell$ to depend on amplitude. t_0 does not depend on amplitude (at any rate, in the same way) because it is associated with the first sound velocity in the gas, and L is calculated from the tube length,

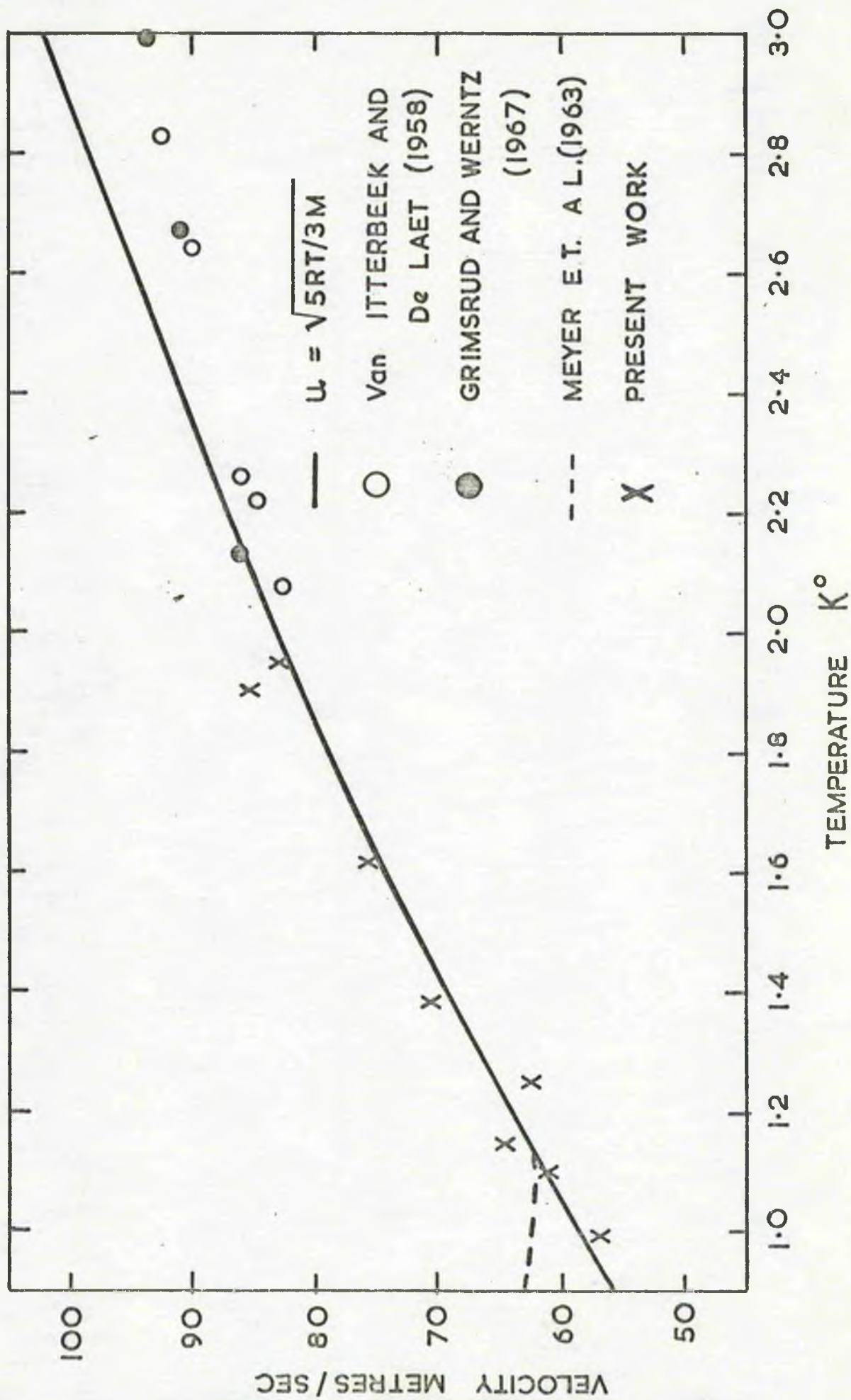


Figure 6.2 The Velocity of First Sound in Helium Vapour.

determined at low amplitude by the method of paragraph 5.2. Nevertheless, the results are in reasonable agreement with $u = (\gamma RT/M)^{\frac{1}{2}}$ and with the other experimental results.

6.4 The amplitude of the vapour pulses.

The expected amplitude of the vapour pulses can be determined from both the Osborne and Chernikova theories. If we define r as the ratio of the amplitude of the vapour pulse to the amplitude of the pulse which produced it, Osborne's theory gives (equations 2.9 and 2.14)

$$r = \frac{4 (A_0 u T / p_0 \xi) (\gamma + 1) / 2\gamma}{(1 + X_L)^2}$$

if we identify p_0 with $V \sigma u$, i.e. neglecting attenuation in the gas and losses at the end of the tube. With the same assumption, Chernikova gives (equations 2.19 and 2.22)

$$r = 4X_L / (1 + X_L)^2$$

To compare these with the measured r , we have to remember that each vapour pulse (apart from the first,) is made up of several components. We have, as a matter of definition

$$H(2,1) = rH(1)$$

$$H(4,1) = RR_B H(2,1) + rH(3)$$

$$= RR_B rH(1) + rH(3)$$

$$= 2rH(3)$$

$$H(6,1) = RR_B H(4,1) + rH(5)$$

$$= 2rRR_B H(3) + rH(5)$$

$$= 3rH(5)$$

Thus $\frac{H(n,1)}{H(n-1)} = \frac{1}{2} nr$ true for n even. 6.2

For the second vapour pulses we have

$$H(4,2) = rH(3,1) = rR_B H(2,1) = r^2 R_B H(1) = (r^2/R)H(3)(1+0)$$

$$H(6,2) = rR_B H(4,1) + RR_B H(4,2)$$

$$= rR_B 2rH(3) + RR_B (r^2/R)H(3)$$

$$= (r^2/R)H(5)(2+1)$$

$$H(8,2) = rR_B H(6,1) + RR_B H(6,2) = (r^2/R)H(7) (3+3)$$

If we now write

$$\frac{H(n,2)}{H(n-1)} = (r^2/R) S(n)$$

6.3

we have

$$S(n) = \frac{1}{2}n-1 + S(n-2)$$

$$= \frac{1}{2}n-1 + \frac{1}{2}(n-2) -1 + S(n-4)$$

$$m = \frac{1}{2}n - 2$$

$$= \frac{1}{2}n-1 + \sum_{m=1} \left[\frac{1}{2}(n-2m)-1 \right]$$

$$= n(\frac{1}{2}n-1)/4$$

We can derive similar expressions for $H(n,3)$ etc., but in practice $H(n,3)$ and subsequent pulses are obscured by the $H(n+1)$ series of pulses.

It is more convenient when doing these experiments to adjust the tube so that the thermometer is on the surface. (This halves the number of pulses visible, making it easier to distinguish between them. It also makes the pulses larger and easier to measure). In this case equations 6.2 and 6.3 are modified. We have, in the notation of Figure 6.1(b)

$$H(1,1) = H(1) r / (1+R)$$

$$H(2,1) = H(2) r / (1+R) + R_B(1+R) H(1,1) = rH(2) \left[\frac{1}{1+R} + \frac{1}{R} \right]$$

$$H(3,1) = rH(3)/(1+R) + R_B(1+R) \cdot rH(2)/(1+R) + \left[rRR_B/(1+R) \right] \left[H(2)/RR_B \right]$$

$$= rH(3) \left[\frac{1}{1+R} + \frac{2}{R} \right]$$

$$\text{and so } \frac{H(n,1)}{H(n)} = r \left[\frac{1}{1+R} + \frac{(n-1)}{R} \right] \quad 6.4$$

For the second vapour pulse we have

$$H(2,2) = rR_B H(1,1) = rR_B \cdot rH(1)/(1+R) = r^2H(2)/R(1+R)$$

$$H(3,2) = R_B H(2,2) + 2R_B r^2H(2)$$

$$= (r^2/R) \cdot H(3) \left(\frac{1}{R(1+R)} + 2 \right)$$

Thus

$$\frac{H(n,2)}{H(n)} = (r^2/R) \left[\frac{1}{R(1+R)} + \left(\frac{1}{2}n-1 \right)(n+1) \right] \quad 6.5$$

About 40 photographs were taken in an experiment of the kind described in 6.2, and using equations 6.2 to 6.5, values of r were calculated from measurements of pulse heights. The results so obtained are shown in figure 6.3 along with all three theoretical curves. R has been taken as 78%, and attenuation in the liquid has been neglected. This is not serious, since l was small (or zero) to give good time resolution of the pulses, and attenuation in the bottom part of the tube below the thermometer can be included in R_B , upon which r does not depend.

The precision of these results is better than 1% in 15%, but a number of systematic errors remain. As already stated, the $H(n,3)$ and the subsequent members of the $H(n)$ series overlap with the $H(n+1)$ series, and this will cause the measured heights of the $H(n+1)$ series to be too large. For n less than 8 this problem does not arise, but for low n $H(n,1)$ and $H(n,2)$ are small and subject to a rather large (up to 33%) error of definition. Finally, to give good resolution when the thermometer is in the liquid $H(2n-1)$ must be close to $H(2n)$ and these two series are superimposed. A correction has been made for attenuation of the pulse in the gas, which was estimated by raising the tube till the thermometer was in the gas, and measuring the decay rate of the pulses observed.

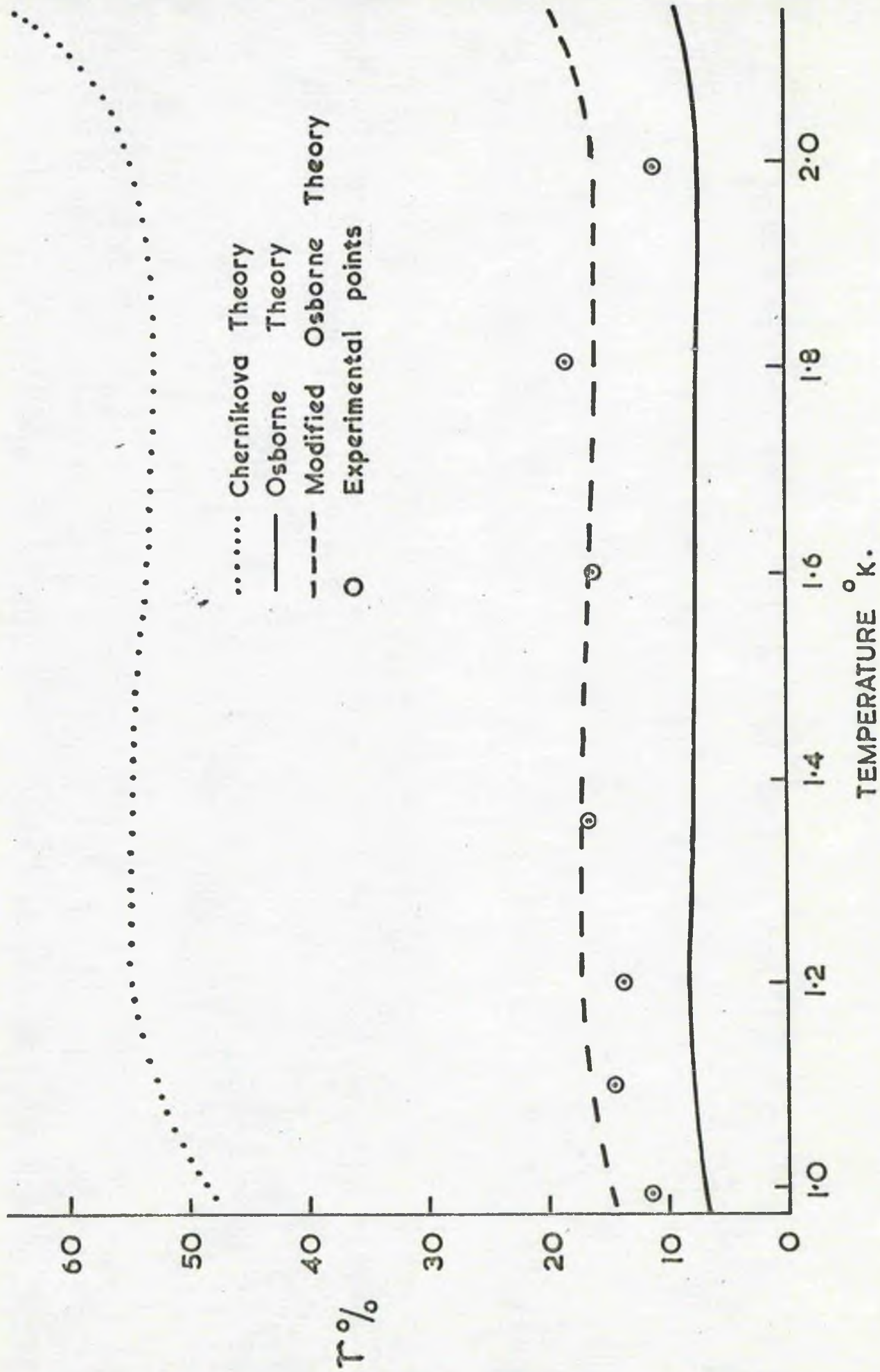


Figure 6.3 The Vapour-Liquid Coupling - the Coefficient r .

The reflection coefficient thus obtained (about 90%) is attributed entirely to attenuation and losses at the closed end. Clearly this neglects losses at the free surface, which are probably the most important. But there are the further problems that (a) the attenuation measured in this way is for a longer length of vapour column than that used in the main experiment (b) the observed pulse train has a fine structure caused by second sound pulse transformations at the surface and (c) most important, the time resolution is only one third of that in the liquid (because of the higher velocity) and the pulses tend to pile up on one another. Nevertheless, the absolute error in r is unlikely to be greater than 5% in 15%. Once again, the modified form of Osborne's theory is in best agreement with the results, although now the tendency is for disagreement in an opposite direction from that of Chapter 5.

6.5 The open tube case.

The observations of 4.3 on the observed pulse shape in open tube experiments are fairly readily explained in terms of secondary pulses produced by first sound in the vapour.

As has already been observed (6.1) the low frequency components of a first sound pulse are reflected from the open end of the tube with a phase change of π , that is, as negative pressure pulses

rather than positive ones. The second sound pulses they produce are likewise negative temperature ones, and so appear upside down on the trace. They appear behind the main pulse on its way down the tube, a time t_0 later, determined by equation 6.1. If a 7 cm tube is used, 5 cm full of helium, t_0 is about 700 μ s. If the main pulse is a 600 μ s one, the vapour pulse following it therefore appears on its tail. The main pulse is always spread over a longer time than the electrical input pulse because of the thermal capacity effects, and with a 7 cm tube and 600 μ s (or longer) pulses, it is never possible to properly resolve the main pulse and the vapour pulse following it.

As the liquid level in the tube rises, t_0 becomes smaller, and the two pulses destructively interfere, giving the appearance of a less marked change of shape. The same is true when longer pulses are used. In fact N , (the pulse number at which the observed pulse is half positive and half negative) is some monotonic function of ζ/t_0 , where ζ is the pulse length.

The dependance of N on temperature amplitude is not so readily explained. However, we would not expect to observe any other dependance of N on temperature. Since $u \propto T^{\frac{1}{2}}$ (a) $t_0 \propto T^{-\frac{1}{2}}$ and (b) the first sound wavelengths are $\propto T^{\frac{1}{2}}$, and the reflection from the open end improves slightly at higher temperatures. But these two effects are

small, and are in opposite directions. And from figure 6.3 we see that r is very insensitive to temperature.

It should be remembered that the closed tube experiments also showed a progressive change of pulse shape, not well understood, but supposed to be a result of the end of the tube not being properly closed. The observed open tube effects are therefore caused by both the poor end geometry and coupling with first sound in the vapour. This is presumably why N is larger for closed tubes than open ones. It is possible that the dependence of N on second sound amplitude is an effect associated with the imperfectly closed end, and cannot, therefore, be explained in terms of vapour pulses, although present in open tube experiments.

It also seems likely that the unexpected resonance plots described in 4.2 were caused by vapour-liquid coupling. Standing waves of first sound in the gas could have been set up by the second sound evaporating liquid at the surface. Since there are large losses at both ends of the vapour column, the first sound resonance would be very broad, and for a large range of lengths of the vapour column the system would be 'close' to resonance. This system would then be coupled back to the second sound resonant system, producing a coupled resonance system. Such an effect would give results at least qualitatively similar to figure 4.1(b).

CHAPTER SEVEN

EVAPORATION ON A MICROSCOPIC SCALE

'Lord! since thou knowest where all these atoms are....'

James Graham, Marquis of Montrose.

CHAPTER 7

Evaporation on a microscopic Scale.

7.1 Introduction.

We now return to the problem raised in Chapter 1, of how condensing atoms can form part of the liquid, with its rather unusual structure. The interpretation of the experiments of Osborne and of Beenaker^k, that the condensing atoms do not exchange momentum with the superfluid, strongly suggests that momentum must be conserved in whatever processes occur when an atom condenses. In other words, the superfluid cannot be used as a source or sink of momentum.

Each condensing atom when it approaches the surface, is pulled into the liquid by the van der Waal's forces which hold the liquid together and are responsible for the surface tension. In this way each atom requires an energy L on condensing, and a corresponding amount of momentum normal to the surface. (L is just the latent heat per atom).

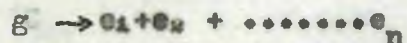
Figure 7.1 shows the energy spectrum of the excitations and that of the free gas atom (i.e. $E = p^2/2m$, m being the mass of a helium atom). An atom when it has condensed has an energy L in addition to its thermal energy, and its momentum is determined by the condition that it lie on the curve $E = p^2/2m$. L is given approximately by (van Dijk and Durieux, 1958b)

$$L = L_0 + 5kT/2$$

where L_0 is the latent heat/atom at the absolute zero. (Throughout this chapter, L and L_0 refer to atomic quantities, rather than molar or specific ones). The error is negligible at 0.8°K and about $+4\%$ at 1.8°K . L_0/k ($=7.15^\circ\text{K}$) is also shown on figure 7.1

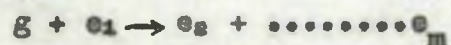
In what follows we shall suppose that the vapour behaves as an ideal classical gas, and that the excitations which form the normal fluid behave as an ideal Bose Einstein gas. We shall neglect interactions between the excitations except in so far as these can be taken into account by the temperature dependence of the excitation spectrum. This limits the discussion to temperatures less than about 1.8°K (Bendt et al., 1959).

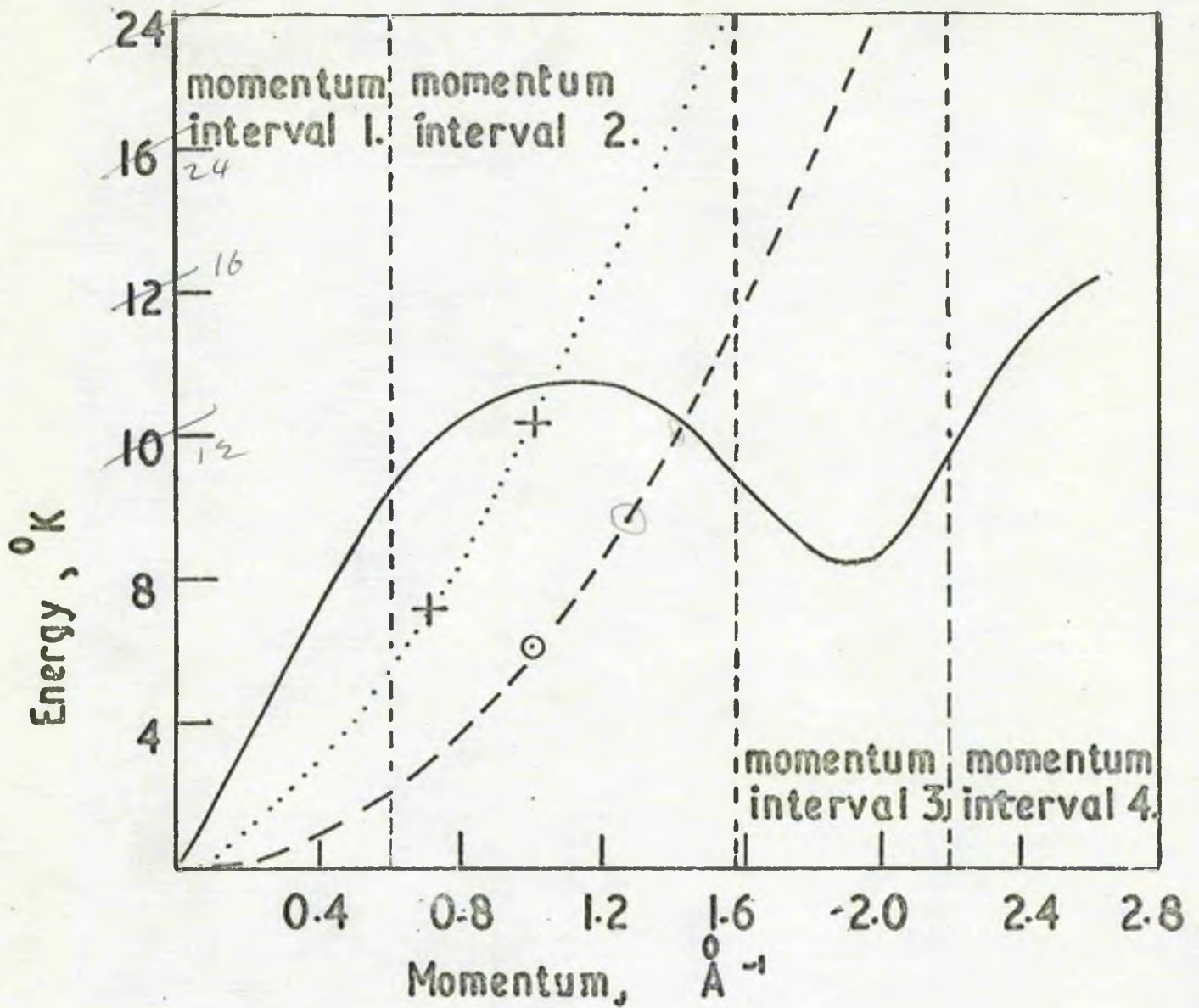
There are two kinds of processes which are probably responsible for condensation. The first is one in which a gas atom decays into several excitations, and we will write this schematically as



where the g represents the gas atom and the e_i the excitations.

The second is one where a gas atom collides with an excitation already in the liquid and the resulting object decays into several excitations.





- Spectrum for bulk excitations
- Spectrum for surface excitations
- Free particle spectrum
- The latent heat at 0°K
- + Possible cut off points for the surface excitation spectrum

Figure 7.1 The Energy Spectrum of Liquid Helium II.

There is no reason why more than two entities should not be involved on the left hand side of such a process, except that the probability of n body collisions falls off rapidly for n greater than 2.

Other processes may be possible, which depend on the fact that the excitations have a finite lifetime, but these will not be considered here. The associated effect, that the spectrum has a finite line width, is also relevant, in that it relaxes slightly the conservation requirements. But the line width is small except near the λ point, and in what follows it will be ignored.

Excitations in helium are normally thought of as two kinds - long wavelength phonons, near the origin of the excitation curve, and rotons, near the minimum. These are the only ones which are appreciably excited at temperatures where the quasi-particle concept is useful, and they make the predominant contribution to the thermodynamic functions. However, as we shall see below, the whole spectrum is probably involved in evaporation and condensation. We therefore split the energy spectrum into four momentum intervals, as shown in figure 7.1. The subdivision is that of Bendt *et al.*, (1959) who chose it so that in each interval the energy could be written as an analytic

function of the momentum. We shall continue to call the excitations in intervals 1 and 3 phonons and rotons, and shall denote them by p and r in process equations. The excitations in intervals 2 and 4 will be called type 2 and type 4 excitations and will be denoted by h_2 and h_4 . It will also be convenient to use the term heavy excitation (h) to mean a roton or a type 2 or 4 excitation.

7.2 Surface excitations.

There is another kind of excitation which may be important in condensation processes, namely surface excitations or quantised surface waves. These were first introduced by Atkins (1953) to explain the temperature dependence of the surface tension, and have since been invoked by Kuper (1956, 1958) and Atkins (1957) to explain critical velocities in superfluid films, and by Brewer, Symonds and Thomson (1965) to explain the specific heat of partially filled superleaks.

For a combined gravitational and surface tension wave on deep liquid, Kuper (1956) gives for the relation between angular frequency ω and wave number k

$$\omega = (gk + \sigma k^3/\rho)^{1/2}$$

where g is the acceleration due to gravity, σ the surface tension and ρ the liquid density. The energy is then given in terms of momentum by

$$E = (g\pi p + \sigma p^3/\pi \rho)^{1/2} \quad 7.1$$

The gravitational and surface tension terms are equal when $p/\pi = 20 \text{ cm}^{-1}$, and $E/k = 10^{-7} \text{ }^\circ\text{K}$. So for thermally excited surface modes we can write 7.1 as

$$E = (\sigma/\pi \rho)^{1/2} p^3/\rho \quad 7.2$$

which is shown in figure 7.1

The number of modes per unit area of surface is then given by

$$\begin{aligned} N_s &= (2\pi/h^2) \int_0^\infty p dp / (\exp(E/kT) - 1) \\ &= (kT/h)^{4/3} (\rho/\sigma)^{2/3} (1/3\pi) \int_0^\infty x^{4/3} dx (\exp x - 1) \quad 7.3 \end{aligned}$$

and the integral is $\Gamma(1/3) \zeta(4/3) = 3.3$

where ζ is the Riemann zeta function.

Atkins (1953) has pointed out that 7.1 is probably not correct for short wavelengths. He noted that the problem was similar to the Debye theory of solids and that the spectrum of normal modes must be cut off at some wavelength of the order of the interatomic spacing.

Since this is 3.2 \AA in helium the maximum wave number is 1.96 \AA^{-1} , and the maximum energy, according to equation 7.2 is about 32°K . Atkins determined the cut off by setting the total number of surface modes equal to the number of atoms in a monomolecular layer at the surface, and obtained a maximum wave number of 1.0 \AA^{-1} , for which equation 7.2 gives an energy of 12.1°K . He then suggested that the zero point energy be subtracted from this figure, to give a maximum energy - 7.2°K , for which equation 7.2 gives 7.1 \AA^{-1} for the maximum wave number.

In order to make some assessment of the role of surface excitations in condensation processes, we will suppose that 7.2 is correct for short wavelengths, even though this is probably not true. But we note that for thermally excited surface excitations, the nature of the short wavelength part of the spectrum is not very important.

7.3 Some numerical calculations relevant to condensation processes.

At this stage it is instructive to do some arithmetic. The numbers of phonons and rotons per unit volume are given by (e.g. Khalatnikov, 1965)

$$N_p = 8\pi(kT/hc)^3 \zeta (3)$$

for phonons, and

$$N_r = (4\pi/h^3)(2\pi\mu kT)^{\frac{1}{2}} p_0^2 \exp(-\Delta/kT)$$

for rotons. Here p_0 , μ and Δ are the parameters of the energy spectrum; their values at 1.1°K are (Yarnell, Arnold, Bendt and Kerr, 1959, Henshaw and Woods, 1961)

$$\Delta/k = 8.65^\circ\text{K}$$

$$p_0/\pi = 1.91 \text{ \AA}^{-1}$$

$$\mu/m = 0.16$$

The number of gas atoms per unit volume is obtained from the gas law.

$$N_G = p/kT$$

In table 7.1 we have calculated the ratios N_r/N_G and N_p/N_G

The mean roton velocity is given by (e.g. Atkins, 1959a)

$$\bar{v}_r = (2kT/\pi\mu)^{\frac{1}{2}}$$

and the mean gas atom velocity is well known to be

$$\bar{v}_G = (8kT/\pi m)^{\frac{1}{2}}$$

Now the flux of gas atoms striking the surface is $N_G \bar{v}_G/4$, and the roton flux is $N_r \bar{v}_r/4$; their ratio is just $(N_r/N_G)(\bar{v}_r/\bar{v}_G) = 1.25(N_r/N_G)$. Phonons all have the same velocity c (the velocity of first sound) and so the corresponding ratio for phonons is $3.3(N_p/N_G)T^{-\frac{1}{2}}$.

Since N_r/N_G and N_p/N_G are always greater than 1, this means that the phonon and roton fluxes striking the surface are always greater than the flux of gas atoms striking the surface.

Also given in the table is the number of surface excitations per unit area (equation 7.3). Finally we calculate the energy E_0 at which the excitation curve intersects the gas atom curve, and the fraction of atoms which have an energy greater than this. The fraction of atoms with energy between E and $E + dE$ is just

$$(4/\pi)^{\frac{1}{2}} (E^{\frac{1}{2}}/(kT)^{3/2}) \exp(E/kT) dE$$

and the fraction with energy between 0 and E_0 , $N(E_0)$ is then

$$\begin{aligned} N(E_0) &= (4/\pi)^{\frac{1}{2}} \int_0^{E_0/kT} (E/kT)^{\frac{1}{2}} \exp(E/kT) \\ &= (4/\sqrt{\pi}) \int_0^{x_0} x^2 \exp(-x^2) dx, \text{ where } x_0^2 = E_0/kT \\ &= \text{erf}(x_0) - (4/\pi)^{\frac{1}{2}} x_0 \exp(-x_0^2) \end{aligned}$$

The fraction f with energy greater than E_0 is then $1-N(E_0)$. The fraction F of incident gas atoms which have enough energy (2Δ) to form two rotons is also given in the table.

The relation given by Yarnell et al (1959)

$$\Delta/k = 8.68 - 0.0084T^7$$

has been used to determine Δ as a function of temperature. E_0 has been calculated from the expression for the excitation energy in the second momentum interval given by Bendt et al

$$E/k = a - 11.5 (p/\hbar - 1.113)^2$$

where a is a function of temperature. ($a = 13.93^\circ\text{K}$ at 1.0°K).

TABLE 7.1

T	Δ/k	L/k	E_0/k	N_r/N_G	N_p/N_G	N_s	f	F
$^{\circ}\text{K}$	$^{\circ}\text{K}$	$^{\circ}\text{K}$	$^{\circ}\text{K}$			$\text{cm}^{-3} \times 10^{18}$	%	%
0.8	8.65	9.15	12.7	6.9	78	1.4	2.9	0.01
1.0	8.65	9.65	12.7	8.0	18	1.9	10	0.16
1.2	8.65	10.1	12.7	8.4	7.1	2.5	21	0.70
1.4	8.59	10.6	12.7	9.1	3.8	3.5	39	2.3
1.6	8.46	10.9	12.5	10.6	2.5	4.4	56	5.7
1.8	8.17	11.2	12.4	11.4	1.8	5.7	72	12

TABLE 7.2

T, $^{\circ}\text{K}$	α'	α
1.0	0.0019	0.019
1.4	0.018	0.22
1.8	0.057	0.81

7.4 Tilley's Theory of evaporation

Tilley (1965) has attempted a calculation of the contribution to the evaporation coefficient α' due to the process

$$g \rightarrow \bullet$$

α' is defined as the fraction of quasi particles striking the surface which decay and enter the vapour as gas atoms. For this process it is related to α by

$$\alpha N_G \bar{v}_G / 4 = \alpha' N_\bullet \bar{v}_\bullet / 4$$

where N_\bullet is the excitation number density and \bar{v}_\bullet the average velocity of an excitation.

He assumes that energy (including the latent heat energy) and momentum parallel to the surface are conserved, but not momentum normal to the surface. He therefore draws figure 7.1 with the origin of the free particle parabola at $E = L$, $p = 0$. The two curves now intersect only for temperatures less than about 1°K. The reason for doing this is that if α is less than one, those atoms which are reflected from the surface must give up their momentum to the liquid as a whole, and Tilley supposes that this is also possible for those atoms which do enter the liquid. But this seems to be at variance with the results of the Osborne and Beenaker^k experiments.

Tilley calculates α' by first determining the probability P that an excitation can cross the surface, expressed as a transmission coefficient. He considers the wave functions on either side of the surface and using the boundary conditions that the wave function and its first derivative are continuous at the surface he obtains an expression for P . He supposes that the matrix element is unity, and obtains an expression for α' by calculating the average

$$N_0 \langle P v_0 \rangle / 4$$

over all excitation energies and momenta. The integration over all energies takes account of the line width of the spectrum.

To get numerical results, Tilley neglects line width effects and puts $P=1$ for all excitation energies greater than L , and zero otherwise. The results of this calculation are given in the table 7.2.

The high values for α are a result of not conserving momentum normal to the surface. If the ideas proposed here are correct, where an atom gains momentum in crossing the surface, then the process $g \rightarrow e$ can occur only where the free particle parabola intersects the excitation curve, if energy and total momentum are to be conserved. The range of energies for which this is possible depends on the spectrum line width at that point, but it is always small in the temperature range where the concept of a gas of excitations is a useful one.

7.5 Condensation processes involving bulk excitations

The probability that a gas atom forms for example, a phonon and a roton will depend amongst other things, on the matrix element for a gas atom \rightarrow phonon + roton transition. No attempt will be made here to calculate these matrix elements, but some qualitative remarks can be made about them.

Since a gas atom is a highly localised entity, we might expect that it will interact strongly only with well localised excitations. In other words we might expect a matrix element to be an increasing function of the momentum of the excitation, and to be largest for rotons and type 4 excitations. It also seems reasonable that the more complicated the process, i.e. the more quasi particles involved the smaller will be the probability of it occurring.

The simplest process by which a gas atom can condense is one in which a gas atom forms a single excitation

$$g \rightarrow \bullet$$

This case has been discussed in detail in the previous section; it is virtually excluded by conservation of energy and momentum. The next possibilities are those involving two excitations

$$g \rightarrow e_1 + e_2 \quad 7.4$$

$$\text{and } g + e_1 \rightarrow e_2 \quad 7.5.$$

The cases when e_1 and e_2 are both phonons are again excluded by the conservation laws. If in the first process e_1 and e_2 are both heavy excitations, then the gas atom must have an energy at least 2Δ . Table 7.1 shows that the fraction F of such atoms is negligible except at the highest temperatures, and these processes will therefore be ignored. Likewise the process

$$g \rightarrow p + h_1$$

will be ignored. The remaining processes of the first kind involving bulk excitations are

$$g \rightarrow p+r \qquad 7.6$$

and $g \rightarrow p+h_2 \qquad 7.7$

The only process of the second kind satisfying the conservation laws is

$$g + p \rightarrow h_2 \qquad 7.8$$

In the special case where both the gas atom and the excitations produced are moving normal to the surface the transition can be simply shown on figure 7.1. If a line of slope $-c$ (representing a phonon moving in the negative direction) is drawn through the roton minimum, say, its point of intersection with the free particle parabola gives the energy and momentum of the gas atom which will condense to give a roton at the minimum (process 7.6) and the difference between the

coordinates of these two points gives the energy and momentum of the phonon. 7.7 is similarly described; for 7.8 a line of slope $+c$ is drawn through some point on the free particle parabola to intersect the excitation curve in the region of the maximum.

The matrix element for 7.6 is perhaps not too small. The wavelength of the phonon required to give a roton at the minimum is only about 10 times the atomic diameter. For 7.7 the matrix element will be rather smaller, the minimum phonon wavelength being about 20 times the atomic diameter. The process 7.8 depends on the gas atom colliding with a phonon already in the liquid. Table 7.1 shows that there are always enough phonons for this to be possible for each atom. But for a phonon momentum p that will allow energy and momentum to be conserved the probability that the transition occurs is proportional to the product of the matrix element (small for p small) and the probability that such a phonon is excited (small for p large). So this process is rather unlikely to occur.

Because of the large value of c processes 7.6 and 7.7 occur only if the gas atom lies above the excitation curve, i.e. only if its energy E is greater than E_0 . Also 7.8 occurs only if E is less than E_0 . Table 7.1 shows that the fraction of gas atoms with energy greater than E_0 falls off rapidly with temperature. If 7.6, 7.7 and 7.8 were the only processes involved 7.6 and 7.7 would be the most important

at 1.8°K, and 7.8 would dominate at 1.0°K. Since 7.8 seems rather unlikely, α might be expected to decrease below about 1.4°K. Since this has not been observed, it must be supposed that there are other processes responsible for condensation in this temperature region. Further, we note that 7.8 is possible only for atoms with a certain minimum energy. Since the phonon is to be a thermally excited one its energy is $\lesssim kT$, and an atom must therefore have an energy $\gtrsim E_0 - kT$ before it can condense.

It has already been mentioned that the probability of processes involving more than one gas atom and two excitations is rather small, because of reduced collision and transition probabilities. There is an additional reason for expecting low transition probabilities for such multiple processes. A gas atom (or a gas atom and excitation) with a total energy E , must distribute this energy among several excitations. The more excitations there are, the less energy each gets, the less momentum each gets and the smaller the matrix element. The exception is processes like



Table 7.1 shows that this process will not be limited by the roton number density, and we may expect the transition probability to be not too low, since only short wavelength excitations are involved. But if the gas atom has an energy (after condensing) less than a certain amount, it cannot collide with rotons which have a reasonable

probability of being thermally excited and still conserve energy and momentum. This threshold energy increases with decreasing temperature as the energy spread of the thermally excited rotons decreases. At 1°K it is about 10°K.

7.6 Processes involving surface excitations.

The discussion of these processes is complicated by the fact that surface excitations have no component of momentum normal to the surface, while most of the momentum which a condensing atom has to dispose of (that due to the attraction of the surface forces) is normal to the surface. This circumstance eliminates the processes 7.4 and 7.5 when the two excitations are two surface excitations, or one surface excitation and one phonon, since a single phonon cannot carry away all the momentum of an incoming atom. This leaves the processes

$$g+s \longrightarrow h \qquad 7.10$$

$$g+r \longrightarrow s \qquad 7.11$$

$$g \longrightarrow s+h \qquad 7.12$$

A proper analysis of these processes is complicated by the fact that the energy of a surface excitation is proportional to the three halves power of its momentum (equation 7.2). The present treatment is therefore limited to low temperatures (1°K, say) where the bulk excitation

processes seem unable to explain the high observed values of α . For the present, we consider only gas atoms normally incident on the surface. Figure 7.2 shows the momentum vector diagrams in this case for the three processes 7.10 to 7.12. In each case conservation of momentum gives

$$p^2 + 2mL + p_s^2 = p_r^2$$

$$\text{or } p^2/2m + L + p_s^2/2m = p_r^2/2m \quad 7.13$$

where p , p_s , p_r are respectively the momentum of the gas atom, the surface excitation and the heavy excitation. Conservation of energy for the process 7.10 gives

$$p^2/2m + L + E_s = E_r$$

where E_s and E_r are the surface excitation and heavy excitation energies.

Since the energy of the thermally excited surface excitations is -1°K , this equation is satisfied only when the gas atom has an energy about 1°K less than an excitation. So process 7.10 is possible only for atoms with energy between about 11.7°K and $E_0 (=12.7^\circ\text{K})$, and at 1°K this is about a quarter of the atoms.

For process 7.12, conservation of energy gives

$$p^2/2m + L = E_r + E_s$$

Subtracting this from 7.13 gives

$$E_s + p_s^2/2m = p_r^2/2m - E_r \quad 7.14$$

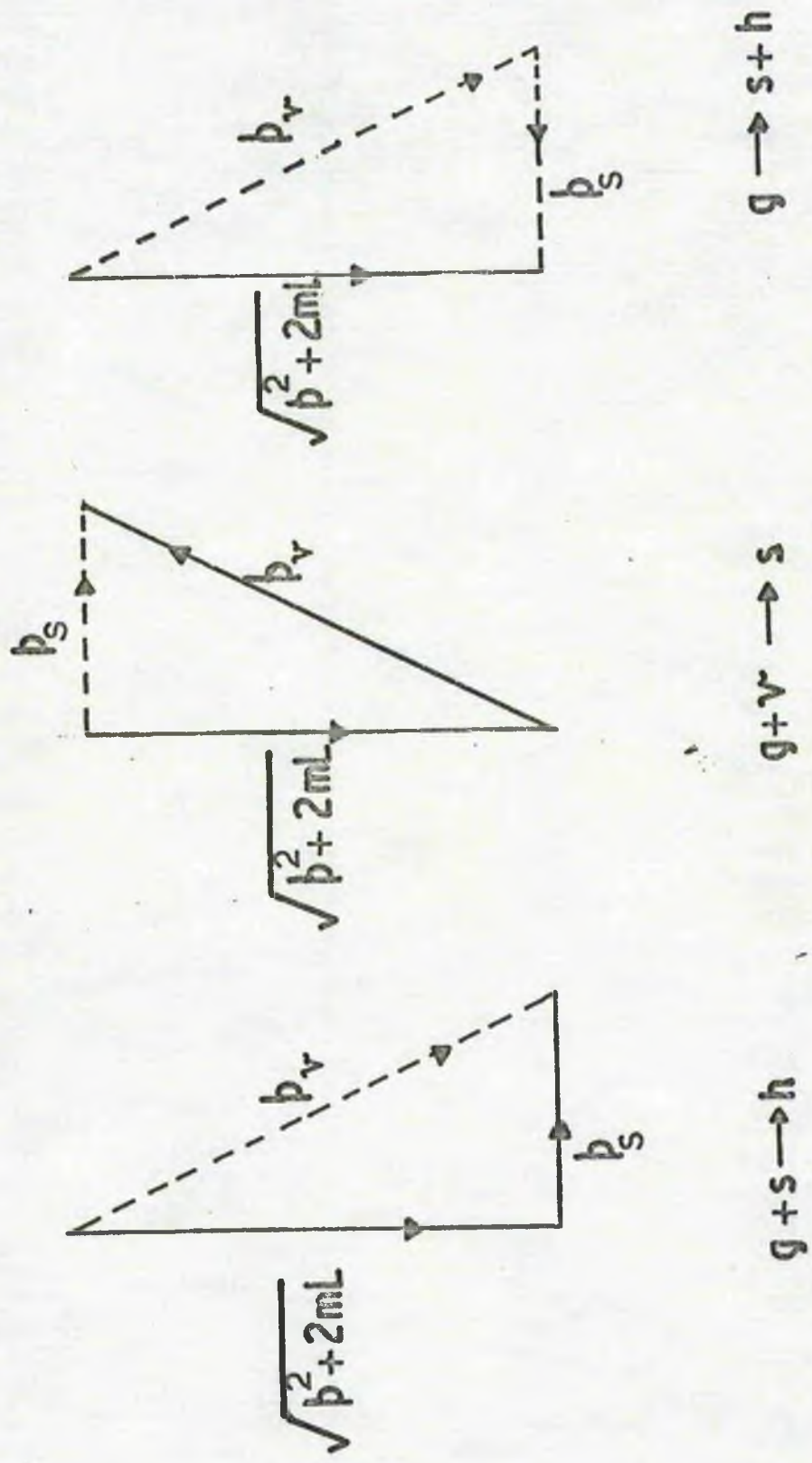


FIG. 7.2 MOMENTUM VECTOR DIAGRAMS FOR SURFACE EXCITATIONS.

This is possible only for excitations with energies less than gas atoms with the same momentum. A more detailed study shows that the minimum value of $E_s + E_r$ satisfying 7.14 occurs when $E_s = 0$ and $E_r = E_0$; consequently only atoms with energies greater than E_0 can condense in this way.

For process 7.11 conservation of energy gives

$$p^2/2m + L + E_r = E_s \quad 7.15$$

Subtracting from 7.13 we get

$$E_s + p_s^2/2m = E_r + p_r^2/2m$$

The bulk excitation must be a thermally excited one, i.e. a roton with energy $\sim \Delta + kT$. At 1°K, the minimum value of $E_r + p_r^2/2m$ is then about 27.5°K. The corresponding value of E_s is about 18°K, and so the minimum energy a gas atom must have to condense is just $E_s - E_r = 8.4°K$.

At temperatures above 0.5°K, all condensing atoms have at least this much energy. But as already noted, the dispersion relation for such high energy surface excitations is probably not equation 7.2, even if these excitations exist. So 7.11 will not occur if high energy, short wavelength excitations do not exist, and even if they do, the gas atom threshold energy will be modified by the short wavelength form of the surface excitation spectrum. The estimate of the momentum cut off

based on the interatomic spacing is almost certainly too high, since the interatomic spacing is greater near the surface. In fact it is hard to see how the cut off can be much larger than Atkins first estimate, obtained by limiting the number of modes. In this case 7.11 is not possible.

7.7 The condensation coefficient at low temperatures.

From what has been said above, it is clear that at high temperatures there are probably enough processes to allow a very large fraction of the incident atoms to condense. But as the temperature is lowered, the latent heat and the average energy per atom decrease, and the energy spectrum moves up slightly. Consequently an increasing fraction of the atoms have too little energy to form two or more excitations, until at 1°K, the only processes left capable of giving significant contributions to α are the collision ones.



7.10 and 7.8 operate only above about 11.5°K (25% of the atoms), and are expected to have small matrix elements (e.g. the wavelength of a 1°K phonon is about 50 atomic diameters). 7.9 operates above

about 10°K (88% of the atoms), but once again the matrix element is expected to be small because three excitations are involved. 7.11 is probably possible for all energies if the appropriate surface excitations exist, and the matrix element should be larger than in the other cases.

But for these processes, we have also to consider the collision probabilities. If an atom which strikes the surface is not to condense, it must be reflected before it has travelled very far into the liquid, say within a distance of 10 interatomic spacings, or 30 Å. At 1°K the number of rotons per cc is $\approx 10^{19}$, and so the number n in the first 30 Å of 1 square cm. of the surface is 3×10^{18} . The probability that an incoming atom collides with one of them is just $n\sigma$, where σ is the atom-roton cross section. σ is related to the matrix element, but we will suppose that for scattering purposes a roton behaves as a hard sphere of diameter equal to its wavelength, i.e. 3.3 Å. Since the atomic diameter is 2.6 Å, σ is $\pi(2.6 + 3.3)^2/4$ Å². So the collision probability $n\sigma$ is about 0.08.

If we now make the optimistic assumptions that the collision probability is the same for 7.10 and 7.8 as it is for 7.9, that the transition probabilities are unity, that all atoms with an energy greater than E_0 can condense, and that none of the above processes are competing for atoms (but taking account of the fact that 7.9 and 7.11 are mutually

exclusive) we get a value of α close to 1 at 1.2°K , about 0.22 at 1°K , and 0.095 at 0.9°K . (It is of little consequence for the present purpose whether 7.11 is possible or not, since it overlaps to a considerable extent with 7.9, and cannot occur if 7.9 occurs, and vice versa).

It is not clear how good an estimate this is; but to give an α of 1 at 1°K would require a collision probability about 7 times higher, and would, in addition, require all the assumptions of the last paragraph to be reasonably good ones.

The discussion in this chapter has neglected various points. Firstly, only atoms incident normally on the surface have been considered. This is unimportant for bulk excitations, since the decay processes are essentially isotropic. For processes involving surface excitations it does not affect our main conclusions, which have mainly been based on energy conservation. A more detailed analysis of the $g+s \rightarrow h$ process suggests the energy range for which condensation is possible is not greater, and may be less, for arbitrary angles of incidence. Secondly we have regarded all the bulk excitation processes as taking place 'in-line'. Again, a detailed analysis of the $g \rightarrow p+r$ process suggests that the extension does not alter the previous conclusions. Finally, for reasons already stated, processes involving more

than two excitations (other than 7.9) have been ignored, as have the effects of the excitation line width.

It seems possible that the ideas presented here could account for the observed values of α above 1.2°K . Below that temperature, the mechanism of condensation is not yet explained, and it is hard to see why the condensation coefficient should not become progressively smaller at lower temperatures.

CHAPTER EIGHT

DISCUSSION

• "The time has come," the Walrus said,

"To talk of many things.

Of shoes - and ships - and sealing wax,

And cabbages and kings.

And why the sea is boiling hot,

And whether pigs have wings." •

Lewis Carroll.

CHAPTER 8

Discussion

8.1 Conclusions

The measurements of the free surface reflection coefficient R , and the vapour liquid coupling coefficient r together suggest that the modified form of Osborne's theory is the correct one to use for interpreting the results. The fact that the two measurements tend to deviate from the theory in opposite directions (R towards Chernikova's theory and r towards Osborne's original theory) is satisfactory in that it implies that the correct answer is somewhere in between. It is very unlikely that there are undetected systematic errors in both sets of results which would bring both into agreement with Osborne's original theory, and it is almost inconceivable that they could produce agreement with Chernikova's theory. It should be remarked that the agreement between theory and experiment suggests that the assumptions about mean energy and momentum transfer used in deriving Osborne's modified theory are in fact justified, even if the real reason is somewhat obscure.

While the accuracy of the measurements is sufficient to determine which theory to use, it is not sufficient to detect any deviation from it which would imply that α is different from unity. But we have

seen that R is rather insensitive to the value of α , and we have concluded therefore that α is probably 1 and not less than about 0.8, between 1.0°K and 2.14°K .

The microscopic reasons for the high observed evaporation rates are not yet properly understood. The approach outlined in the last chapter leads to values of α less than one below about 1.4°K , and the value of about 0.2 at 1.0°K is definitely incompatible with the experiments. The calculation is capable of considerable refinement, but it seems unlikely that the increase to be expected by including line width effects and higher order processes would outweigh the decrease expected by calculating the matrix elements.

8.2 Johnston and King's experiment

It is perhaps relevant at this stage to discuss recent work by Johnston and King (1966). They used a molecular beam technique to measure the velocity distribution of atoms evaporating from liquid helium. Between 0.59 and 0.7°K they found the distribution to be Maxwellian, but with a mean velocity corresponding to a temperature $(1 \pm 0.1)^\circ\text{K}$ hotter than the supposed temperature of the liquid. The helium II bath was in thermal contact with a liquid He^{II} pot, and the temperature of the helium II bath was deduced from the He^{II} vapour

pressure. A control experiment in which He^4 gas was used as the molecular beam source gave a Maxwellian velocity distribution which corresponded to the gas temperature deduced in this way. Further, they calculated the beam intensities which should be observed if the vapour pressure of the helium II was that corresponding to the temperature of the He^3 bath, and found them to be in agreement with the observed beam intensities. The results were found to be independent of factors like vibration level and cryostat geometry.

Since the ideas presented in the last chapter do not properly explain the present results at 1°K it is perhaps unwise to expect them to be adequate at even lower temperatures. Nevertheless, they seem capable of giving at least a qualitative explanation of Johnston and King's rather surprising results.

As we have seen it is possible for a gas atom to condense only if it has an energy greater than some threshold energy E_1 , which will be the threshold energy for the process with the lowest threshold energy. We might also expect that atoms which are evaporated will appear in the vapour with energies $\gg E_1 - L$, since evaporation is presumably due to the same process proceeding backwards. On these grounds we might therefore expect that evaporating atoms would have a mean energy approximately $E_1 - L$ larger than that corresponding to the liquid temperature. The liquid is behaving rather as if it had a latent

heat E_1 rather than L , and for the reasons discussed in Chapter 2 a Maxwellian velocity distribution in the evaporating atoms might reasonably be expected.

If E_T is the mean energy the evaporating atoms would have if they could all evaporate (i.e. $3kT/2$) and E_B the mean energy actually found, then

$$E_B - E_T = E_1 - L$$

Using Johnston and King's values for E_B this gives $E_1 = 10.15^\circ\text{K}$ at 0.6°K and 10.3°K at 0.7°K . This is about the threshold energy for process 7.9. If this is the correct explanation, then E_1 would be expected to increase as the temperature is lowered, and not decrease as found above. But the error in determining E_1 from Johnston and King's results is about $\pm 0.15^\circ\text{K}$, so the difference is hardly significant.

However, at 0.6°K the roton density has decreased by a factor of 5 from its value at 1°K , and so the collision probability for 7.9 is five times smaller. And since at 0.6°K only about 20% of the gas atoms have enough energy to condense, only about 0.3% could do so. This should mean that the beam intensities observed by Johnston and King should have been only 0.3% of those calculated from the vapour pressure data. This was not the case, and the above treatment is clearly not a complete explanation, though it seems possible that the true explanation will be along similar lines.

8.2 The condensation coefficient in Helium films.

So far we have only been concerned with the condensation coefficient of the bulk liquid. The theoretical discussion in Chapter 7 suggests that the condensation coefficient in films will be the same as in the bulk liquid. There are two qualifications to this statement, however. The first is that if surface excitations play a predominant role in the evaporation process, they will be of a different kind in the film (Atkins, 1957, Kuper, 1958). And as already noted, it is perhaps unwise to attach too much weight to the predictions of chapter 7 when the present results are unexplained at 1°K.

There is no direct experimental evidence on evaporation from films, but some indirect evidence is provided by third sound experiments. Atkins (1959b) derived an expression for the third sound velocity u_s which can be written as

$$u_s^2 = \frac{\rho_s}{\rho} \frac{(Cdf/ST + S - \eta p/\rho T) - i(\alpha\alpha_c \eta pf/\rho wT)(L/ST+1)}{C/ST - i(\alpha\alpha_c \eta pL/\rho wdST^2)}$$

8.1

where ρ_s is the superfluid density, f the force acting on unit mass of the liquid at the film surface, d is the film thickness, w is the angular frequency, S and C are the entropy and specific heat of the liquid, and the other symbols have their previous meanings^s (see Chapter 2). We can write this expression in the form

$$u_s^2 = A(1-i\alpha\omega_1/\omega)/(1-i\alpha\omega_2/\omega)$$

Now at frequencies $\omega \ll \alpha\omega_1$ and $\omega \ll \alpha\omega_2$, the velocity is

$$u_s^2 = A\omega_1/\omega_2$$

and there is no dispersion and no attenuation. As the frequency is increased, we would expect to find maximum dispersion and attenuation at frequencies $\sim \alpha\omega_1$ and $\alpha\omega_2$. Everitt, Atkins and Denenstein (1962, 1964) have measured the velocity at frequencies up to 1.3 kc/s at 1.2°K, and found it to be frequency independent. Since at this temperature $\omega_1/2\pi = 135$ kc/s and $\omega_2/2\pi = 15$ Mc/s, this suggests that α is not less than about 10^{-4} . The observed attenuation, however, is much greater than that implied by equation 8.1, but Pollack has suggested that this is because Atkins theory neglects the motion of the normal fluid. If the normal fluid is allowed to move, and a viscous drag term proportional to the normal fluid velocity is introduced into Atkins equations, a much larger attenuation is predicted (Pollack 1966a). A further consequence of this approach (Pollack 1966b) is that another wave mode is possible, coupled to the third sound, and presumably always excited with it. The new mode is heavily damped, and the two effects together qualitatively explain the high observed attenuation. By what appears to be a numerical coincidence, the

values of w_1 and w_2 are unaltered at 1.2°K, which is the only temperature at which the velocity has been measured as a function of frequency. So the more complete theory does not require a revision of our previous estimate of a lower limit to α .

The condensation coefficient in the film is of particular interest because of recent work on film flow rates. Allen and Matheson (1966) have measured the film flow rates out of a beaker which had been filled (a) by film flow and (b) by submersion in the bath. The outflow rates in the latter case were found to be significantly higher and they interpreted these results by supposing that submersing the beaker formed a thick film on the wall, which slowly drained away. Tilley and Kuper (1966) and Tilley (1965) have shown that such a mechanism does indeed explain the observed flow rates. However, it has been pointed out (Mate, unpublished, see Tilley, 1965) that in a thick film the normal fluid will move only very slowly, because of its viscosity, and will hold up the excess superfluid by the fountain effect. Consequently the top of the film will be hotter than the bottom by a small amount, and Mate calculates that it should evaporate (until it reaches the equilibrium thickness) in about 10^{-1} to 10^{-2} seconds. His calculation assumes $\alpha = 1$, and is to be compared with the time interval over which enhanced film flow rates were observed by Allen and Matheson, i.e. about 10^0 seconds. So if a thick film is not to evaporate during

the experiment, α must be $\sim 10^{-5}$. This contradicts the third sound evidence and in any case seems unlikely in view of the present results for the bulk liquid. However Keller and Hammel (1966) have suggested that it may not be necessary to invoke the thick film hypothesis to explain these results, but that changes in the profile of the chemical potential along the film path may be responsible for the different flow rates observed.

8.3 Suggestions for future work

The present measurements do not give very accurate values for α , and in particular do not preclude the possibility that α is different from, but close to, unity. Measurements of reflection coefficients would have to be about ten times as accurate to determine α to within 1%. While this is no doubt possible, it is probably better to use a resonance method and measure Q 's. Measurements of Q to 1% accuracy would determine α to within about 2%, compared with about 20% for 1% measurements of the reflection coefficient. Such measurements would also show explicitly the existence of any relaxation effects present. Extension of the measurements to lower temperature becomes increasingly difficult, since the reflection coefficient tends to 1. For instance at 0.7°K, all three theories are predicting reflection coefficients greater than 95%, and at 0.6°K the reflection coefficient

is greater than 99% (essentially because the vapour pressure falls exponentially with temperature). In these circumstances the advantages of the resonance method over the pulse method becomes even more pronounced. But in this region no second sound experiments will be easy to perform, since the attenuation is very high, and the energy loss at the surface, which is the quantity of interest, is small compared with the energy loss elsewhere. That is, all the measured Q 's or R 's will be small and not easy to measure. But measurements on Q would still give more information about α .

Measurements of Q rather than R would require some modification to the present experimental procedure. It would be necessary, for instance, to mount the thermometer at the bottom of the tube. The wire thermometer originally used in this work might be suitable if it were sealed through the tube wall. It might also be necessary to suppress the signal generated by first sound in the vapour rather better than has been done with cotton wool. Removing the cotton wool, and using a wider tube and higher frequencies would help, but an acoustic matching horn on the end of the tube would probably be necessary. A wider tube and higher frequencies would make vertical adjustment of the tube more critical, and higher frequencies would require a thermometer with a better response time. It is suspected

that the original wire thermometer was quite fast, and that the rise time was limited by the heater. So it would be advisable to replace the conducting glass heater, e.g. by an aquadag on mica one.

The discussion on Chapter 7 suggests that α ought to fall off rapidly with decreasing temperature (which, if true, would make measurement even more difficult at lower temperatures). But it also suggests that the effect should be significant at 1°K, contrary to the experimental evidence. It is also suspected that a more refined treatment of the theoretical ideas proposed here will make the disagreement with experiment worse rather than better. So further experiments ought probably to await a satisfactory theoretical explanation of the results already obtained.

APPENDICES

APPENDIX A

The Surface Area of a Liquid Meniscus.

We wish to find $A_0 = A/\pi r^2$ where A is the area of the liquid surface and r is the radius of the tube. To do this we require the surface profile of the liquid, from which the area of revolution can be calculated. The surface profile has been investigated by Rayleigh (1916) and his relevant results are reproduced below.

Let the x - y plane be the free liquid surface and the z -axis the axis of the tube. Then Rayleigh gives the second order equation of the liquid surface as

$$\frac{d^2 z}{dx^2} + \frac{1}{x} \frac{dz}{dx} \left[1 + \frac{dz}{dx}^2 \right] = \frac{z}{a^2} \left[1 + \frac{dz}{dx}^2 \right]^{3/2}$$

where $a^2 = T/\rho g$, T is the surface tension and ρ the liquid density. To solve this, he supposes that the tube can be split into two regions, a central part where $dz/dx \ll 1$, and an outer part near the rim where $r - x \ll r$. In this region, the curvature of the surface is $\gg r$, and a two dimensional solution is adequate. This implies that the tube is wide, or more precisely $r \gg a$. Since for liquid helium a is ≈ 0.05 cm, this condition is satisfied. We shall therefore calculate A in two parts; A_1 will be the area out to a radius x_0 and A_2 will be the area from x_0 to r . x_0 is to be chosen such that $r - x_0 \ll r$ and $\left(\frac{dz}{dx}\right)_{x=x_0} \ll 1$. Now the area of a surface of revolution about the

z axis is

$$\int 2\pi x ds = \int 2\pi x \left[1 + \left(\frac{dz}{dx} \right)^2 \right]^{\frac{1}{2}} dx \quad \text{A.1}$$

and we see that for the central part, where $\frac{dz}{dx} \ll 1$,

$$A_1 = \int_0^{x_0} 2\pi x dx = \pi x_0^2$$

In the outer annulus, where only one curvature is important, Rayleigh gives

$$1/R = \frac{d\theta}{ds} = \frac{d\theta}{dz} \sin\theta = z/a^2$$

where $\tan\theta = dz/dx$

This integrates to

$$z^2/2a^2 = C - \cos\theta = 1 - \cos\theta \quad \text{A.2}$$

the constant being determined by the condition that when $\theta = 0$,

$$z^2/2a^2 \ll 1$$

Thus $z/a = 2\sin\frac{1}{2}\theta$

$$dx/a = dz/\tan\theta = (1/\sin^2\theta - 2\sin^2\theta) d(\theta/2)$$

$$x/a = \log \tan(\theta/4) + 2\cos^2\theta + C_1$$

At the wall, $x = r$, $\theta = \pi/2$ (zero angle of contact). Thus

$$(x - r)/a = \log \tan(\theta/4) + 2\cos^2\theta - \log \tan(\pi/8) - \sqrt{2}$$

When $\theta \ll 1$ this reduces to

$$(x - r)/a = \log \theta - \log \tan(\pi/8) + 2 - \sqrt{2} - 2 \log 2$$

or

$$\begin{aligned} \theta &= 4 \tan(\pi/8) \exp(-r/a - 2 + \sqrt{2}) \exp(x/a) \\ &= \theta_0 \exp(x/a) \end{aligned} \quad \text{A.3}$$

Using these results of Rayleighs we can now calculate the integral

A.1. We make the substitution

$$t = z/2a$$

Then A.2 becomes

$$2t^2 = 1 - \cos \theta \quad \text{A.4}$$

from which we get

$$1 + \tan^2 \theta = 1/\cos^2 \theta = 1/(1-2t^2)^2 \quad \text{A.5}$$

whence

$$\tan \theta = 2t(1-t^2)^{\frac{1}{2}}/(1-2t^2) \quad \text{A.6}$$

Also

$$dx = 2a dt/\tan \theta \quad \text{A.7}$$

Substituting from A.6 and integrating

$$\begin{aligned} x &= 2a \int (1-2t^2) dt / 2t(1-t^2)^{\frac{1}{2}} \\ &= a \left[\int dt/t(1-t^2)^{\frac{1}{2}} - 2 \int t dt/(1-t^2)^{\frac{1}{2}} \right] \end{aligned}$$

$$= a \left[\log t - \log \left\{ 1 + (1-t^2)^{\frac{1}{2}} \right\} + 2(1-t^2)^{\frac{1}{2}} \right] \quad \text{A.8}$$

$$\text{Now } A_2 = 2\pi \int_{x_0}^r x \left[1 + (dy/dx)^2 \right]^{\frac{1}{2}} dx$$

$$= 2\pi \int_{x_0}^r x (1 + \tan^2 \theta)^{\frac{1}{2}} dx$$

Substituting from A.5 to A.8 gives

$$A_2 = 2\pi a^2 \int \left[\log t - \log \left\{ 1 + (1-t^2)^{\frac{1}{2}} \right\} + 2(1-t^2)^{\frac{1}{2}} \right] dt/t(1-t^2)^{\frac{1}{2}}$$

$$= 2\pi a^2 \left[\int \left[\log t - \log \left\{ 1 + (1-t^2)^{\frac{1}{2}} \right\} \right] dt/t(1-t^2)^{\frac{1}{2}} + 2 \int dt/t \right]$$

To evaluate the first integral we write

$$F(t) = \log t - \log \left\{ 1 + (1-t^2)^{\frac{1}{2}} \right\} \text{ and } f(t) = 1/t(1-t^2)^{\frac{1}{2}}$$

and note that

$$dF/dt = f$$

Thus the integral is

$$\int Ff dt = \int FdF = F^2/2$$

and so

$$A_2 = 2\pi r^2 \left[\log t^2 + \frac{1}{2} \left\{ \log t / (1 + (1 - t^2)^{\frac{1}{2}}) \right\}^2 \right]$$

Substituting from A.4 and A.8 gives

$$A_2 = 2\pi r^2 \left[\frac{1}{2} (x/a)^2 - (x/a) \left\{ 2(1 + \cos\theta) \right\}^{\frac{1}{2}} + 1 + \cos\theta + \log \frac{1}{2} (1 - \cos\theta) \right] \begin{array}{l} x = r \\ \\ x = x_0 \end{array}$$

Now at $x = r$ $\theta = \pi/2$ and at $x = x_0$ $\theta = \theta_0 \exp(x_0/a)$ and $\theta \ll 1$

$$\text{Thus } A_2 = 2\pi r^2 \left[(r^2 - x_0^2)/2a^2 - (r/a) \sqrt{2} - 1 + \log 2 - 2 \log \theta_0 \right]$$

$$\begin{aligned} \text{Now } A_0 &= (A_1 + A_2)/\pi r^2 \\ &= 1 + 2(a/r)^2 \left[\log 2 - 1 - (r/a) \sqrt{2} - 2 \log \theta_0 \right] \end{aligned}$$

Substituting for θ_0 , and putting in numerical values, gives

$$A_0 = 1 + 1.172(a/r) - 0.290(a/r)^2$$

which is the required result. Values of surface tension from Atkins and Narahara (1965) were used, giving for a 1cm diameter tube

$$A_0 = 1.12 \text{ at } 1.2^\circ\text{K decreasing to } 1.11 \text{ at } 2.1^\circ\text{K.}$$

There is a second meniscus effect which should be considered but which turns out to be self cancelling. Consider a liquid in equilibrium with its vapour. Then the pressure at the liquid surface is the same on both sides of the surface, namely p , the vapour pressure.

If now the liquid is contained in a tube of finite radius, then the pressure $p(x)$ at the surface is a function of the distance x from the centre of the tube. In fact

$$p(x) + \rho gz = p(0) \quad \text{A.9}$$

where z is the height of the meniscus measured from the liquid level in the centre of the tube ($x=0$). The mass evaporating/unit time from the whole liquid surface is

$$\begin{aligned} & \int_0^r \alpha_{op}(x) \cdot 2\pi x \sqrt{1 + \left(\frac{dz}{dx}\right)^2} \cdot dx \\ &= A\alpha_{op}(0) - 2\pi\alpha_{op}\rho g \int_0^r x \sqrt{1 + \left(\frac{dz}{dx}\right)^2} dx \end{aligned}$$

$$= A\alpha_{op}(0) - A\alpha_{op}\Delta p$$

and in equilibrium this must be equal to the mass condensing, which is just $A\alpha_{op}$. (There is a similar effect in the vapour, but it is negligible in that the vapour density is small compared with the liquid density).

Therefore

$$p(0) = p + \Delta p \quad \text{A.10}$$

Thus in the centre of the tube there is a net evaporation, since $p(0) > p$, which is balanced at the sides by a net condensation, when $p(x) < p$. To treat the non equilibrium case we must replace p in $G(T+\theta)$ (equation 2.5) by the $p(x)$ of equation A.9. If θ is independent of x the integration across the whole tube may be carried out as above. If we divide by A , to give the average evaporation rate/sq.cm., and use A.10, we get the same equation 2.5 as before.

APPENDIX B

The Kinetic Theory Calculations on Evaporation

B.1 The distribution functions close to the surface

We assume that the number of atoms with components of velocities between v_z and $v_z + dv_z$ is

$$f_{z+} dv_z = \beta_1 \exp(-mv_z^2/2kT_1) dv_z$$

for the atoms travelling upwards, and

$$f_{z-} dv_z = \beta_2 \exp(-mv_z^2/2kT_2) dv_z$$

for the atoms travelling downwards. Normalising these distribution functions gives

$$\beta_1 = 2(m/2\pi kT_1)^{\frac{1}{2}}$$

$$\text{and } \beta_2 = 2(m/2\pi kT_2)^{\frac{1}{2}}$$

The number of atoms travelling upwards with a speed between v and $v+dv$ is then given by the speed distribution function $F_1(v)$,

$$F_1(v)dv = \int f_x f_y f_{z+} dv_x dv_y dv_z$$

where f_x is the usual Maxwell-Boltzmann component velocity distribution function

$$f_x = (m/2\pi kT_1)^{\frac{1}{2}} \exp(-mv_x^2/2kT_1)$$

and the integration is to be performed over all possible directions. We transform to spherical polar coordinates in the usual way, but note that the integration over θ is to be carried out only from 0 to $\pi/2$, since the atoms occupy only half of phase space. Thus

$$F_1(v)dv = f(v_x) f(v_y) f_{z+}(v_z) v^2 dv \int_0^{2\pi} d\phi \int_0^{\pi/2} \sin\theta d\theta$$

$$= 4\pi(m/2\pi kT_1)^{3/2} \exp(-mv^2/2kT_1) v^2 dv$$

which is the usual Maxwell-Boltzmann distribution. Clearly a similar result holds for F_2 , the distribution function for the atoms travelling downwards.

It remains to derive a distribution function for all the atoms in the region close to the surface. If the number density of these going up is $\frac{1}{2}n_1$, then $\frac{1}{2}n_1 F_1 dv$ of these going up have a speed between v and $v + dv$, as do $\frac{1}{2}n_2 F_2 dv$ of those going down. Thus the normalised distribution function F for all the atoms is

$$F(v) = (n_1 F_1 + n_2 F_2) / (n_1 + n_2) \quad \text{B.1}$$

B.2 Momentum and mass flux

We have to calculate the z momentum crossing unit area of the x - y plane per unit time. Consider an element of area dS on the

x-y plane. Then the atoms with velocities close to \underline{v} which cross in a time dt are all contained in an oblique cylinder, of slant height $v_z dt$ and base area dS . The volume of this cylinder is $v_z dt dS$, the number of atoms in it is $nv_z dt dS$, and of these atoms $nv_z dt dS f_x f_y f_z dv_x dv_y dv_z$ have the specified velocity. The z momentum they carry across the x-y plane per unit area per unit time is then

$$nmv_z^2 f_x f_y f_z dv_x dv_y dv_z$$

where the f 's are general component distribution functions which must, however, be mutually independent and normalised. Integrating this gives the total momentum flux M . Since the integral is independent of x and y

$$M = nm \int v_z^2 f_z dv_z \quad \text{B.2}$$

and the integral is over all possible values of v_z .

By a similar argument, we find that the mass flow G is given by

$$G = nm \int v_z f_z dv_z \quad \text{B.3}$$

B.3 Momentum, mass and energy conditions close to the surface.

The mean energy E of the atoms close to the surface is

$$E = \frac{1}{2} m \overline{v^2} = \frac{1}{2} m \int_0^{\infty} v^2 F(v) dv$$

where $F(v)$ is given by equation B.1. Thus

$$E = \frac{m}{2(n_1+n_2)} \left[n_1 \int_0^{\infty} v^2 F_1(v) dv + n_2 \int_0^{\infty} v^2 F_2(v) dv \right]$$

$$= (3k/2)(n_1 T_1 + n_2 T_2) / (n_1 + n_2) \quad \text{B.4}$$

which is the first of the results required on p. 25. The momentum flux due to the atoms moving up the tube is, from equation B.2

$$\frac{1}{2} n_1 m \int_0^{\infty} v_z^2 f_{z+} dv_z = \frac{1}{2} n_1 k T_1$$

Similarly the momentum flux due to the atoms moving down is $\frac{1}{2} n_2 k T_2$, and so the total momentum flux is

$$\frac{1}{2} n_1 k T_1 + \frac{1}{2} n_2 k T_2 \quad \text{B.5}$$

the second result required on p. 25.

From equation B.3 we get that the mass flow upwards is

$$\frac{1}{2} n_1 m \int_0^{\infty} v_z f_{z+} dv_z = n_1 k T_1 \left(m / 2\pi k T_1 \right)^{1/2}$$

and the mass flow downwards is

$$n_2 k T_2 (m/2\pi k T_2)^{\frac{1}{2}}$$

Since $m/k = M/R$, we can write the net mass flow as (see page 27)

$$n_1 k T_1 (M/2\pi R T_1)^{\frac{1}{2}} - n_2 k T_2 (M/2\pi R T_2)^{\frac{1}{2}} \quad \text{B.6}$$

B.4 Momentum and energy conditions far from the surface.

In this region the z velocity component distribution function is

$$f_z = (m/2\pi k T_2)^{\frac{1}{2}} \exp \left[-m(v_z - v_0)^2 / 2k T_2 \right]$$

and the x and y distribution functions are the usual ones, e.g.

$$f_y = (m/2\pi k T_2)^{\frac{1}{2}} \exp(-mv_y^2 / 2k T_2)$$

Then the mean energy of an atom is

$$E = \frac{1}{2} m \bar{v}^2 = \frac{1}{2} m \int v^2 f_x f_y f_z dv_x dv_y dv_z \quad \text{B.7}$$

We integrate this by writing $v^2 = v_x^2 + v_y^2 + v_z^2$. Then equation B.7 splits into the sum of three triple integrals each of which separates; the last, for example, is

$$\int_{-\infty}^{+\infty} f_x dv_x \int_{-\infty}^{+\infty} f_y dv_y \int_{-\infty}^{+\infty} v_z^2 f_z dv_z$$

The first two integrals are 1 since the f 's are normalised, the third is evaluated by the substitution $V = v_z - v_0$. It then becomes

$$\left(\frac{m}{2\pi kT_0} \right)^{\frac{1}{2}} \left[\int_{-\infty}^{+\infty} v^2 \exp(-mV^2/2kT_0) dV + 2v_0 \int_{-\infty}^{+\infty} V \exp(-mV^2/2kT_0) dV + v_0^2 \int_{-\infty}^{+\infty} \exp(-mV^2/2kT_0) dV \right] \quad \text{B.8}$$

The first of these integrals contributes $\frac{1}{2}kT_0$ to E , as do each of the other two triple integrals in B.7. The second integral in B.8 is zero, the third gives a contribution $\frac{1}{2}mv_0^2$ to E . Thus

$$E = 3kT_0/2 + \frac{1}{2}mv_0^2 \quad \text{B.9}$$

From equation B.2 the momentum flux is

$$n_0 m \int_{-\infty}^{+\infty} v_z^2 f_z dv_z = n_0 kT_0 + n_0 m v_0^2 \quad \text{B.10}$$

Equations B.9 and B.10 are the two results used on page 26.

APPENDIX C

The Computer Programme

The program is written in FORTRAN, which is a problem orientated language as opposed to a machine orientated language. That is to say it is a language which is basically similar to mathematics, but quite unintelligible to a computer until it has been translated into a more basic machine language. The translation is done by the computer using a machine language programme called a compiler. Each instruction in FORTRAN is called a FORTRAN statement, and is punched on one or more 80 column cards, 1 character per column. The first 5 columns are used for labelling statements for programming purposes, e.g. to have a computation repeated with different data. The sixth column is used to indicate that a statement occupies more than one card, and the last 8 columns are used for external labelling purposes, and are ignored by the compiler.

The basic FORTRAN statement is the arithmetic statement, e.g. $A=B+C$. This simply means that the value of the expression on the right hand side of the equality sign is to be assigned to the variable on the left hand side. Note that the symbol = does not have its mathematical meaning, since $M=M+1$ is a meaningful FORTRAN statement but not a mathematical one. Apart from ordinary variables we can have subscripted variables, e.g. h_1 , which is written as $H(I)$. (Only capital

letters are allowed in FORTRAN statements).

To do useful calculations it is necessary to be able to decide the next stage in the calculation on the basis of the results already calculated. The basic method for doing this is to use an IF statement, e.g. IF(A) 1,2,3. This means that if A is negative the next statement to be carried out will be the one labelled 1 in columns 1 to 5, if A is zero it will be statement 2, and if positive, statement 3. If any of 1, 2, or 3 is the physically next statement, then the label may be omitted and replaced by 0. An extension of this facility is the DO loop, e.g.

```
DO 100 I = M, N,L
```

This causes all the statements after the DO statement up to and including the statement labelled 100 to be executed, first with $I = M$, then with $I = M+L$, then $I = M+2L$, and so on for all such values of I up to N . If $L=1$ it is usually omitted.

Using these statements and some others (mostly concerned with getting information into and out of the machine) it is possible to build up programmes of considerable complexity. However there are many advantages to be gained by splitting large programmes into sections called subroutines. Each subroutine is given a name, and information is transferred between routines by listing after the name of each subroutine

all the variables whose names and values it is desired to transfer.

We are now in a position to describe the programme used in this work for calculating the reflection coefficients. It consists of a main routine and four subroutines, called EXPLOT, GEMEAN, AVER and GHLESQ. Most of the calculation is done in the subroutines, and the main programme just controls the data input and output. As soon as the programme reads data in from cards it writes it out again on magnetic tape, and in this way it is possible to recalculate all the results using different numbers of points per line in only one programme run.

The first act of the compiler programme is to list on the line printer all the cards it reads, and such a listing is shown in Figure C.1. The numbers at the left hand side are the statement label numbers, those at the right are reference numbers which will be used for purposes of exposition.

The first statement (9) is merely a job number to distinguish this programme from all the others on the machine. Statements 15 and 16 allocate storage space for the subscripted variables. 17 and 18 cause the parameter NK to be read in; NK is the number of times the calculation is to be repeated for different numbers of points per line. 20 is the DO statement which does this; the statement labelled

MASTER E01B	009
DIMENSION H(20), VA(10),EVA(10),VB(10),EVB(10),VT(10),EVT(10	010
1),V(20),EV(20) ,S(50),DS(50) ,KOD(4)	010
4 1 2 3	
READ(1,105)NK	011
105 FORMAT(12)	012
M=1	014
DO 102 JJ=1,NK	020
LL=0	021
READ(1,20)KODE,KP1,KP2,KP3,KP4	022
20 FORMAT(12,411)	023
KOD(1)=KODE	024
READ(M,2)NFILMS	025
IF(JJ-1)0,0,106	026
WRITE(0,2)NFILMS	027
106 CONTINUE	028
2 FORMAT(12)	029
READ(M,103)NG	030
IF(JJ-1)0,0,107	031
WRITE(0,103)NG	032
107 CONTINUE	033
103 FORMAT(12)	034
KK=0	035
NGS=NG	036
KKS=0	037
DO 11 L=1,NFILMS	038
READ(M,1)NRUN,NFILM,NFS	039
IF(JJ-1)0,0,109	040
WRITE(0,1)NRUN,NFILM,NFS	041
109 CONTINUE	042
1 FORMAT(12,11,12)	043
KOD(2)=NRUN	044
KOD(3)=NFILM	045
WRITE(2,3)NRUN ,KODE	046
3 FORMAT(12H1HELIUM RUN ,12,2X,30HREFLECTION COEFFICIENT BY PULSE ME	047
1THOD,6X,25HMAXIMUM POINTS PER LINE =,13)	048
WRITE(2,16)	049
16 FORMAT(21HO R(ALL),12X,6HR(ODD),12X,7HR(EVEN),11A,7HD	050
DELTA R,11X,9HR(BOTTOM),9X,6HR(TOP))	051
DO 4 K=1,NFS	052
READ(M,8)N,(H(I),I=1,N)	053
IF(JJ-1)0,0,110	054
WRITE(0,8)N,(H(I),I=1,N)	055
110 CONTINUE	056
8 FORMAT(12,20F5.1)	057
IF(H(1)-1.0E-4)0,0,15	058
IF(H(2)-1.0E-4)4,4,0	059
15 CONTINUE	060
N=2*(N/2)	061
IF(N-KODE)201,0,0	062
N=KODE	063
201 CONTINUE	064
CALL EXPLOT(1,N,1,H,K1,KA,ERA,AA,BA,DAA,DBA)	065
IF(K1)6,6,0	066
NG=NG-1	067
GO TO 101	068
6 CONTINUE	069
KK=KK+1	070
VA(KK)=BA	071
EVA(KK)=DBA	072
CALL EXPLOT(1,N,2,H,K1,RO,ERO,AU,BO,DAO,DBO)	073
IF(K1)12,12,0	074
NGS=NGS-1	075
GO TO 104	076

Figure C.1 The Computer Programme.

12	CONTINUE	077
	KKS=KKS+1	078
	V(2*KKS-1)=BO	079
	EV(2*KKS-1)=DBO	080
	CALL EXPLOT(2,N,2,H,K1,RE,ERE,AE,BE,DAE,ORE)	081
	IF(K1)7,7,0	082
	NGS=NGS-1	083
	KKS=KKS-1	084
	GO TO 104	085
7	CONTINUE	086
	V(2*KKS)=BE	087
	EV(2*KKS)=DBE	088
	LL=LL+1	089
	S(LL)=RE-RO	090
	DS(LL)=SQRT(ERE*ERE+ERO*ERO)	091
	RBORT=EXP(AO-AE)	092
	RB=RA*RBORT	093
	RI=RA/RBORT	094
	DR=SQRT((ERA/A)**2+DAO*DAO+DAE*DAE)	095
	ERB=RB*DR	096
	ERT=RI*DR	097
	VB(KKS)=BA+AO-AE	098
	EVB(KKS)=SQRT(VBA*DBA+DAO*DAO+DAE*DAE)	099
	VT(KKS)=BA-AO+AE	100
	EVT(KKS)=EVB(KKS)	101
	WRITE(2,10)NRUN,NFILM,K,RA,ERA,RO,ERU,RE,ERE,S(LL),DS(LL),RB,ERB,RT,ERT	102
10	FORMAT(313,6(F11.3,F7.3))	103
	GO TO 101	104
104	CONTINUE	105
	WRITE(2,13)NRUN,NFILM,K,RA,ERA	106
13	FORMAT(313,F11.3,F7.3)	107
101	CONTINUE	108
	IF(KK-NG)100,0,0	109
	KOD(4)=K	110
	NGT=NGS*2	111
	CALL GMEAN(VA,EVA,NG,RAB,ERAB,ZA,DZA,NSA,KOD,KP1)	112
	CALL GMEAN(V,EV,NGI,ROB,EROB,ZO,DZO,NSO,KOD,KP2)	113
	CALL GMEAN(VB,EVB,NGS,RBB,ERBB,ZB,DZB,NSB,KOD,KP3)	114
	CALL GMEAN(VI,EVI,NGS,RIB,ERIB,ZI,DZI,NSI,KOD,KP4)	115
	WRITE(2,17)RAB,ERAB,NG,ROB,EROB,NGT,RBB,ERBB,NGS,RTB,ERIB,NGS,ZA,D	116
	ZA,NSA,ZO,DZO,NSO,ZB,DZB,NSB,ZI,DZI,NSI	117
17	FORMAT(17H AVERAGES,2(F8.2,F5.2,2H (,12,2H),33X,2(F8.2,F5.2,2H (118
	1,12,2H))/9X,2(6H Z= ,	119
2	F5.2,F6.2,13),30X,2(6H Z= ,F5.2,F6.2,13)//)	120
	KK=0	121
	KKS=0	122
	READ(M,103)NG	123
	IF(JJ-1)0,0,108	124
	WRITE(0,103)NG	125
108	CONTINUE	126
	NGS=NG	127
100	CONTINUE	128
4	CONTINUE	129
	CALL AVER(S,DS,LL,R1,ER1,AA,B,A,Z,DZ)	130
	WRITE(2,5)LL,R1,ER1,Z,DZ	131
5	FORMAT(136HWEIGHTED MEAN AND ERROR OF THE LAST,12,1X,8HREADINGS,2F	132
	17.2,20X,3HZ =,2F7.3)	133
	WRITE(2,9)AA,B,A	134
9	FORMAT(17	135
2	H ZIGMA X(I)W(I) =,E13.5,5X,12HZIGMA W(I) =,F13.5,5X,24HZI	136
	IGMA(X(I)-XBAR/2W(I) =,E13.5)	137
	LL=0	138
11	CONTINUE	139
	M=0	140
	REWINDO	141
102	CONTINUE	142
	STOP	143
	END	144

Figure C.1 The Computer Programme (contd.).

SUBROUTINE AVER(V, EV, N, RB, ERB, AA, B, A, Z, DZ)	140
DIMENSION V(N), EV(N)	149
AN=N	150
A=0.	151
B=0.	150
DO 7 I=1, N	159
C=1./ (EV(I)*EV(I))	160
A=A+V(I)*C	161
B=B+C	162
7 CONTINUE	163
RB=A/B	164
AA=A	165
A=0.	160
DO 5 I=1, N	167
C=1./ (EV(I)*EV(I))	163
A=A+(V(I)-RB)*(V(I)-RB)*C	169
5 CONTINUE	170
ERB1=SQRT(A/((AN-1.)*B))	171
ERB2=SQRT(1./B)	172
IF(ERB1-ERB2)4,6,6	173
4 ERB=ERB2	174
GO TO 1	175
6 ERB=ERB1	175
1 CONTINUE	177
Z=ERB1/ERB2	178
DZ=1./SQRT(2.*(AN-1.))	179
RETURN	180
END	181
SUBROUTINE GMEAN(V, EV, N, VB, EVB, Z, DZ, NS, KOD, KP)	182
DIMENSION V(N), EV(N), KOD(4)	183
CALL AVER(V, EV, N, RB, ERB, A, B, C, Z, DZ)	184
VB=EXP(RB)*100.	185
EVB=VB*ERB	186
IF(KP)1,1,0	187
WRITE(3,2)N, RB, ERB, A, B, C, KP, (KOD(I), I=1,4)	188
2 FORMAT(12,5E13.5,12,213,12,13)	189
1 CONTINUE	190
IF(Z-1.)5,0,0	191
NS= ALOG(Z)/ALOG(1.+DZ)+1.	192
GO TO 4	193
3 CONTINUE	194
NS=-(ALOG(Z)/ALOG(1.-DZ)+1.)	195
4 CONTINUE	196
RETURN	197
END	198

Figure C.1 The Computer Programme (contd.).

	SUBROUTINE EXPLOT(K,N,L,H,K1,R,ER,A,B,DA,DB)	199
	DIMENSION H(N)	200
	DIMENSION Y(20),X(20),EH(20)	201
	II=0	202
	K1=0	203
	DO 6 J=K,N,L	204
	IF(H(I)-1.0E-4)6,6,12	205
12	II=II+1	206
	Y(II)=ALOG(H(I))	207
	X(II)=I	208
	EH(II)=1./H(I)	209
6	CONTINUE	211
	IF(II-4)0,1,1	212
	K1=1	213
	GO TO 2	214
1	CONTINUE	215
	CALL GHLESQ(X,Y,EH,A,B,1,II,DA,DB)	216
	R=EXP(B)*100.	217
	ER=R*DB	218
2	CONTINUE	219
	RETURN	220
	END	221

	SUBROUTINE GHLESQ(X,Y,DY,A,B,NS,NF, DA, DB)	222
	DIMENSION X(NF),Y(NF),DY(NF)	228
	DIMENSION W(100)	229
	AN=NF-NS+1	230
	ZIGW =0.	231
	ZIGWX =0.	232
	ZIGWY =0.	233
	ZIGWXY=0.	234
	ZIGWX2=0.	235
	ZIGDEN=0.	236
	ZIGBRA=0.	237
	DO 2 I=NS,NF	238
2	W(I)=1. / (DY(I)*DY(I))	239
	DO 3 I=NS,NF	240
	ZIGW =ZIGW +W(I)	241
	ZIGWX =ZIGWX +W(I)*X(I)	242
	ZIGWY =ZIGWY +W(I)*Y(I)	243
	ZIGWXY=ZIGWXY+W(I)*Y(I)*X(I)	244
3	ZIGWX2=ZIGWX2+W(I)*X(I)*X(I)	245
	XBAR=ZIGWX/ZIGW	246
	YBAR=ZIGWY/ZIGW	247
	DO 4 I=NS,NF	248
	ZIGDEN=ZIGDEN+W(I)*(X(I)-XBAR)*(X(I)-XBAR)	249
4	ZIGBRA=ZIGBRA+W(I)*(X(I)-XBAR)*(Y(I)-YBAR)	250
	A=(YBAR+ZIGWX2-XBAR*ZIGWXY)/ZIGDEN	251
	B=ZIGBRA/ZIGDEN	252
	DO 6 I=NS,NF	253
6	DY(I)=ABS(Y(I)-A-B*X(I))	254
	DYY=0.	255
	DO 7 I=NS,NF	256
7	DYY=DYY+DY(I)*DY(I)*W(I)	257
	DD=SQRT(DYY/(AN-2.)*(ZIGW*ZIGWX2-ZIGWX*ZIGWX))	258
	DA=DD*SQRT(ZIGWX2)	259
	DB=DD*SQRT(ZIGW)	260
	RETURN	261
	END	262

Figure C.1 The Computer Programme (contd.).

102 is the last statement in the programme, and so the entire programme calculation is done NK times. JJ is a dummy variable which does not appear again in the course of the programme. 22 and 23 read in the parameters KODE, KP1, KP2, KP3 and KP4. KODE is the maximum number of points which are to be fitted to a line. Some of the results are punched out (so that averages of the results in several groups can be recalculated) and the KP's are control numbers to suppress the punching of unwanted cards. It is convenient in a later part of the programme to express KODE as an element of an array of reference numbers and this is the function of line 21. 25 to 29 read in NFILMS, and (on the first run through) write it out again on magnetic tape. (Line 19 is also concerned with the use of magnetic tape). It is necessary to have an indexing system for the photographs; each photograph is labelled by three numbers - the helium run number (NRUN), the film number during that run (NFILM) and the frame number on that film. NFILMS is the total number of films to be processed.

Similarly 30 to 34 read in NG, which is the number of frames which are to be grouped together for averaging. 38 is an instruction to repeat the calculation for all the films. 39 to 43 then read in NRUN, NFILM and NFS, the total number of frames in that film. 44 and

45 set `NRUN` and `NFILM` in array form, and 46 to 51 print out headings for the results. At statement 52, we reach the inside loop, with an instruction to repeat the calculation for all frames, and start the calculation proper.

53 to 57 read in $H(I)$, the pulse height measurements, and N , the number of them. Normally, K , the loop parameter (line 52) will be the same as the frame number, but occasionally (see Chapter 5) a photograph is omitted. If a card with the first two values of $H(I)$ punched as zero is fed in instead, 58 to 60 cause K to be incremented by 1 without any other action being taken, thus keeping K in correspondence with the frame numbers. (The `CONTINUE` statement means just what it says - go on to the next statement).

One of the `FORTRAN` conventions is that variables whose names begin with the letters `I, J, K, L, M, N` are to be regarded as integers, while other variables are regarded as decimal numbers. Division of two integers gives an integer answer which has been truncated towards zero, rather than rounded off. 61 therefore ensures that the number of points used is even so that odd and even lines have the same number of points, and one straight line fits are obtained from the same data as two line fits. 62 to 64 ensures that the maximum number of points fitted is `KODE`. 65 calls the subroutine `EXPLOTT`, which is listed separately, starting at line 199. From the parameter list we see that

N and H are already defined, and are the numbers we put into the subroutine. The other parameters are those which are to be calculated in the subroutine and then transferred back to the main routine. For example, R is a parameter calculated in the subroutine, but which is transferred back to the main routine, where it is called RA. Similarly K is a parameter transferred from the main routine, on this occasion with the value 1. We turn now to the calculations performed in EXPLOT.

200 and 201 allocate array storage. The loop 204 to 211 sets up the values of X and Y which will be fitted to a straight line $Y = A + BX$ by the general subroutine GHLESQ. Sometimes low frequency noise causes the tops of some pulses (not necessarily the first) to be off scale, and these are punched as zero. 205 and 206 ensure that these points are not included, and that the total number of points is correct. 202 ensures that II is initially zero, and that the final value of II is therefore correct. (This is a general procedure when using DO loops for calculating sums). 207 calculates $\log_{10} H(I)$. $EH(II)$ is a number proportional to the error in $Y(II)$. 212 and 214 ensure that no line is fitted to less than four points (GO TO 2 means that the statement labelled 2 is to be executed next) and the parameter K1 (203 and 213) indicates this fact to the main programme. 216 now

calls the subroutine GHLESQ (listed from line 222) which fits the straight line.

228 and 229 of GHLESQ again allocate array storage. 230 sets AN equal to the total number of points. 231 to 237 ensure that all the sums to be calculated will be correct. 238 and 239 calculate the weighting factors w_i , and 240 to 245 the sums $\sum w_i$, $\sum x_i w_i$, $\sum y_i w_i$, $\sum x_i y_i w_i$ and $\sum x_i^2 w_i$ (* means x). 246 and 247 calculate $\bar{x} = \sum x_i w_i / \sum w_i$ and $\bar{y} = \sum y_i w_i / \sum w_i$. 248 and 250 calculate $\sum (x_i - \bar{x})^2 w_i$ and $\sum (x_i - \bar{x})(y_i - \bar{y}) w_i$. 251 and 252 then calculate the intercept A and the slope B of the plotted straight line. 253 and 254 give the deviation of the points from the fitted line, and 256 to 260 use this information to calculate the standard errors DA and DB of A and B. 261 returns control of the programme to the next statement after the CALL GHLESQ statement just executed in EXPLOT. 262 is an instruction to the compiler to stop compiling the subroutine.

EXPLOT now (217 and 218) calculates the reflection coefficient R and standard error ER corresponding to the slope and error of the fitted line, and then returns control to the main routine at line 66.

66 now determines whether a straight line has or has not been fitted. If not, the number of results in the group to be averaged

is reduced by 1 (17). Since in the EXPLOT routine just completed K and L were set equal to 1, it was a straight line fit through all the points that was attempted. If there were too few points 68 directs that no attempt be made to fit two lines.

70 to 72 now accumulate the results of fitting one line to all the data in VA (the slopes) and EVA (the errors). Since KK has been previously set equal to zero outside the NFILM loop (35), the accumulation is from 1 to NG.

73 fits the odd line and 74 tests to see that it has in fact been done. If it has not, then the number of frames contributing to the average of odd and even lines (NGS) is no longer equal to NG (line 36) and must be reduced (75). In this case the even line is not fitted (76 and 77). 37 with 78 to 80 accumulate the odd line results in V and EV. 81 to 88 repeat all this for the even lines, and 84 erases the previous odd line result if no line can be fitted to the even points. 21 with 89 to 91 accumulates in S and DS, the difference between the slope of the odd and even lines, and the error in that quantity. (S and DS have lost their significance since the programme was written).

92 to 97 calculate the top and bottom reflection coefficients (equations 5.3 and 5.4) and their errors and 98 to 101 accumulate the

answers in VT, VB, EVT and EVB. 102 to 109 now print out the results, taking account of the fact that it may not have been possible to fit odd and even lines. 110 enquires if all the results in one group are yet complete. If so K, equivalent to the frame number of the last member is put into the reference number array (111), the total number of odd and even lines NGT is evaluated (112), and all the averages calculated by the subroutine GEMEAN. 113 gives the average obtained by fitting one line to all the data, 114 the average of both odd and even lines and 115 and 116 the averages of the bottom and top reflection coefficients.

GEMEAN (starting on line 182) at once calls the subroutine AVER (146). 157 to 163 calculates $\sum v_i w_i$ and $\sum v_i$. 164 gives \bar{v} (denoted by RB) and 165 retains $\sum v_i w_i$ for future reference. 166 to 170 calculates $\sum (v_i - \bar{v}) w_i$ and 171 to 172 the two standard errors of Chapter 5. 173 to 177 determine which is the larger and 178 and 179 give Z and its standard error.

Control returns to GEMEAN, which calculates the reflection coefficient and its error corresponding to the mean slope given by AVER. 187 to 190 cause punched card output of the results (and the reference array KOD) to be produced if KP is 1, but suppress it otherwise. 191 to 196 determine the deviation of Z from 1 in terms

of the standard error in $Z, \Delta Z$. Control now returns to the main programme, at 117, where all the results are printed out (117 to 121). The results registers are cleared (122 and 123) the next value of NG read in (124 to 127), and NGS set equal to it (128). At 130 we reach the end of the K loop, i.e. the end of the calculations on one frame. The programme returns to line 52 and repeats the calculation until it has done so for all the frames on one film. The average value of S is then calculated (131), printed out (132 to 138) along with some other information, and the S register cleared (139). At 140, we reach the end of the $NFILM$ loop, i.e. the programme returns to 38 and repeats the calculation for each film. Having done that it rewinds the magnetic tape (142) and reaches the end of the NK loop. It therefore returns to 20 and repeats the entire calculation for a different number of points per line. Finally, at 144, it stops.

The programme was run on an I.C.T. 1905 computer. It fitted 3 lines to some 500 sets of data, each of from 8 to 16 points, and calculated 4 averages for each of some 150 groups. For two values of $KODE$ (8 and 16) the calculation took about 15 minutes. Since it occupied about 5k words of core store it is a small to medium sized programme. It took about two months to write and debug in which time

perhaps one quarter of the basic information about reflection coefficients and averages could have been calculated by hand. The probability that such a hand calculation would be free from numerical error is rather low, and no attempt could have been made at a proper calculation of the standard errors in that time.

REFERENCES

- Allen, J.F. and C.C. Matheson. (1966). Proc. Roy. Soc., A290, 1.
- Alty, T. and C.A. MacKay. (1935). Proc. Roy. Soc., A149, 104.
- Atkins, K.R. (1953). Canad. J. Phys., 31, 1165.
- Atkins, K.R. (1957). Physica, 23, 1143.
- Atkins, K.R. (1959a). Liquid Helium, p 107. Cambridge University Press.
- Atkins, K.R. (1959b). Phys. Rev., 113, 962
- Atkins K.R. and K.H. Hart. (1954). Canad. J. Phys., 32, 81.
- Atkins, K.R. and Y. Narahara. (1965). Phys Rev., 138, 437.
- Atkins K.R., B. Rosenbaum, and H. Saki (1959). Phys. Rev., 113, 751.
- Bendt, P.J., R.D. Cowan and J.L. Yarnell (1959). Phys. Rev., 113,
1386.
- Brewer, D.F., A.J. Symonds and A.L. Thomson (1965). Phys. Rev. Letters,
15, 182.
- Chernikova, D.M. (1964). J. Exp. Theor. Phys. USSR, 47, 537
(translated in Soviet Physics -JETP, 20, 358, 1965).
- Cunsolo, S., M. Santini, and M. Vincenti-Missoni. (1965).
Cryogenics 5, 168
- Dessler, A.J. and W.M. Fairbank. (1956). Phys Rev., 104, 6.
- van Dijk, H. and M. Durieux. (1958a). Physica, 24, 920.

- van Dijk, H. and M. Durieux. (1958b). *Physica*, 24, 1.
- Dingle, R.B. (1948). *Proc. Phys. Soc. A*, 61, 9.
- Everitt, C.W.F., K.R. Atkins and A. Denenstein. (1962).
Phys. Rev. Letters, 8, 161.
- Everitt, C.W.F., K.R. Atkins and A. Denenstein. (1964).
Phys. Rev., 136, A1494.
- Fairbank, W.M., H.A. Fairbank and C.T. Lane. (1947).
Phys. Rev., 72, 645.
- Grimrud, D.T. and J.H. Werntz. (1967). *Phys. Rev.*, 157, 181.
- Henshaw, D.G. and A.D.B. Woods (1961). *Phys. Rev.*, 121, 1266.
- Hirth, J.P. and G.M. Pound (1963). Condensation and Evaporation,
p 77 et seq. London; Pergamon Press.
- van Itterbeek, A. and W. de Laet. (1958). *Physica*, 24, 59.
- Jamieson, D.T. (1964). *Nature*, 202, 583.
- Johnston, W.D. and J.G. King. (1966). *Phys. Rev. Letters*, 16, 1191.
- Keller, W.E. and E.F. Hammel. (1966). *Phys. Rev. Letters*, 17, 998.
- Khalatnikov, I.M. (1952a). *J. Exp. Theor. Phys. USSR*, 23, 821.
- Khalatnikov, I.M. (1952b). *J. Exp. Theor. Phys. USSR*, 22, 687.
- Khalatnikov, I.M. (1965). An Introduction to the Theory of Superfluidity, pps. 11-12. New York; W.A. Benjamin.
- Kinsler, L.E. and A.R. Frey (1962). Fundamentals of Acoustics,
p 199. New York; John Wiley and Sons.

- Knudsen, M. (1915). *Ann. Phys.*, 47, 697.
- Kuper, C.G. (1956). *Physica*, 22, 1291.
- Kuper, C.G. (1958). *Physica*, 24, 1009.
- Landau, L.D. (1941). *J. Phys. USSR.*, 5, 71.
- Landau, L.D. (1947). *J. Phys. USSR.*, 11, 91.
- Lane, C.T., H.A. Fairbank and W.M. Fairbank. (1947). *Phys. Rev.*,
71, 600.
- Lane, C.T., H.A. Fairbank, H. Schultz and W.M. Fairbank, (1946).
Phys. Rev., 70, 431.
- Loeb, L.B. (1961). *The Kinetic Theory of Gases*, 3rd. ed., p. 106
et. seq. New York; Dover.
- Meyer, D.T., H. Meyer, W. Halliday and C.F. Kellers. (1963).
Cryogenics, 3, 150.
- Osborne, D.V. (1948). *Nature*, 162, 213.
- Osborne, D.V. (1962a). *Proc. Phys. Soc.*, 80, 103.
- Osborne, D.V. (1962b). *Proc. Phys. Soc.*, 80, 1343.
- Pellam, J.R. (1948). *Phys. Rev.*, 73, 608.
- Pellam, J.R. (1949). *Phys. Rev.*, 75, 1183.
- Peshkov, V. (1944). *J. Phys. USSR*, 8, 381.
- Pollack, G.L. (1966a). *Phys. Rev.*, 143, 103.
- Pollack, G.L. (1966b). *Phys. Rev.*, 149, 72.
- Present, R.D. (1958). *Kinetic Theory of Gases*, p 47. New York:
McGraw-Hill.

- Rayleigh, Lord. (1916). Proc. Roy. Soc., A92, 184.
- Tilley, J. (1965). Ph.D. Thesis, University of St. Andrews.
- Tilley, J. and C.G. Kuper. (1966). Proc. Roy. Soc., A 290, 14.
- Tisza, L. (1940). J. Phys. Radium, 1, 165, 350.
- Topping, J. (1962). Errors of Observation and their Treatment,
3rd. ed., p 91. London; Chapman and Hall.
- Yarnell, J.L., G.P. Arnold, P.J. Bendt and E.C. Kerr (1959).
Phys. Rev., 113, 1379.
- Zinoveva, K.N. (1956). J. Exp. Theor. Phys. USSR, 31, 31.
(Translated in Soviet Physics -JETP, 4, 36, 1957).

ACKNOWLEDGEMENTS

I would like to thank the following people for their assistance at various stages of this work.

Professor D.V. Osborne for suggesting the project, for his advice, encouragement and assistance while it was being carried out, and for reducing the number of wild goose chases up blind alleys by a factor of at least 2.

Professor J.F. Allen, F.R.S., for offering me the facilities of the Physics department at St. Andrews, and for his local supervision during a year when Professor Osborne was in Norwich.

Mr. R.H. Mitchell for his invaluable advice and assistance on all cryogenic matters, and he and his staff at St. Andrews for providing liquid helium.

Mr. McNab and his staff at St. Andrews for teaching me most of what I know about workshop practice, and for making some of the apparatus.

Mr. Howard Cairns for lending choke s and transformers unobtainable elsewhere.

Mr. V. Rose and his staff at East Anglia, for the considerable time and skill they devoted to building a cryostat virtually from scratch; and for installing a 16 inch booster pump in record time and overcoming their professional distaste of unpolished pipework to do so.

Mr. E.J. Critchfield and his staff at East Anglia for cheerfully and efficiently obtaining equipment and supplies amid all the chaos of a new department, and for processing more films than I care to count.

The programming staffs of the St. Salvators College Computing Laboratory, St. Andrews, the S.R.C. Atlas Computing Centre at Harwell and the University of Sussex computing centre, for their assistance with the programme, especially while it was being debugged.

Mrs. Audrey Ower for her rapid and efficient typing of this thesis.

Mr. D.O. Meyer for drawing the diagrams, and Mr. J.R. Carter and his staff for preparing the photographs.

My wife Elspeth for her encouragement during the past four years, and especially for typing a first draft of this document from my illegible handwriting.

A large number of other people, too numerous to catalogue, who, at various times and places have provided stimulating conversation or critical listening.

And last but not least, the Science Research Council for the award of a Research Studentship, during the tenure of which this work was carried out.